AD-A104 415 NAVAL OCEANOGRAPHIC OFFICE NSTL STATION MS F/G 11/1
ASSESSMENT OF TACTICAL SONOBUOY COMPUTER PROGRAMS FOR ENVIRONME--ETC(U)
FEB 81 L J FUSILLO
UNCLASSIFIED NOO-TR-260 NL

(12) LEVEL II

TR 260

TECHNICAL REPORT

ASSESSMENT OF TACTICAL SONOBUOY COMPUTER PROGRAMS FOR ENVIRONMENTAL SOFTWARE SYSTEMS

LAWRENCE J. FUSILLO
ENVIRONMENTAL SYSTEMS DIVISION

FEBRUARY 1981

APPROVED FOR PUBLIC RELEASE;
DISTRIBUTION UNLIMITED.

Prepared by
COMMANDING OFFICER,
NAVAL OCEANOGRAPHIC OFFICE
NSTL STATION, BAY ST. LOUIS, MS 39522

Prepared for
COMMANDER
NAVAL OCEANOGRAPHY COMMAND
NSTL STATION, BAY ST. LOUIS, MS 39529

FOREWORD

The area of Sonobuoy performance prediction is of vital importance for continued improvement in our Antisubmarine Warfare (ASW) capabilities. As part of the Naval Oceanographic Office's investment in ASW, the Environmental Systems Division specializes in on-scene predictions. This report identifies the major on-scene sonobuoy performance prediction programs and analyzes the characteristics of each. This information should prove a valuable contribution to future fleet improvements in on-scene prediction.

C. H. Bassett
Captain, USN
Commanding Officer

UNCLASSIFIED

SECURITY CLASSIFICATION OF THIS PAGE (When Data Entered)

REPORT DOCUMENTATION PAGE	READ INSTRUCTIONS BEFORE COMPLETING FORM
1. REPORT NUMBER: TR-260	2. GOVT ACCESSION NO.: AD-A104415
3. RECIPIENT'S CATALOG NUMBER	
4. TITLE (and Subtitle): Assessment of Tactical Sonobuoy Computer Programs for Enviromental Software Systems	5. TYPE OF REPORT & PERIOD COVERED
	6. PERFORMING ORG. REPORT NUMBER
7. AUTHOR(s): J. Fusillo	8. CONTRACT OR GRANT NUMBER(s)
9. PERFORMING ORGANIZATION NAME AND ADDRESS: Naval Oceanographic Office, Environmental Systems Division (Code 9200), NSTL Station, Bay St. Louis, MS 39522	10. PROGRAM ELEMENT, PROJECT, TASK AREA & WORK UNIT NUMBERS
11. CONTROLLING OFFICE NAME AND ADDRESS: Naval Oceanographic Office, NSTL Station, Bay St. Louis, MS 39522	12. REPORT DATE: February 1981
	13. NUMBER OF PAGES: 137
14. MONITORING AGENCY NAME & ADDRESS (if different from Controlling Office)	15. SECURITY CLASS. (of this report): Unclassified
	15a. DECLASSIFICATION/DOWNGRADING SCHEDULE

16. DISTRIBUTION STATEMENT (of this Report)

Approved for public release; distribution unlimited.

17. DISTRIBUTION STATEMENT (of the abstract entered in Block 20, if different from Report)

18. SUPPLEMENTARY NOTES

19. KEY WORDS (Continue on reverse side if necessary and identify by block number)

Sonobuoy	AZOI
On-scene prediction	SPAM
Tactical software	ADEPS
	TASDA

20. ABSTRACT (Continue on reverse side if necessary and identify by block number)

The Integrated Command ASW Prediction System (ICAPS) developed by the Naval Oceanographic Office reflects the impact of a changing ocean environment on tactical sensor performance. Four tactical sonobuoy programs, ADEPS, TASDA, AZOI, SPAM, were investigated to identify parameters and techniques used in the prediction of sonobuoy sensor performance. Each program uses mathematical techniques based on assumptions about the variance of figure of merit (FOM), the amount of signal excess (SE) necessary to detect a target,

DD FORM 1 JAN 73 1473 EDITION OF 1 NOV 65 IS OBSOLETE
S/N 0102-014-6601

UNCLASSIFIED 25045

SECURITY CLASSIFICATION OF THIS PAGE (When Data Entered)

and the dependence of sonobuoys contributing to a detection. Results show that in an open ocean environment these tactical programs often give different predictions because of differences in modeling assumptions.

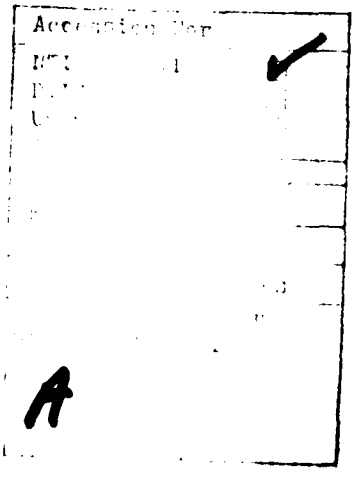

TABLE OF CONTENTS

TABLE OF CONTENTS (Cont'd)

LIST OF FIGURES

TABLE OF CONTENTS (Cont'd)

LIST OF FIGURES

LIST OF TABLES

EXECUTIVE SUMMARY

Many features of tactical programs ADEPS, TASDA, AZOI and SPAM are comparable, some are not. Each of the programs offers different advantages in user input, computation time, and output measure of effectiveness. This report describes the comparable and unique features of each program. No attempt has been made to evaluate the accuracy of output values.

In an open environment where there is little or no information about the target, the simulation programs give varying results. The data in this report show that these programs evaluate probability of detection (POD) differently for the same set of patterns and input values. By analyzing cumulative POD curves there are general relationships that can be observed between the models: (1) TASDA tends to be conservative in comparison with AZOI and SPAM at low figures of merit since it assigns a POD of 0 or 1 during a Monte Carlo trial. (2) SPAM is the most optimistic of the three at low figures of merit since it uses a cumulative time window and a weighted average to obtain POD. (3) At all frequencies and FOMs, AZOI shows small variance between probability values for each of the patterns since the calculation of POD is time independent. (4) SPAM is more conservative in its POD values at high FOMs since the cumulative time window builds detection probabilities. (5) Both AZOI and TASDA have a sharp breakoff point for FOM below which POD values decline rapidly to zero because of the probability of detection vs. range curves used in each model. Output for ADEPS was not analyzed since the number of patterns it evaluates is limited and the output is a conditional probability of detection. Differences between computer models need to be investigated further. However, further investigation should be based on a real world application of the sonobuoy programs.

I. INTRODUCTION

Deciding on a "best" pattern is not an easy task. Ideally, after input of all available data and execution of a sonobuoy program, program output provides an optimal sonobuoy pattern. There are, however, many complex decisions to make in specifying a pattern including:

where to drop each sonobuoy,

number of sonobuoys to drop in a pattern,

sonobuoy depth settings,

length of time to monitor a pattern, and

number of patterns to drop.

All of these decisions are interrelated. For example, the number of patterns depends on the size of the search area, the aircraft on-station time and the availability of other aircraft. Additionally, the number of buoys required for a particular pattern depends on sonobuoy depth settings and monitoring time for each buoy. Operational constraints and mission goals must also be considered to provide the decision maker with the best possible choices for each decision.

Four of the tactical sonobuoy computer programs which aid in these decisions were investigated to determine their functional effectiveness as an aid to planning search patterns. The programs studied were:

1. Tactical Sonobuoy Decision Aid (TASDA)

2. Algorithm for Zone Optimization and Investigation (AZOI)

3. Search Pattern Assessment Model (SPAM)

4. Automated Deployment of Sonobuoys (ADEPS)

This report provides a description of the simulation techniques used in each model in Section II. Input parameters of target intelligence, environmental data, buoy data, and aircraft characteristics are compared in Section III followed by a discussion of computer output from four scenarios in Section IV. Sonobuoy pattern definition is included in Appendix A. The propagation loss environment is described in Appendix B. Output data analyzed for this report are included in Appendix C.

II. DESCRIPTION OF COMPUTER SIMULATION MODELS

The tactical programs ADEPS, TASDA, AZOI and SPAM provide measures of effectiveness for sonobuoy patterns. ADEPS uses a mathematical technique based on the symmetric properties of certain sonobuoy fields to calculate conditional probability of detection. The other models, TASDA, AZOI and SPAM, use Monte Carlo simulation techniques. In these latter three models satistical distributions are used to simulate initial target location. If target position and speed can be estimated, a normal statistical distribution is used. Otherwise, a uniform statistical distribution is used and the target is considered equally likely to be anywhere in a search area.

Model Description for ADEPS

Two search methods are available in ADEPS (Allison, 1970). An area search routine predicts effectiveness from a latticed sonobuoy pattern with equally spaced sonobuoys. This routine includes the following possibilities for buoy placement: 4-4, 2-2-2-2, 3-3-3, 8-8, 5-6-5, 4-4-4-4, 6-6-6-6, 16-16, 11-10-11, 8-8-8-8. A barrier search routine assumes that a submarine is on a course perpendicular to a row of sonobuoys. Only the area search method is examined in this report.

In the ADEPS area search routine, symmetric characteristics of the sonobuoy field are used to divide the field into identical subareas as shown in Figure 1. A lateral range routine computes POD versus range values to give the probability that a sonobuoy will detect a target when the target is at a given range from the sonobuoy. Individual buoy

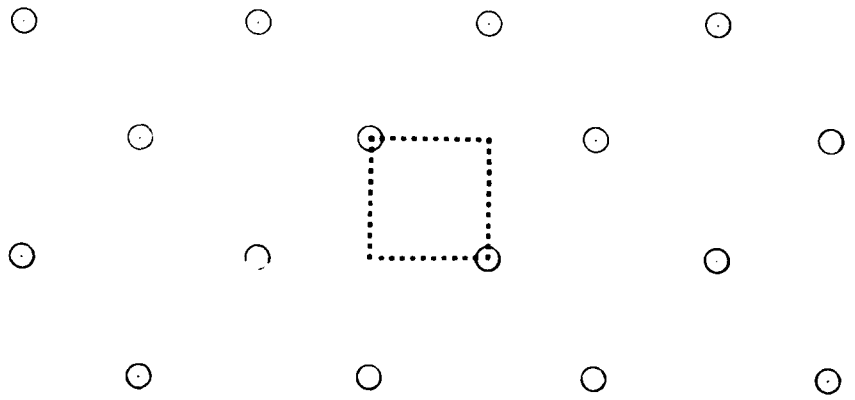

Figure 1. A Symmetrical Subsection of a 4-4-4-4 Buoy Field in ADEPS. Probability of Detection is calculated for a symmetrical subarea of the buoy field and is used as indicator of effectiveness for the entire field.

lateral range curves are combined to determine probability of detection at equally spaced points in a subarea. Conditional probability (P(t)) is computed from the sample points in a subarea where the combined probability of detection is greater than or equal to 0.5. The average distance D between consecutive detections is computed by sampling each point sequentially (as shown in Figure 5) and averaging the distances between POD $\geq$ 0.5 sample

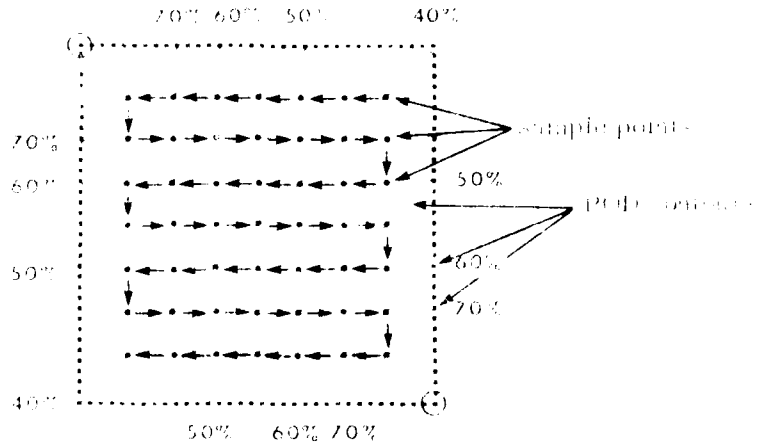

Figure 2. Example of Probability of Detection Contours in a 4-4-4-4 Buoy Field in MDPS. A detection is recorded when a point sample is within a contour greater than or equal to .5 or 50%. Arrows indicate the target track.

points. The target speed S divided by the distance D gives an average rate of occurrence R. In equation 1, P(t) is a conditional probability of detection in a subarea during time t.

$$P(t) = 1 - e^{-Rt} \quad Rt \geq 0 \qquad (1)$$

Although it is not the probability that a submarine will be detected by the entire sonobuoy field, it is a measure of the effectiveness of the field. The final product of the model is the average conditional probability of detection ($\hat{P}$) given that a target enters a symmetrical subsection of the buoy field. It is determined by averaging the values for P(t) over the on station time period.

Model Description for TASDA

TASDA operations (NADC, 1976) are divided into two functional objectives: (1) creation of a sonobuoy tactics file, and (2) application of Monte Carlo simulation to produce optimum sonobuoy field deployment for ASW threats. The tactics file is created by a geometry definition program (GEOMT). TASDA uses Monte Carlo game theory to stimulate 100 random tracks of a target through a sonobuoy field selected by GEOMT. Aircraft time on station is divided into time steps. The position along a target track is computed for each time step. If signal excess is greater than zero for two consecutive time steps, a detection is recorded. The frequency of detected target tracks to total tracks is used as an estimate of the expected and cumulative probability of detection. The total time a target is detected by one or more sonobuoys divided by the number of unbroken detection intervals is output as mean holding time. The time of first detection for each target track is recorded and the total of these times divided by the number of detected tracks is output as mean time to first detection.

Model Description for AZOI

AZOI (Birnbaum and Doray, 1975) is a tactics package which includes four subprograms LOOP, OPTI, WAIT, and GAME. Expected probability of detection (EPOD) by a sonobuoy field is computed in LOOP. OPTI determines the pattern spacing which provides maximum EPOD. WAIT calculations include cumulative probability of detection. GAME uses EPOD obtained by LOOP to estimate an optimum buoy spacing for a given pattern with several different sonobuoy characteristics, such as figure of merit (FOM) or buoy depth.

In AZOI, EPOD is estimated by Monte Carlo simulation. A lateral range curve of probability of detection versus signal excess is given by a receiver operating curve (ROC) which is determined from a probability of false alarm of 10^{-4} and a specific spectrum analyzer set for a five-minute integration time. Signal excess versus range is determined from the FOM and the propagation loss curve. The two tables of values are combined to produce POD versus range values. Range from a sonobuoy is determined from a statistical target distribution. Detection probability, $P_{i,j}$, for the jth sonobuoy at range r_i from the target is found from POD versus range values (Figure 3). In equation 2, $Z(X_i, Y_i)$ is the expected value for detection when the target is at a particular position (X_i, Y_i). The subscript i is an index used to number target positions from 1 to N.

$$Z(X_i,Y_i) = 1 - (1 - P_{i,1})(1 - P_{i,2})(1 - P_{i,3}) \ldots (1 - P_{i,j}) \ldots (1 - P_{i,n}) \qquad (2)$$

n = number of sonobuoys

EPOD for a pattern is calculated by taking a random sample of N target positions. Probability is calculated for each position i as in equation 2. The probabilities are summed and divided by N to calculate EPOD in equation 3.

$$EPOD = \left[Z(X_1,Y_1) + Z(X_2,Y_2) + Z(X_3,Y_3) + \ldots \ldots Z(X_N,Y_N) \right] / N \qquad (3)$$

N = number of target positions

Cumulative probability of detection (CPOD) is also estimated by Monte Carlo simulation. The mathematical function used in the computation of CPOD is binomial and gives the probability of at least one detection in N trials. A time t_i is chosen randomly from a time interval I using a random number generator. The interval I is defined by equation 4.

$$I = T - T_f \qquad \begin{array}{l} T = \text{aircraft time late} \\ T_f = \text{time when sonobuoys can no longer be monitored} \end{array} \qquad (4)$$

An uncertainty about the target position at time t_i is calculated from a normal statistical distribution. Detection probability at a position is calculated as in equation 2. The maximum expected value for detection by sonobuoy j (Figure 1) over N target tracks at each time t_i is summed to yield cumulative probability of detection in equation 5.

$$CPOD(t_i) = 1 - (1 - P^*_{i,1})(1 - P^*_{i,2})(1 - P^*_{i,3}) \ldots (1 - P^*_{i,j}) \ldots (1 - P^*_{i,n}) \qquad (5)$$

$P^*_{i,j}$ = maximum expected POD at time t_i by sonobuoy j

n = number of sonobuoys

The CPOD in equation 5 is an estimate for the lower limit of cumulative probability of detection at time t. A large number of target tracks must be generated to obtain an estimate of CPOD with a small variance. The number of simulations required depends on the signal excess and the desired accuracy of output data. The probability of detecting a target that has not yet been detected is calculated from CPOD using Bayes theorem of probability.

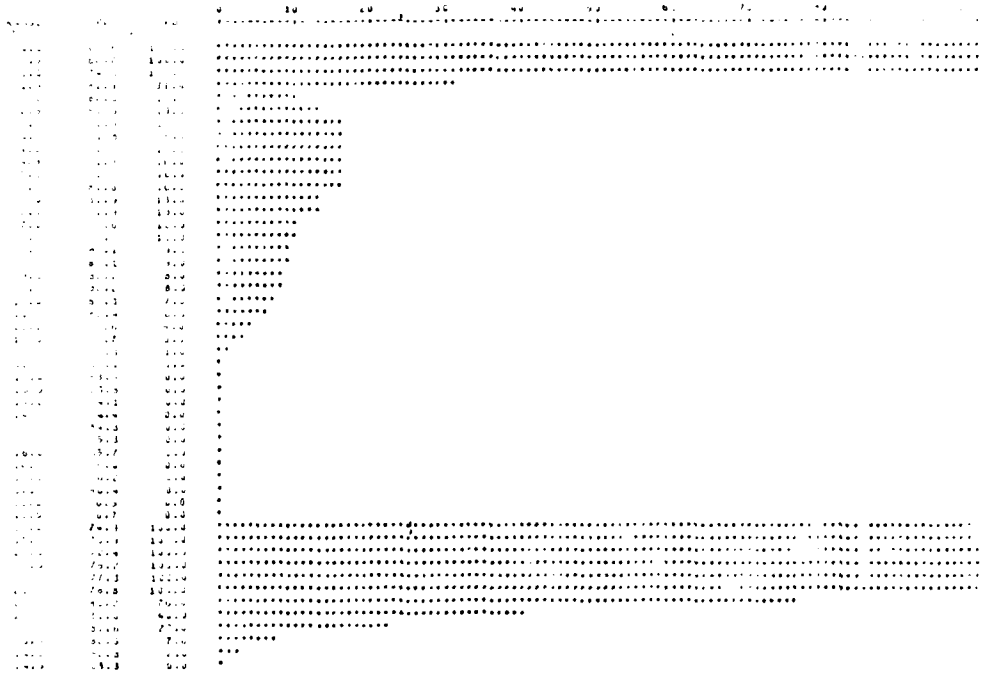

Figure 3. A Graph of POD vs. Range Values Computed in the AZOI Tactics Package.

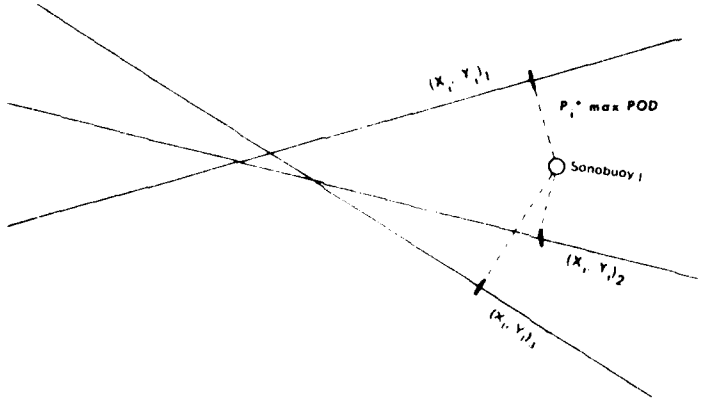

Figure 4. Maximum POD $P_{i,j}^*$ of 3 Target Tracks at Time t_i for a Sonobuoy j in AZOI.

Model Description for SPAM

The SPAM program computes CPOD by Monte Carlo simulation (Marin, 1976). The range of the target from a sonobuoy is found by a stochastic process. Signal excess (SE) at time t is found from a normal distribution with mean SE(r) and a standard deviation of 6, 8, 10, or 12 dB. The probability that the signal excess is greater than zero at range r is given by equation 6 (Marin, 1976).

$$P_j(SE(r_i) \quad 0) = \frac{1}{\sqrt{2\pi}} \int e^{-\frac{(x - SE(r_j))}{2}} dx \qquad (6)$$

$$= \text{standard deviation of signal excess}$$

To use equation 6 in a simulation model, it is necessary to introduce a time element. The expression $P_j(t_i)$ is introduced as the probability that a target is not detected at range r_i during time t_i. The following equations are assumed for the time element.

$$P_j(t_i) = \lambda_i t_i + 0(t_i) \quad \text{where } \lim_{t \to 0} 0(t)/t = 0 \qquad (7a)$$

$$P_j(t_i) + M_j(t_i) = 1 \quad \text{where } M_i(0) = 1 \qquad (7b)$$

$$M_j(t_i + t) = M_j(t_i) * M_j(t) \qquad (7c)$$

Equation 7a states that the probability of detection $P_j(t_i)$ is proportional to some constant λ_i plus some higher order terms. The higher order terms in equation 7a can be neglected for a small time period t. Equation 7b states that the target is either detected or not detected where the probability $M_i(0)$ of no detection at any range with no time elapsed at that range is one. Equation 7c assumes that no detection at time t and no detection at time $t+\Delta t$ are independent events. The assumptions lead to an exponential statistical distribution for $P_j(t_i)$. The SPAM program uses the equation (Marin, 1975)

$$P_j(t_i) = 1 - e^{-\lambda_i t} \quad \text{for } t \quad 0 \qquad (8)$$

in a simulation technique called the cumulative time window (CTW). The length of time t_0 necessary for a sonobuoy j to detect a target and the length time t_1 between time steps are input. Probabilities $P_j(t_i)$ are computed and compared with random numbers to determine when a detection occurs. A program trial ends either when a detection occurs or when the aircraft on station time expires. The upper limit for cumulative probability of detection is obtained by combining single buoy probabilities independently in equation 9.

$$CPOD_{max}(t_i) = 1 - [1 - P(t_i)] \ldots [1 - P_j(t_i)] \ldots [1 - P_n(t_i)] \qquad (9)$$

n = number of sonobuoys

A lower limit for probability of detection at time t_i is obtained assuming complete dependence as in equation 10.

$$CPOD_{min} = MAX(P_j(t_i)) \qquad j=1, \qquad (10)$$

n = number of sonobuoys

SPAM outputs cumulative probability slightly less than halfway between the two extremes using equation 11.

$$CPOD = .45\ (CPOD_{max} + CPOD_{min}) + CPOD_{min} \qquad (11)$$

Summary of Model Descriptions

Each of the models calculates probability of detection at some time t_i in order to arrive at an estimate for EPOD. ADEPS calculates the average conditional probability $\hat{P}$ in a symmetrical subarea of a buoy pattern. TASDA computes probability of detection by one or more buoys (PDI) using Monte Carlo simulation of 100 target tracks and a detect (POD = 1) or no detect (POD = 0) analysis for each track. AZOI uses a binomial distribution function to calculate EPOD where a value along a time track is chosen randomly. SPAM uses Monte Carlo simulation and averages $P_j(t_i)$ (previously defined) obtained by assuming dependence of sonobuoys with $P_j(t_i)$ obtained by assuming independence of sonobuoys.

Each of the models estimates cumulative probability of detection. ADEPS uses an exponential expression to estimate CPOD. TASDA uses a detect-no detect Monte Carlo mathematical technique. AZOI uses some of the EPOD calculations to obtain an estimate for the lower limit of CPOD. In the uniform case CPOD is time independent and is equal to EPOD. SPAM uses a cumulative time window (CTW) defined by t_0 and t_1 to calculate CPOD.

III. SCENARIO DEFINITION

Five sonobuoy patterns employed by ASW tacticians were chosen for data analysis in scenario 1: the circle (ellipse in the normal case), 4-4-4-4, chevron (chevron skew in the normal case), 5-6-5, and brushtac patterns. Their configurations are defined in Appendix A. The same input for target intelligence, environmental data, and aircraft characteristics were used so as to evaluate the effectiveness of each pattern. Output was generated for one-half hour, one hour, and four hours of flight time in all cases preceding the aircraft's arrival on-station. The aircraft remained on-station four hours in all cases for scenario 1. The circle, ellipse, 4-4-4-4 and chevron skew patterns were evaluated in scenario 2. The on-station time was extended from four to 16 hours in the second scenario and output was generated for one hour time late. In scenario 3, the circle, ellipse, 4-4-4-4 and chevron skew patterns were searched in quarters by four planes with one hour time late and four hours on station. Scenario 4 used the same target data, buoy data, and aircraft data input as scenario 3, however, environmental input was changed for other comparison purposes.

Scenarios 1-3 were based on the following environmental input. An XBT temperature profile to 750 meters recorded 6 July 1971 in the Pacific Ocean at latitude 35° 38' North and longitude 125° 59' West was input into the Integrated Command ASW Prediction System (ICAPS) PROFGEN computer program. This program merged the observed depth-temperature pairs with a deep historical profile to yield a total temperature profile with bottom depth at 4000 meters. The program then calculated a sound speed profile from the total temperature profile and historical salinity values. The sound speed profile, which exhibited a depth excess indicative of convergence zone environment (Figure 5), was input into the ICAPS Fast Asymptotic Coherent Transmission (FACT) program to determine acoustic propagation loss. By varying the target depths, receiver depths, and detection frequencies inserted into the FACT program nine propagation loss (PL) curves were generated. These curves appear in Appendix B.

The environmental input for scenario 4 was a Gulf Stream profile from latitude 39° 36' North longitude 70° 29' West recorded 17 November 1969. It was merged with ICAPS deep history data to produce a total profile with bottom depth 2400 meters (Figure 6). An Atlantic slope water profile at latitude 39° 35' North, longitude 71° 30' West recorded 18 November 1969 was merged to produce a total profile with the same bottom depth (Figure 7). Two different profiles were used in scenario 4 in order to show the effect of varying the environment on the tactical programs. Since scenario 4 uses environmental input which is different from the other 3 scenarios, its output does not directly compare with output from the first three scenarios.

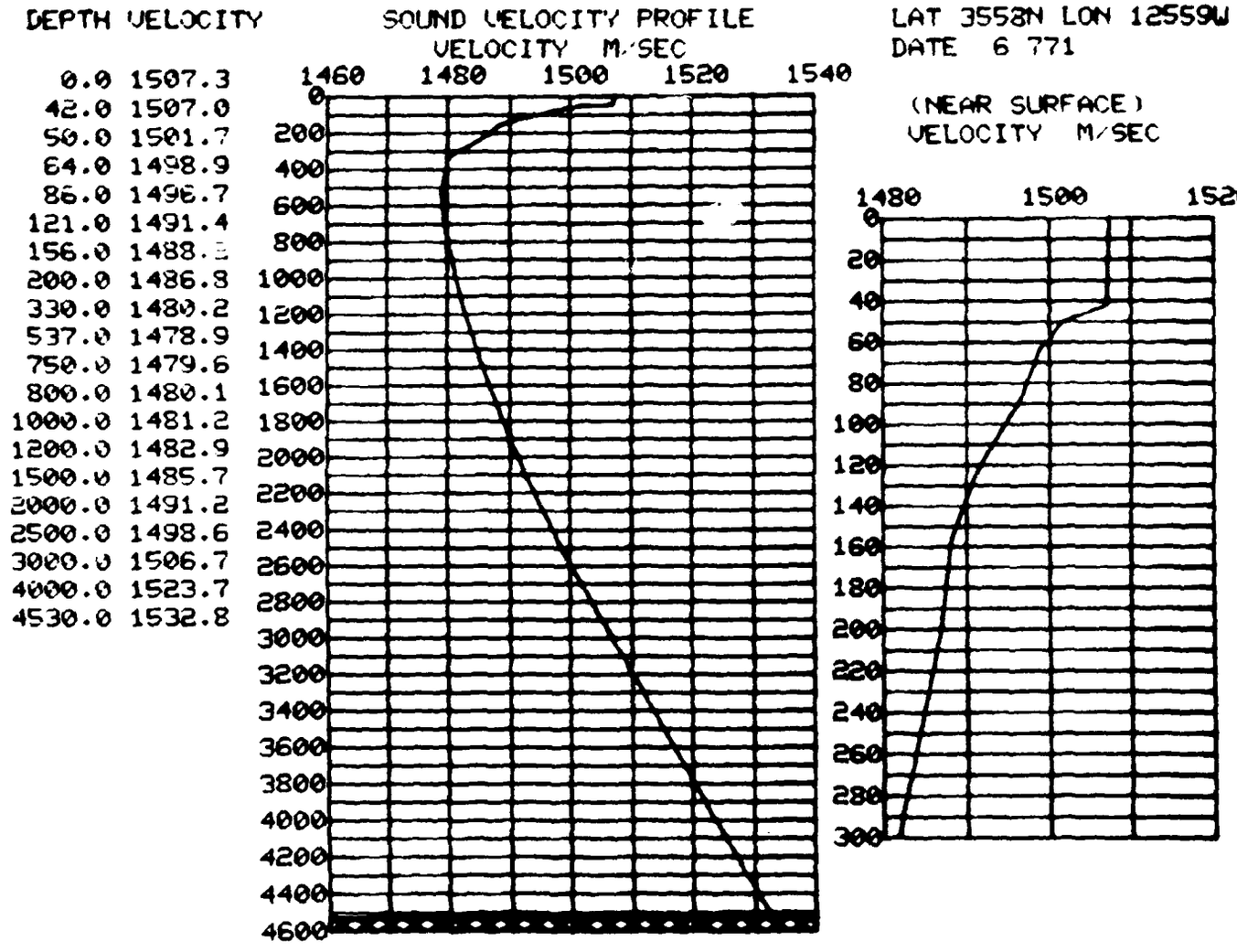

Figure 5. Pacific sound speed profile used to generate propagation loss curves in scenarios 1, 2, and 3. (The depth excess in sound speed from 3100 m to 4530 m indicates strong convergence zone environment).

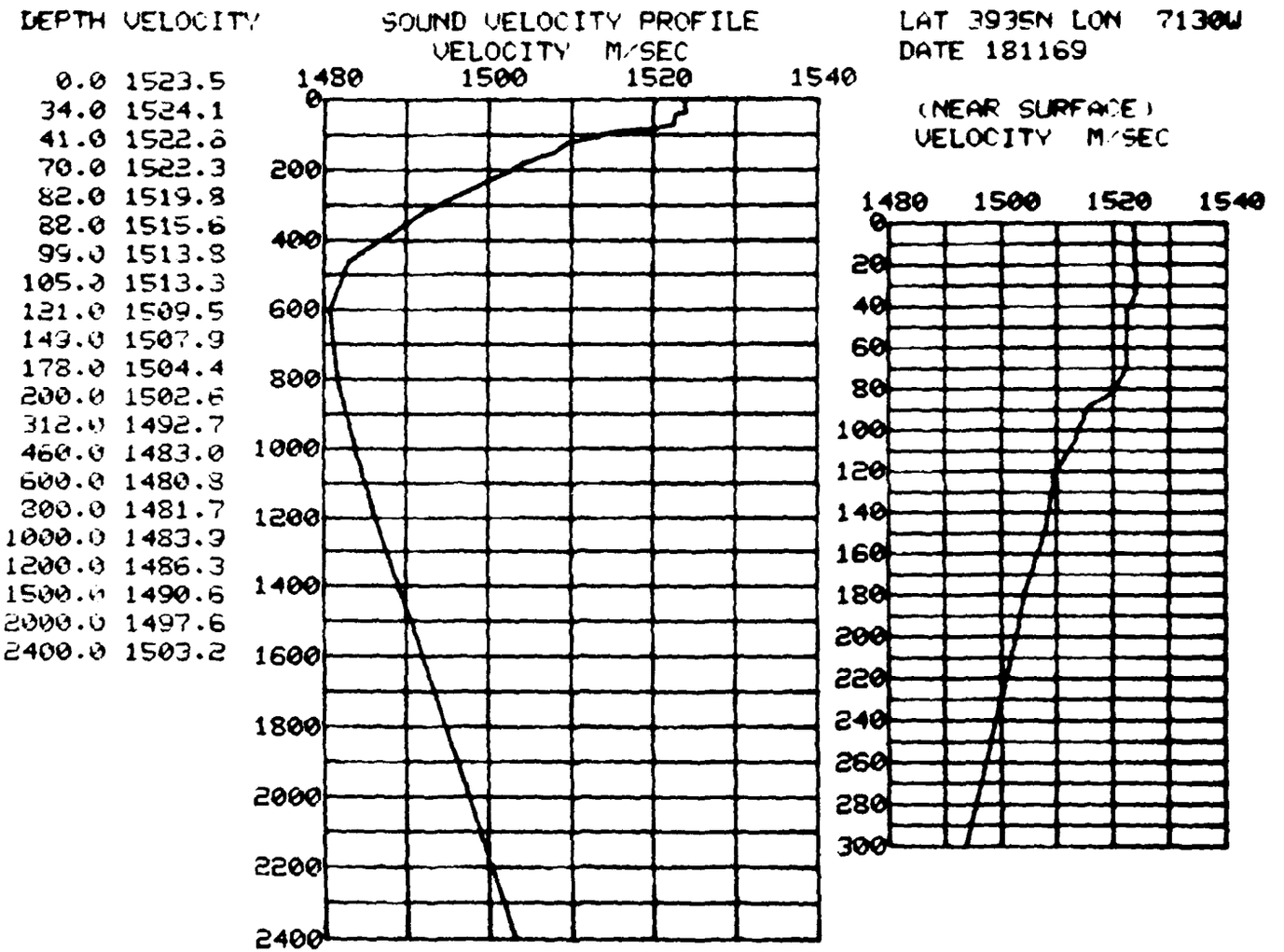

Figure 6. Atlantic Gulf Stream sound speed profile used to generate propagation loss curves for scenario 4. (The predominant mode of sound propagation is by direct path.)

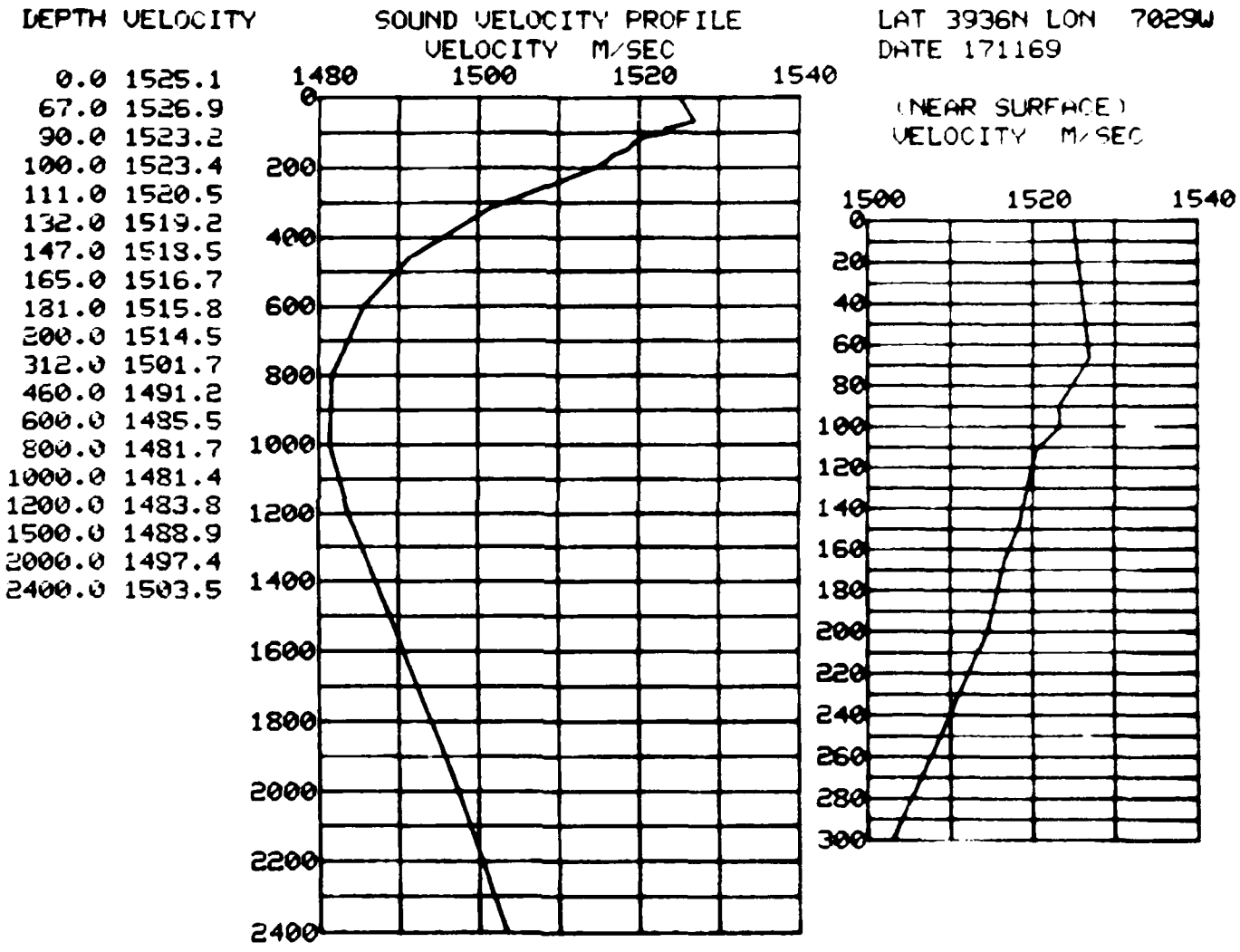

Figure 7. Atlantic slope water sound speed profile used to generate propagation loss curves for scenario 4. (The predominant mode of sound propagation is by direct path).

IV. PROCESSING REQUIREMENTS

All four tactical sonobuoy computer programs require buoy input, target input, and environmental input. ADEPS does not require aircraft input. Some input values are preset in each program so that the user need not specify a long list of values. Data processing inputs for the four scenarios considered in section V are given in Table 1.

Buoy Input

Buoy input which define sonobuoy patterns for evaluation is shown in Table 2. In ADEPS the total number of sonobuoys input must be a multiple of eight. Area dimensions are required and are used to calculate a buoy spacing. The buoys are equally spaced to cover an entire area. ADEPS is the most limited program in terms of buoy input, but the symmetric patterns allow rapid processing. The only geometries available in the ADEPS preset pattern package, applicable for this study, were the 4-4-4-4 pattern and the 5-6-5 pattern with a uniform target distribution.

TASDA requires the number of sonobuoys, buoy position assignment, the number of different spacings, and buoy spacing limits as input. Patterns are input using a sonobuoy position planner chart. Optionally, the user may input buoy positions in x-y coordinates to define a pattern. GEOMT is a preprocessor program for TASDA and creates a tactics file of up to 20 sonobuoy patterns with as many as 64 buoys in each pattern. This preprocessing

Table 1. Data Processing Requirements

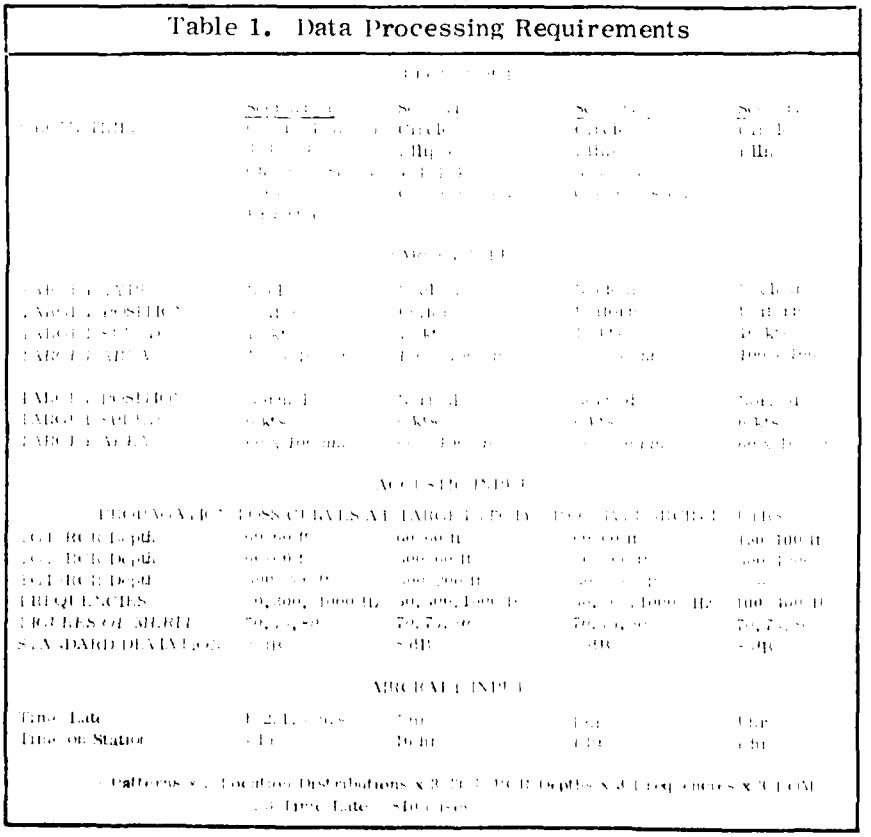

feature combines 810 cases shown in Table 1 into 162 runs for processing. Run time and buoy input time are reduced since buoy positions are simply recalled from GEOMT rather than routinely entered.

Table 2. Buoy Input

	ADEPS	TASDA	AZOI	SPAM
Coordinates		X	X	X
Spacing	X	X	X	X
Buoy Transformation			X	X
Preset Patterns	X			
Geometries		X		
Ambient Noise SDev		X		

In AZOI a pattern geometry is defined by specifying a set of x-y coordinates for each buoy. A factor for converting relative distance to nautical miles must be specified. Four types of transformations may change the basic pattern: x-spacing expansion, y-spacing expansion, pattern shift along the x-axis, and rotation of the pattern about the origin.

In SPAM the user specifies the number of sonobuoys and the x-y coordinates in nautical miles for each buoy. Buoy coordinates are input in the order in which the buoys are deployed. As the buoys are dropped, the user-specified radio-frequency (RF) range is used to determine if a sonobuoy can be monitored. After the pattern is complete, SPAM simulates monitoring constraints. The user specifies the average number of buoys that an aircraft can monitor and the monitoring time. Using the value for the average number of buoys, the program randomly selects buoys from the pattern and only these buoys will be used to determine if a detection occurs.

Target Input

There are twenty target inputs as shown in Table 3. In ADEPS only four of the inputs are applicable. Target speed is input. The area search option corresponds to an evenly spaced position input where the target remains in the search area at fixed positions. The barrier search option corresponds to the univariate normal input where the target is assumed to progress towards a barrier with a target track perpendicular to the barrier. Only the evenly spaced input is used in this study to search an area with 5-6-5 and 4-4-4-4 patterns.

Twelve of the twenty target inputs apply to TASDA. Target speed is required. The target type must be specified as nuclear or conventional, holding or transiting. A nuclear holding target was used for this study (see Table 1). Target location may be described in two ways:

1. A uniform time-dependent density function assumes that the target density is random over a designated rectangle (Figure 8).

2. A Bessel normal distribution function is generated from an initial bivariate normal density function that is expanded at a rate equal to input target speed (Figure 9).

Both target location functions were used in this study.

Table 3. Target Input

Target Movement	ADEPS	TASDA	AZOI	SPAM
Course		X		X
Course Standard Deviation				X
Course Limits		X		
Speed	X	X	X	X
Speed Standard Deviation			X	X
Velocity Vector			X	
Conventional		X		
Nuclear		X		
Holding		X		
Transiting		X		
Distance Traveled		X		
Snorkel Cycle		X		
Target Location Standard Deviation	X	X		
Initial Target Location Density Functions				
Evenly spaced positions	X			
Uniform Time-dependent		X		
Uniform Time-independent			X	X
Univariate normal	X			X
Bessel normal		X	X	
Bivariate normal			X	X
Time-dependent bivariate normal			X	

AZOI uses seven of twenty target inputs. Target speed and speed standard deviation are input directly or in terms of a speed covariance matrix. The following four target location density functions are used to predict initial target location for Monte Carlo simulation:

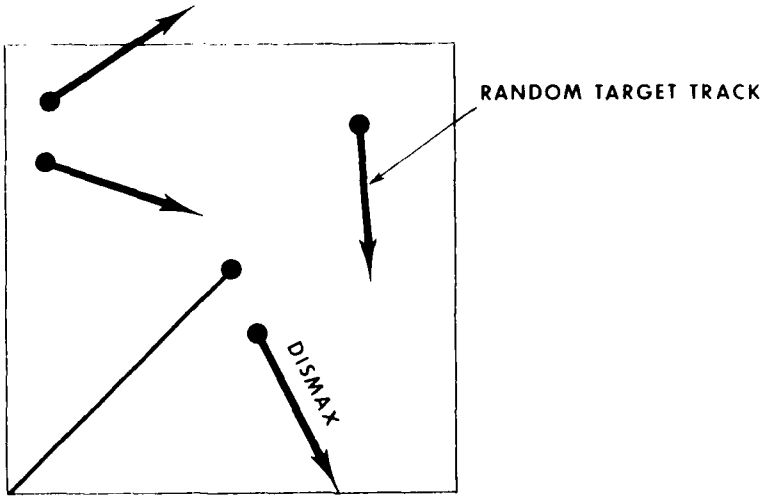

Figure 8. Uniformly Distributed Initial Target Area in TASDA. The target location is random over a designated area. The same type of target area definition is available in AZOI and SPAM. However, the statistical distribution is time-dependent for TASDA.

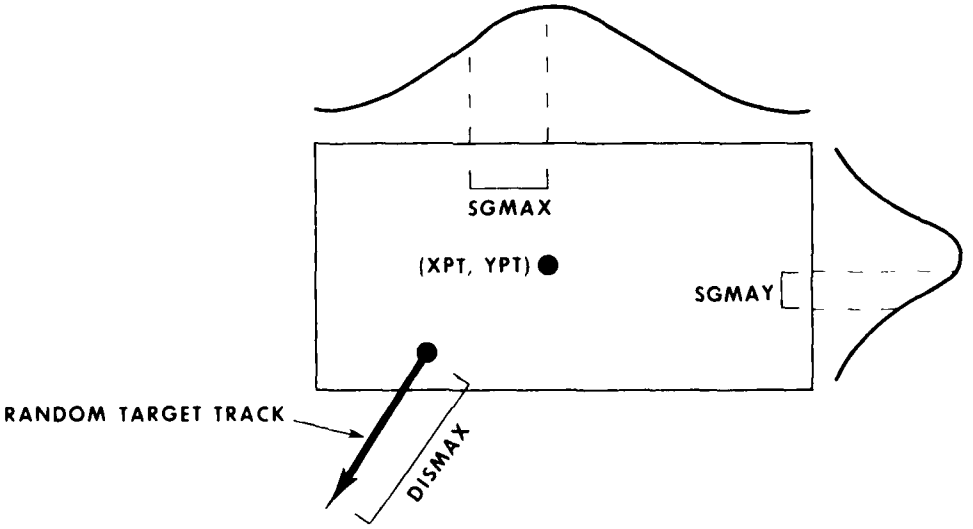

Figure 9. Normally Distributed Initial Target Area in TASDA. The initial target location is normally distributed around (XPT, YPT) with standard deviation SGMAX in the x-direction and SGMAY in the y direction. The same type of area definition is available in AZOI and SPAM. However, the statistical distribution is bivariate normal for SPAM.

1. A uniform time-independent density function assumes that target density is constant over a designated area.

2. A Bessel normal density function is generated from an initial bivariate normal density function and expands at a rate equal to the best estimate of target velocity.

3. A time-dependent bivariate normal density function predicts a target position when target tracking has been successful. This function describes a target being tracked when it is imperative to re-establish target contact.

4. A bivariate normal distribution function assumes that a target is normally distributed in an area generated from a single DIFAR buoy fix, a SOSUS contact, or a radar contact. This distribution does not expand with time.

The first and second functions were used for uniform and normal cases in this study (Table 1).

SPAM uses seven of the twenty inputs listed in Table 3. Required input is speed, speed standard deviation, course and course standard deviation. Target location can be assigned using three distribution functions:

1. A uniform time-independent distribution function with the property that a target is equally likely to be at any point within a bearing box of length L and half-width H.

2. A bivariate normal distribution function which has a user specified mean and standard deviation.

3. A univariate normal distribution function which has a normal distribution in an x direction and a uniform distribution in a y direction.

Functions 1 and 2 were used for data analysis in this study.

Acoustic Input

Acoustic input for each program is listed in Table 4. The acoustic input, source level (SL), ambient noise (AN), and recognition differential (RD) are used to determine FOM as in equation 12.

$$FOM = SL - AN - RD \qquad (12)$$

Probability of detection is defined to be 0.5 when signal excess (SE) in equation 13 is zero for propagation loss (PL) at range R.

$$SE = FOM - PL(R) \qquad (13)$$

In each program a probability curve is used to assign probability values to values of signal excess. When signal excess is greater than zero, the probability values will be greater than 0.5. When signal excess is less than zero probability values will be less than 0.5.

Table 4. Acoustic Input

	ADEPS	TASDA	AZOI	SPAM
Prop Loss (PL)	X	X	X	X
Source Level	X			
Ambient Noise	X			
Recognition Differential	X			
Figure of Merit		X	X	X
Multiple FOM		X	X	X
ROC Curve			X	
Multiple PL		X	X	X
Convergence Zones		X	X	

ADEPS considers propagation loss (PL) curves, source level (SL), ambient noise (AN), and recognition differential (RD), but ADEPS does not have a provision for time late. As a result ADEPS could only be applied for 54 of the 810 possible cases. There is no provision for multiple frequencies or multiple FOMs and a separate run was required for each case. In order to reduce the number of runs, an FOM of 75 was selected with a frequency of 300 Hz. Eighteen computer runs were processed for scenario 1.

The TASDA program can accept up to three propagation loss curves and up to four FOMs. These two features reduced the number of runs required from 162 to 18. The user may input convergence zone ranges and widths instead of propagation loss curves.

In AZOI, a receiver operating characteristic (ROC) curve is required input. This curve gives probability values as a function of signal excess. Other inputs are a table of propagation loss versus range and a figure of merit. Two subprograms of AZOI were modified in May 1978 to process multiple FOMs, multiple propagation loss curves, and multiple patterns. The number of required data sets for input were thereby reduced from 810 to eight.

SPAM accepts one propagation loss file with frequency and receiver-source (RCR-SRC) depth identification numbers. Any number of propagation loss curves may be input to the file with any number of frequencies. The program automatically searches through the input propagation loss file for the appropriate propagation loss curve. The main program SPAM was modified in September 1977 for multiple FOM, multiple time late, and multiple propagation loss input. The number of executions was reduced from 810 to eight. A propagation loss curve is classified as shallow-shallow (S-S) for a shallow target and receiver, deep-deep (D-D) for a deep target and receiver, or shallow-deep (S-D) for either a shallow target or receiver on output.

Aircraft Input

ADEPS does not consider aircraft parameters except for monitor degradation as shown in Table 5. For TASDA, the flight path is described only to the extent of specifying the elapsed time before arrival on station. The radio frequency (RF) range is the maximum allowable distance between the aircraft and a sonobuoy which permits radio reception. For TASDA, the position of the aircraft is fixed at the center of the field for the simulation. AZOI uses time late, aircraft velocity, and on-station time to calculate CPOD. SPAM includes time late and time on station as well as aircraft ground speed. The user specified ground speed in SPAM determines the time at which each buoy comes up. Only those buoys within a user-specified RF range are monitored. After all buoys are in the water, the user can specify a sonobuoy monitoring scheme that reflects RF constraints.

Table 5. Aircraft Input

	ADEPS	TASDA	AZOI	SPAM
RF Range		X		X
Time Late		X	X	X
Time on Station			X	X
Monitoring Sequence				X
Ground Speed				X
Monitor Degradation	X			

Search Model Input

Each of the programs uses different mathematical formulations to describe a tactical situation in an open ocean environment. The formulations are based on assumptions about the variance of the FOM, the amount of signal excess necessary to detect a target, and the dependence (or independence) of sonobuoys collectively contributing to a detection.

ADEPS has preset patterns. The preset package cannot be modified. TASDA also has a preset pattern package, but the package can be modified. AZOI and SPAM have no preset pattern files. ADEPS has a normal initial target location distribution. TASDA, AZOI and SPAM all have options for uniform target location distributions and normal location distributions.

All models input a propagation loss curve. TASDA may input propagation loss curves at three different depths. Therefore, one sonobuoy pattern may have sonobuoys placed at different depths. AZOI inputs a receiver operating characteristic (ROC) curve which assigns a probability to values of SE. In ADEPS and SPAM this curve has a normal density distribution with probability equal to 0.5 at the mean of the normal distribution. In TASDA cumulative probability is determined from a Rician density Distribution. TASDA assumes all sonobuoys are activated at the same time. In SPAM, the user specified ground speed determines the time each buoy comes up.

V. ANALYSIS OF RESULTS

Two types of program output are compared by this study: expected probability of detection (EPOD) and cumulative probability of detection (CPOD). EPOD follows the statistical definitions for expectation. CPOD is computed from a probability density function which follows the statistical definition of a density function. Each program uses different assumptions to arrive at EPOD and different density functions to calculate CPOD. Since methods of calculations are different in each program the output have different numerical values. The analysis in this section examines mathematical techniques to explain the CPOD and EPOD numerical output.

A list of all program output is given in Table 6. Although CPOD and EPOD parameters in Table 6 are listed for TASDA, AZOI, and SPAM, numerical output for these measures of pattern effectiveness are not the same. The output values were analyzed in reference to four scenarios. Three target-receiver depth combinations, shallow-shallow (S-S), shallow-deep (S-D), and deep-deep (D-D), were used to generate propagation loss curves for the first 3 scenarios. Probability of detection was predicted for three FOMs and for a low frequency range, middle frequency range, and a high frequency range in scenario 1, 2 and 3. Scenario 4 uses two target-receiver depth combinations, two frequencies and one FOM.

Scenario 1

Expected probability of detection was calculated for five patterns with a uniform and normal initial target location distribution. Time late was not a factor in the uniform case because that parameter did not change the initial target location distribution for AZOI and SPAM. Therefore, values for 1 and 4 hrs time late have been omitted and only values for 30 min time late appear in Appendix C. Cumulative probability of detection was analyzed using the method shown in Figure C-1. Using this method cumulative probability of detection was converted to a single eventual probability of detection value for comparison purposes. Both the eventual POD values and the original CPOD curves appear in Appendix C for TASDA, AZOI, and SPAM. The 18 CPOD curves that were generated for ADEPS are shown in Figure 10 with the corresponding curves for TASDA, AZOI and SPAM. Since ADEPS could process only two of the patterns the results were not analyzed for inclusion in Table 7. However, the relationship between ADEPS output and output from the other

three models can be deduced from Figure 10. One characteristic of the ADEPS curves is that they always rise to 100% POD.

Table 6. Measures of Effectiveness

ADEPS	TASDA	AZOI	SPAM	PROGRAM OUTPUT
	X	X	X	CPOD
	X	X	X	EPOD
	X			PD2
	X			PD3
	X			MHT1
	X			MHT2
	X			MHT3
	X			MHFD
X				$\hat{P}$
X				P(t)
		X		SIGMA
		X		P(DE/NDT)

CPOD	cumulative probability as a function of time on station
EPOD	expected probability of detection on one or more sonobuoys
PD2	probability of detection on two or more sonobuoys
PD3	probability of detection on three or more sonobuoys
MHT1	mean holding time on one or more sonobuoys
MHT2	mean holding time on two or more sonobuoys
MHT3	mean holding time on three or more sonobuoys
MTFD	mean time to first detection
$\hat{P}$	average conditional probability in a section where the submarine is assumed to be a random target
P(t)	cumulative probability that a submarine has entered part of a buoy field where signal excess SE is greater than zero
SIGMA	standard deviation of POD
P(DE/NDT)	probability that a target will be detected given that it has not been detected in the past

Uniform Case

EPOD values for the uniform case were averaged over three FOMs and three frequencies and the averages are present in Table 7. For a shallow target and receiver, TASDA shows the 1-1-1-1 pattern as most effective over the frequencies and FOMs with a value of 51.9% EPOD. For the shallow-deep target-receiver combination, TASDA shows the chevron pattern as most effective. For a deep-deep target receiver propagation loss curve, TASDA selected the chevron pattern, AZOI selected the circle pattern and SPAM

+ ADEP

· TASDA

△ AZOI

⊙ SPAM

5-6-5 PATTERN

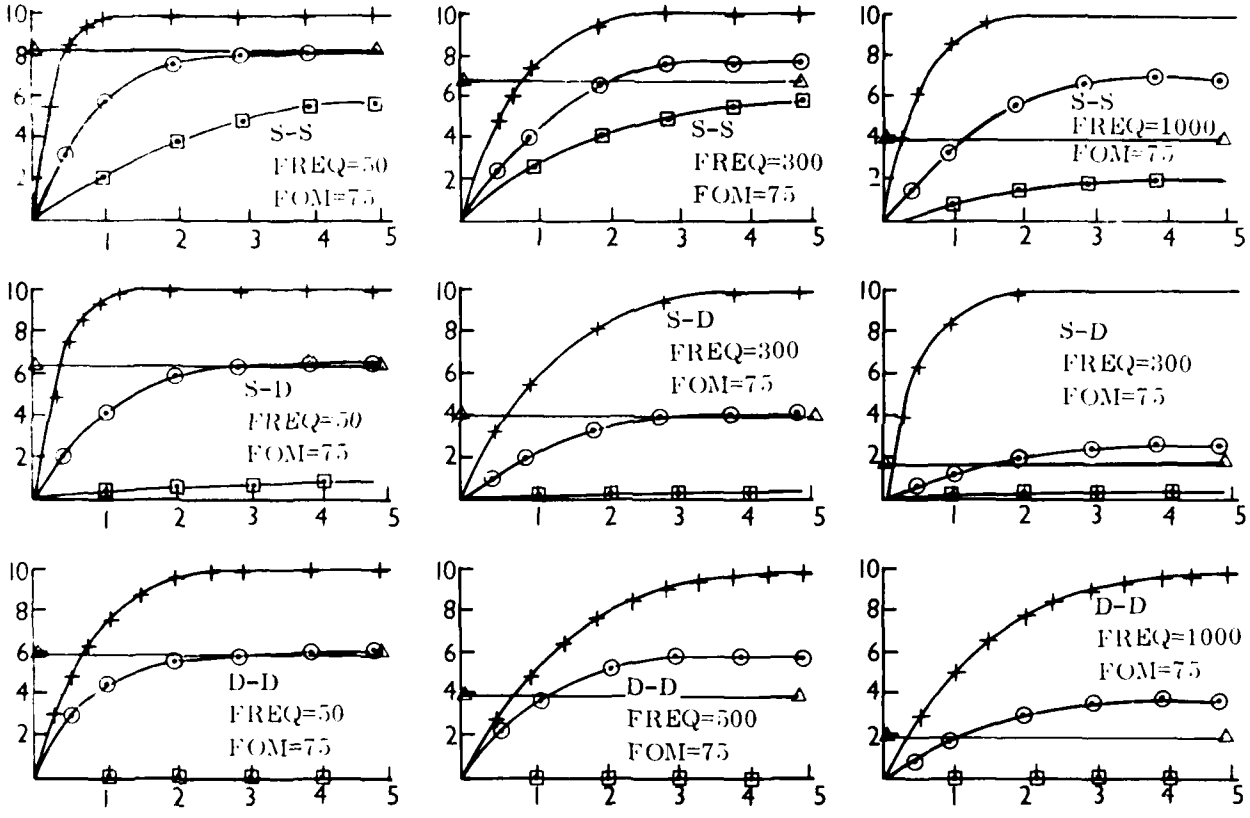

Figure 10. Probability of Detection versus Elapsed Time on Station for Scenario 1 with a Uniform Target Location Distribution.

· ADEP

· TASDA

△ AZOI

⊙ SPAM

4-4-4-4 PATTERN

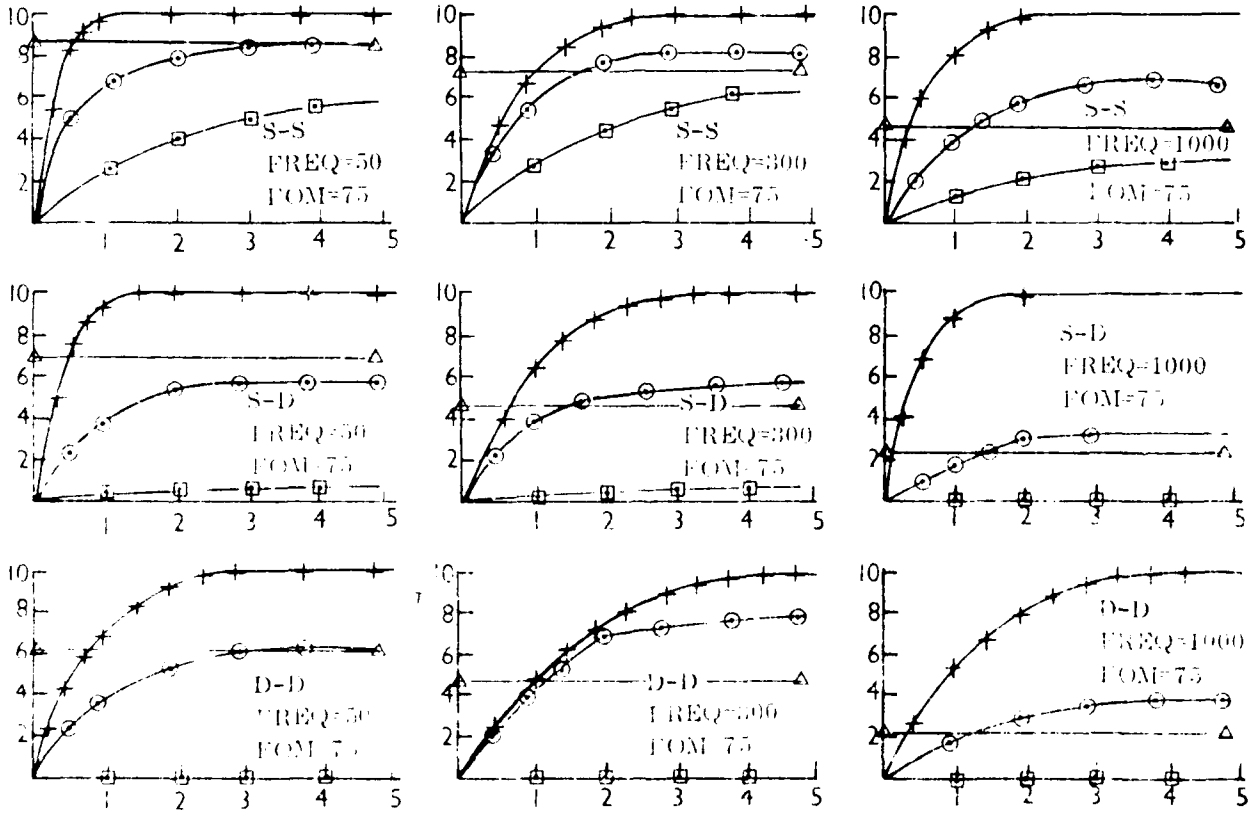

Figure 10. Probability of Detection versus Elapsed Time on Station for Scenario 1 with a Uniform Target Location Distribution (continued).

Table 7. Percent Probability of Detection for Scenario I

	[illegible]			
	8-8	8-10	[illegible]	Average
ELLIPSE (FASDA)	66.2	29.9	21.2	38.8
ELLIPSE (AZOD)	96.8	84.6	94.0	91.8
ELLIPSE (SPAM)	79.9	64.1	57.4	67.1
BRUSHTAC	65.3	28.7	19.7	37.9
BRUSHTAC	97.1	86.7	94.4	92.7
BRUSHTAC	76.2	56.3	55.7	62.7
4-4-4-4	65.7	29.1	20.0	38.3
4-4-4-4	[illegible]	86.2	94.3	92.2
4-4-4-4	[illegible]	[illegible]	58.2	64.3
5-6-5	[illegible]	[illegible]	21.9	[illegible]
5-6-5	95.4	80.3	93.0	[illegible]
5-6-5	71.9	55.8	56.0	61.2
CHEVRON SKEW	66.1	27.4	22.2	38.6
CHEVRON SKEW	97.0	85.6	94.3	92.4
CHEVRON SKEW	79.8	60.7	60.0	[illegible]

	[illegible]			
	8-8	8-10	[illegible]	Average
ELLIPSE	57.1	23.0	16.9	[illegible]
ELLIPSE	81.7	95.8	94.0	[illegible]
ELLIPSE	75.2	61.4	54.2	63.6
BRUSHTAC	51.1	17.6	12.0	26.9
BRUSHTAC	81.6	95.2	93.9	[illegible]
BRUSHTAC	75.1	55.6	54.8	61.8
4-4-4-4	58.1	21.3	16.6	32.0
4-4-4-4	81.6	97.4	93.9	90.3
4-4-4-4	72.0	53.7	56.9	60.9
5-6-5	56.7	21.8	14.4	31.0
5-6-5	76.8	93.2	90.7	86.9
5-6-5	69.6	53.2	54.3	59.0
CHEVRON SKEW	56.7	20.9	16.6	31.4
CHEVRON SKEW	82.3	95.6	94.7	90.9
CHEVRON SKEW	74.2	57.8	57.6	63.2

selected the 4-4-4-4 pattern as most effective. Note that there is very little agreement in pattern selection. This is because of the different modeling in each program. Since the patterns were defined at a near optimum sonobuoy spacing, the models give about the same probability averages for each pattern they evaluate. However, the difference in average probability of detection from one model to another is very noticeable. Differences in model output is as much as 34% predicting the performance of the same pattern. Since there was not much difference in EPOD between the five patterns using one model, the number of patterns considered was reduced to two. Only the circle and 4-4-4-4 pattern were processed in subsequent scenarios.

Normal Case

Time late is a factor for EPOD in the normal case. The time it takes an aircraft to arrive on station changes the distribution for initial target location. At time late equal zero TASDA, AZOI, and SPAM all have the same normal target location distribution as shown in Figure 11. At 30 min time late, the normal distribution spreads out as shown in Figure 12 and Figure 13. After 30 min the probability that the target is at the original estimated position is smaller. Since the target location distribution does change, the eventual probability of detection values are different for each time late. These values are given in Appendix D under Normal Case. In this study normal case output CPOD values were averaged over three FOMs and three frequencies and over each time late. Table 7 shows averaged values. The three sets of output show that AZOI is consistently the most optimistic of the three programs. This is a change from the uniform case where SPAM was the most optimistic. As in the uniform case, the averaged values were very close for different patterns using the same model. The ellipse and chevron skew patterns were processed subsequent scenarios.

Scenario 2

Cumulative probability of detection was calculated for two patterns with a uniform and normal initial target location distribution. The first flight arrives on station after one hour time late and remains on station for four hours. A standard deviation in target speed is introduced. The last three flights arrive on station with no time late and remain on station for four hours. This scenario is simulated by a computer run with one hour time late and 16 hours on station.

The values in Table 8 were obtained by examining CPOD curves and attaching a numerical value to each curve. In order to arrive at a numerical value the slope of the curve and

Table 8
Percent Probability of Detection for Scenario 2

UNIFORM CASE			
	S-S	S-D	D-D
[illegible]	[illegible]	[illegible]	[illegible]
[illegible]	[illegible]	[illegible]	[illegible]
[illegible]	[illegible]	[illegible]	[illegible]
[illegible]	[illegible]	[illegible]	[illegible]
[illegible]	[illegible]	[illegible]	[illegible]
[illegible]	[illegible]	[illegible]	[illegible]

NORMAL CASE			
	S-S	S-D	D-D
[illegible]	[illegible]	[illegible]	[illegible]
[illegible]	[illegible]	[illegible]	[illegible]
[illegible]	[illegible]	[illegible]	[illegible]
[illegible]	[illegible]	[illegible]	[illegible]
[illegible]	[illegible]	[illegible]	[illegible]
[illegible]	[illegible]	[illegible]	[illegible]

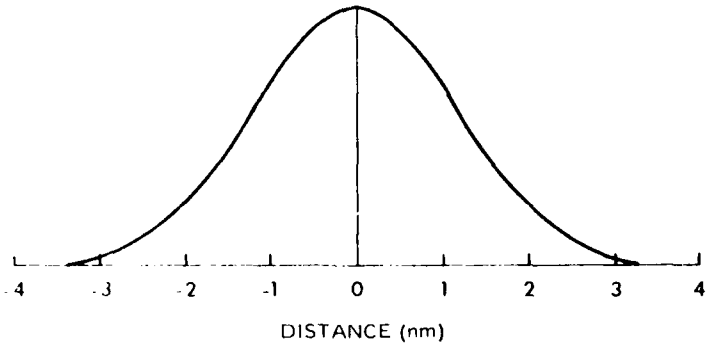

Figure 11. Normal Target Location Distribution for TASDA AZOI and SPAM at 0 min Time Late.

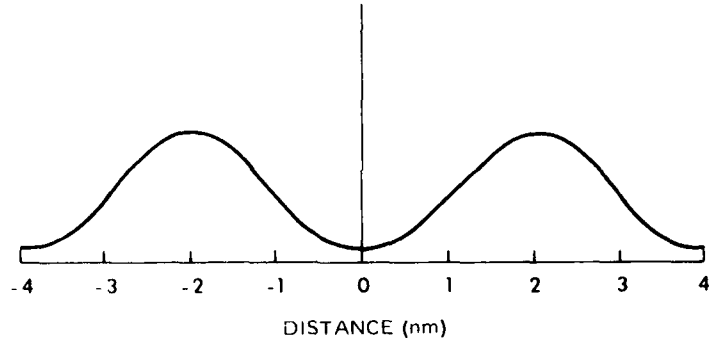

Figure 12. Normal Target Location Distribution for TASDA and AZOI at 30 min Time Late.

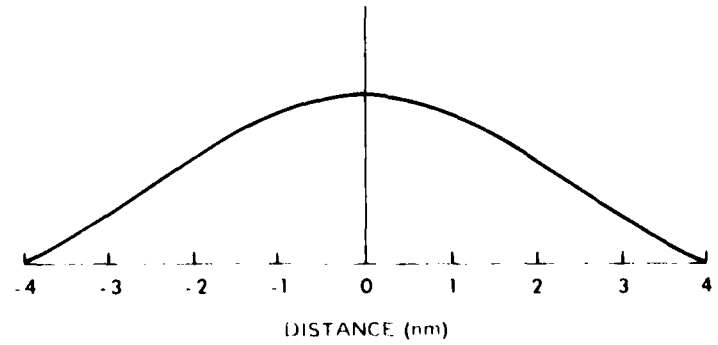

Figure 13. Normal Target Location Distribution for SPAM at 30 min Time Late.

its maximum value should be considered. A numerical value based on area under a curve was used since area under a curve depends on rise time and curve height. For example, in Figure 14, Curves A and B rise to the same probability of detection equal to 20.8. However, curve A rises to that POD faster than curve B and has a higher numerical indicator attached. In Figure 15, curve C rises as fast as curve A, but curve C rises to a smaller POD maximum. Therefore, the tactic associated with curve A has a higher measure of effectiveness than curve C and thus, has a higher numerical indicator.

The area under the CPOD curves was estimated by visually inspecting the curves. The method used to calculate the CPOD curve indicator values is shown in Figure C-2 in Appendix C.

Uniform Case

CPOD indicator values for the uniform case were averaged over three FOMs and three frequencies, and the averages are presented in Table 8. The indicator values for each curve are shown in Appendix C. In this scenario only two patterns were considered and computer output showed only partial agreement. However, it is important to remember that in the uniform case initial target position is unknown. For all three models indicator values fell within a few percentage values of each other for the 4-4-4-4 and circle patterns. However, the difference between models is as much as 37 in the D-D case and is noticeable in all cases.

Normal Case

CPOD indicator values for the normal case were averaged over three FOMs and three frequencies and the averages are shown in Table 8. The indicator values are shown in Appendix C. In this case, initial target location points are clustered toward the center of the operation area for TASDA, AZOI and SPAM. One would expect these three models to evaluate the patterns similarly since there is now some control on target location. Table 8 shows average probability of detection values remain noticeably different. Note that the maximum difference is 17 for the S-S depth with the ellipse whereas in the uniform case the maximum difference was 24 for the circle for the S-S depth. This relationship of the differences can be observed for both patterns at all depths. The long on station time of 4 hours appears to have an affect on the large differences.

[illegible]

[illegible] probability of detection casual was calculated for two patterns with a uniform [illegible] initial target location distribution. Four flights arrive on station with 1 [illegible] and remain on station for four hours. Each flight searches a quadrant of [illegible] field. Since the sonobuoy patterns are symmetric with respect to the center [illegible], each quadrant has an identical sonobuoy geometry. Therefore, only computer simulation on one quadrant were necessary. Instead of obtaining CPOD indicator values [illegible] sporting curves, average values were obtained by dividing the CPOD curves into time steps as shown in Figure C-2 of Appendix C. CPOD indicator values for the uniform [illegible] case were averaged over three FOMs and three frequencies and are shown [illegible].

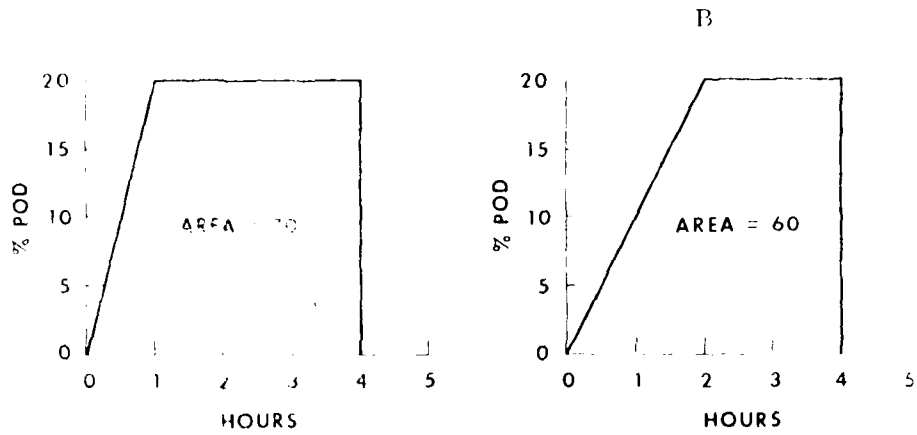

Figure 14. Curves A and B: Numerical Value for Pattern Selection by Rise Time.

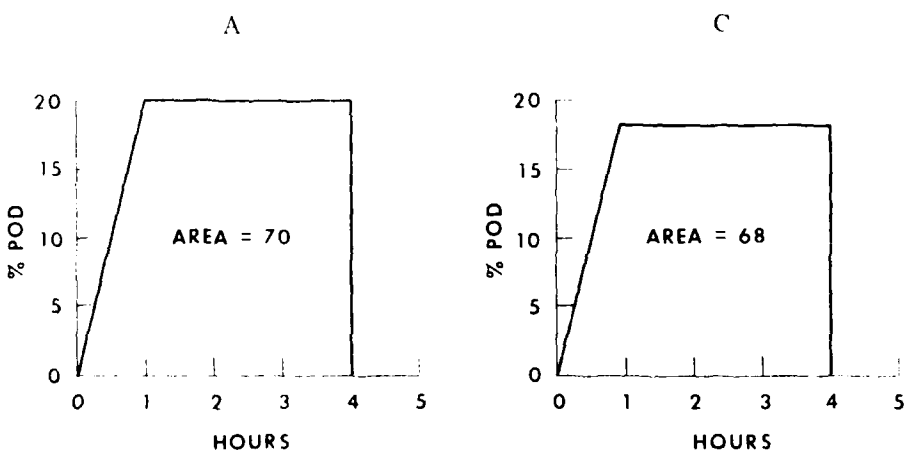

Figure 15. Curves A and C: Numerical Value for Pattern Selection by EPOD.

Table 9
Percent Probability of Detection for Scenario 3

UNIFORM CASE			
	S-S	S-D	D-D
[illegible]	16.0	18.0	9.6
[illegible]	26.8	23.0	7.4
[illegible]	16.2	37.1	36.3
[illegible]	15.2	19.2	10.0
[illegible]	28.7	19.6	14.1
[illegible]	41.2	33.6	35.7

NORMAL CASE			
	S-S	S-D	D-D
[illegible]	62.7	26.8	20.7
[illegible]	62.7	36.0	13.1
[illegible]	62.1	13.1	12.0
[illegible] BEARING SKEW	64.7	30.3	19.8
[illegible] BEARING SKEW	62.2	34.0	11.1
[illegible] BEARING SKEW	62.1	15.7	39.4

In the uniform case results in Table 9 show that there are still significant differences in model outputs at all depths. However, shortening the on station time appears to have brought the values closer together in the normal case. There is only 2.3°F maximum difference at the S-S depth.

Scenario 4

The circle and chevron skew (Appendix A) buoy fields were considered. The environment was changed from the Pacific to the Atlantic for a different type of comparison. The sound speed profiles in Figures 2 and 3 show that there is no CZ so sound propagation is by direct path. The propagation loss curves in Appendix B indicate bottom bounce is present with a 1[illegible]-100 ft source receiver depth combination. Values in Table 10 show average POD values obtained for the Atlantic environment. Hydrophone depths of 100 and 1900 ft were chosen for simulation and the results are shown in Table 10.

This scenario was chosen to show how the models respond in a direct path environment. As expected, the values are lower than in the other scenarios because of the absence of a convergence zone environment. The one noticeable result in the output averaged in Table 10 is the high evaluation by AZOL using the chevron skew pattern in the normal case. Actually, this is what one would predict for the chevron skew pattern since the coverage is greatest at the center where the target is most likely. The other two models, however, did not increase their predictions significantly from the uniform case.

Table 10
Percent Probability of Detection for Scenario 4

UNIFORM CASE			NORMAL CASE		
	S-S	D-D		S-S	D-D
GULF STREAM			GULF STREAM		
CIRCLE (TASDA)	15.1	8.7	CHEVRON SKEW	28.8	12.3
CIRCLE (AZOI)	28.6	28.4	CHEVRON SKEW	67.3	39.9
CIRCLE (SPAM)	28.7	25.7	CHEVRON SKEW	24.1	32.0
SLOPE WATER			SLOPE WATER		
CIRCLE	6.0	8.4	CHEVRON SKEW	10.1	9.1
CIRCLE	24.3	23.7	CHEVRON SKEW	41.8	36.1
CIRCLE	32.4	30.7	CHEVRON SKEW	32.0	32.5

VI. CONCLUSIONS

Expected probability of detection is calculated using four different methods. ADEPS calculates the average conditional probability in a symmetrical subsection of a buoy field pattern where the submarine is assumed to be a random target. TASDA computes probability of detection by one or more buoys using Monte Carlo simulation of 100 random tracks through a buoy field and a detect (POD = 1) or no detect (POD = 0) analysis for each track. AZOI uses a binominal probability function to calculate EPOD where a value for time along a track is chosen randomly. SPAM uses a Monte Carlo simulation and calculates EPOD by averaging a probability obtained through assuming independence of buoys with a probability obtained by assuming complete dependence of buoys. Since the methods of calculation are different in each program, the output for EPOD is not exactly the same.

ADEPS, TASDA, AZOI and SPAM all calculate cumulative probability of detection as a function of time. However, the method of calculation is different in all four programs. ADEPS uses an exponential expression to estimate a conditional cumulative probability P(t) as discussed in Section I. TASDA uses a detect - no detect Monte Carlo methodology. AZOI uses EPOD calculation to obtain an estimate for the lower limit of CPOD. In the case where the target location is assumed to have a uniform distribution, the CPOD does not change with time and is equal to EPOD. In the normal case, EPOD and CPOD are different since calculations for the normal case are time dependent. SPAM uses a cumulative time window to limit POD calculations for CPOD. Since different techniques are used for each program, it is not expected that CPOD output will be exactly the same for each program. ADEPS outputs P and P(t); TASDA outputs CPOD, EPOD and mean time to first detection (MTFD); AZOI outputs CPOD, EPOD, standard deviation (SIGMA) and probability that a target will be detected given that it has not been detected in the past (P DE/NDT); SPAM outputs CPOD and EPOD. Although the symbols CPOD and EPOD in Table 6 are used for TASDA, AZOI, and SPAM, the output for these parameters may not be the same.

The following conclusions are indicated by this study.

1. TASDA is Conservative at Low FOMs

Unlike AZOI or SPAM, TASDA requires contact during two consecutive time steps before a detection is made. TASDA constructs probability areas around each buoy bounded by two concentric circles as in Figure 16. These areas represent the locations where the

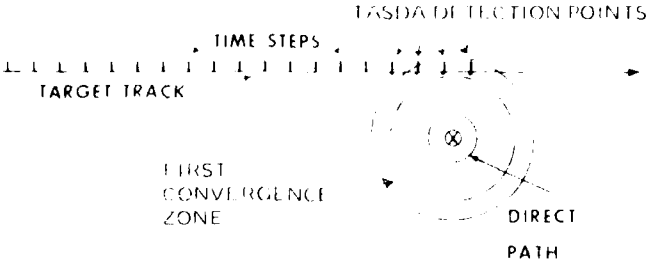

Figure 16. Target Track for TASDA and SE ≥ 0 Region Around a Sonobuoy. POD = 1.

signal excess SE is greater than zero. If the target remains in one of these areas during two consecutive time steps, then the POD = 1 for that time period. Otherwise, the POD = 0. There will be a set of these values for each of the 100 TASDA trials. The values are summed over 100 trials to come up with CPOD values for each time interval. At low FOMs the areas bounded by concentric circles become very small and as a result, the CPOD values drop rapidly to zero. AZOI and SPAM compute POD versus range for each buoy rather than assigning a 0 or 1 value at a particular range.

2. SPAM is Optimistic at Low FOMs

If the target is at a range such that a faint line will be created on a gram, then there must be some amount of time during which the target remains at a detectable range in order for the operator to see a line; call it t_0. Even after t_0 time has passed, the operator may not see the line. The probability that the operator sees the line increases up until some time, t_z. These two values for time are incorporated into a cumulative time window (CTW) model which examines the probabilities between these times in increments of time t_1. The smaller the value of t_0, the higher the POD value. Standard operating values for SPAM are (t_0, t_1, t_z) = (.25, .05, .50). This means that the target must remain at a detectable range for only 15 minutes to achieve the probability of detection predicted by the standard passive sonar equation. The values t_0, t_1, t_z in the CTW caused predictions for SPAM to be optimistic at low FOMs. Detection can occur at any time before or after t_0, depending on chance.

3. SPAM Results are more Conservative at High FOMs

The CTW model builds detection probabilities experimentally for a target remaining at a fixed range until time t_z with the probability predicted by the sonar equation achieved after time t_0 has passed. This function also smoothes the jump from low probabilities associated with low FOMs to high probabilities associated with high FOMs.

4. TASDA and AZOI Show a Jump in CPOD as FOM Increases

A normal distribution around the figure of merit is used in the SPAM model. The belief is that the area under a normal curve is equal to the probability of detection. SE = 0 when FOM = PL. At that point there is a 50% POD. As shown in Figure 17, SPAM POD gradually increases as SE increases. Truncation has an effect on CPOD values for AZOI with low FOMs. For low FOMs there is very little signal excess and probability depended on the left half of the curves above; therefore, the CPOD values dropped quickly to 0. TASDA uses a Rician Distribution to simulate short-term fluctuation in the PL curve and calculations are based on the assumption that below the FOM an operator is unlikely to detect a target. Detection is either YES or NO based on SE 0 after employing the Rician fluctuations. As is apparent from the graphs in Figures 17, 18 and 19. AZOI and TASDA have probability distributions which drop off quickly to zero below the FOM. Therefore, TASDA and AZOI exhibit breaking points when the FOM reaches a small enough value. At these FOMs CPOD falls rapidly to zero.

5. AZOI Shows Small Variance Between Patterns

AZOI differs from TASDA and SPAM in that TASDA and SPAM use successive time steps along a target track for a particular trial. After a track has been generated for a particular trial, AZOI picks random points along that track and evaluates POD values at those points. Therefore, the time increments are not evenly spaced but randomly spaced. At each point, the range to each buoy is calculated and the probabilities associated with each buoy are summed to give a POD for the target at a point along the track. In this manner, all contributions are considered. The probability at a point along the track is not zero or one as with TASDA, nor is execution terminated when a detection is encountered as with SPAM. So this method yields more values for POD along a track; and a cumulative time window is not employed as is the case with TASDA and SPAM.

These five differences in the three computer simulation models result from various interpretations of the tactical sonobuoy situation under consideration. These interpretations result in different output values for each of the three simulation programs.

The large differences between computer models require further investigation. Future studies should be based on a real world application of the sonobuoy programs. Real world mission planners usually have SOSUS or other intelligence information for input to the model and are interested in POD versus buoy spacing. The output data sets in this report are not designed to reflect a real world application of the sonobuoy programs, but acquaint the reader with the amount and type of data output generated by considering a few pattern configurations under several different conditions.

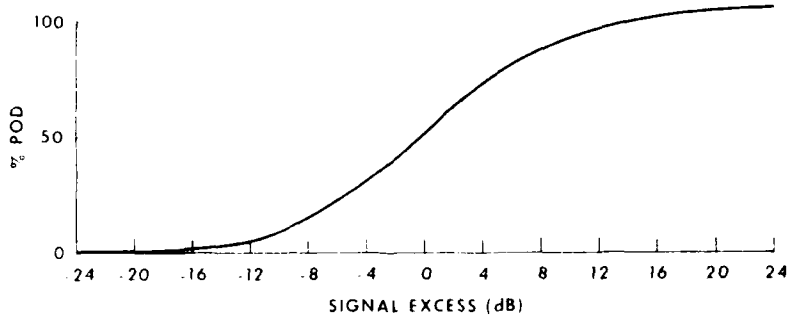

Figure 17. SPAM: POD vs SE Used in the Calculation of a Lateral Range Curve (Normal Distribution).

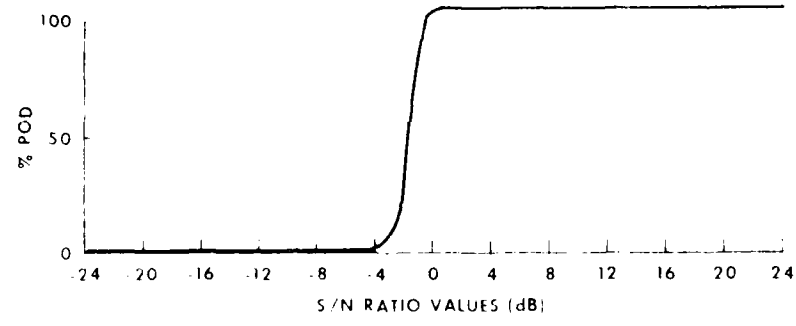

Figure 18. AZOI: POD vs SE Used in the Calculation of a Lateral Range Curve (ROC Curve).

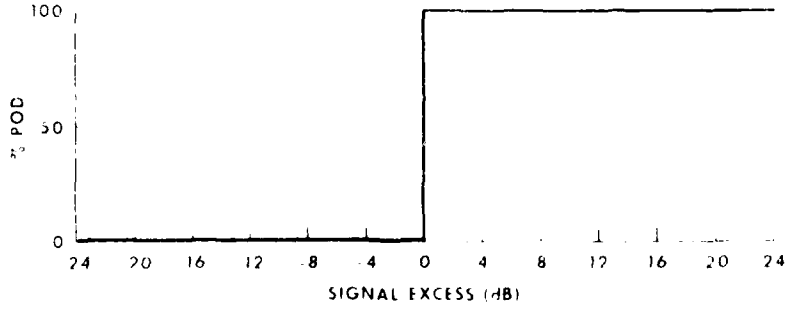

Figure 19. TADA: POD vs SE Used in the Calculation of a Lateral Range Curve (Detect-No Detect Assumption).

ACKNOWLEDGMENTS

Special thanks go to Dave Birnbaum and Gale Katz of the Naval Air Development Center for a review of the data and technical content of text material for AZOI and TASDA. Suggestions from George Hanssen, former Program Manager for ICAPS, are appreciated. Al Crumpler provided valuable guidance through several working drafts and enhanced the data analysis by providing input for the Atlantic environment in the fourth scenario. Final text review by Jeff Heaton produced many changes which helped improve the report.

REFERENCES

Allison, Commander K. L., ADEPS Passive Sonobuoy Detection Prediction Models, Naval Command Systems Support Activity (NAVCOSSACT) Washington Navy Yard Washington, D.C. 20390., 1970

Birnbaum, David and Ronald Doray, A Detection Algorithm for Real-Time Optimization of the Deployment of Passive Sonobuoy Fields, Systems Analysis and Engineering Dept., Naval Air Development Center, Warminster, Pennsylvania 18974, 1975.

Marin, Gerald A., ASW Detection Simulation and the Cumulative Time Window Model, Center for Naval Analysis, Arlington, VA. 1975.

Marin, Gerald A., Search Pattern Assessment Model, Center for Naval Analysis, Arlington, VA. 1976.

Naval Air Development Center, TASDA System Functional Document, Naval Air Development Center, Warminster, Pennsylvania 18974, 1976.

APPENDIX A

SONOBUOY PATTERN DEFINITION

Figure A-1. Circle pattern used in scenarios 1, 2, 3, and 4 for a uniform target distribution.

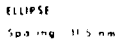

Figure A-2. Ellipse pattern used in scenarios 1, 2, 3, and 4 for a normal target distribution.

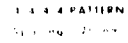

Figure A-3. 4-4-4-4 pattern used in scenario 1 for a uniform and normal target location distribution and in scenarios 2, 3 and 4 for a uniform distribution.

Figure A-4. Chevron or X pattern used in scenario 1 for a uniform target distribution.

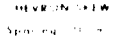

Figure A-5. Chevron skew pattern used in scenarios 1, 2, 3, and 4 for a normal target distribution.

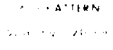

Figure A-6. 5-6-5 pattern used in scenario 1 for a uniform and normal target location distribution.

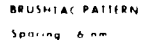

Figure A-7. Brushtac pattern used in scenario 1 for a uniform target distribution and for a normal target distribution.

APPENDIX B

PROPAGATION LOSS CURVES

PROPAGATION-LOSS GRAPHICS DATE = 7 / 6 71

WAVE HEIGHT..... 5 FT
SONIC LAYER DEPTH.. 0 FT
SOURCE DEPTH... 60 FT
RECEIVER DEPTH. 60 FT
FREQUENCY..... 50 HZ

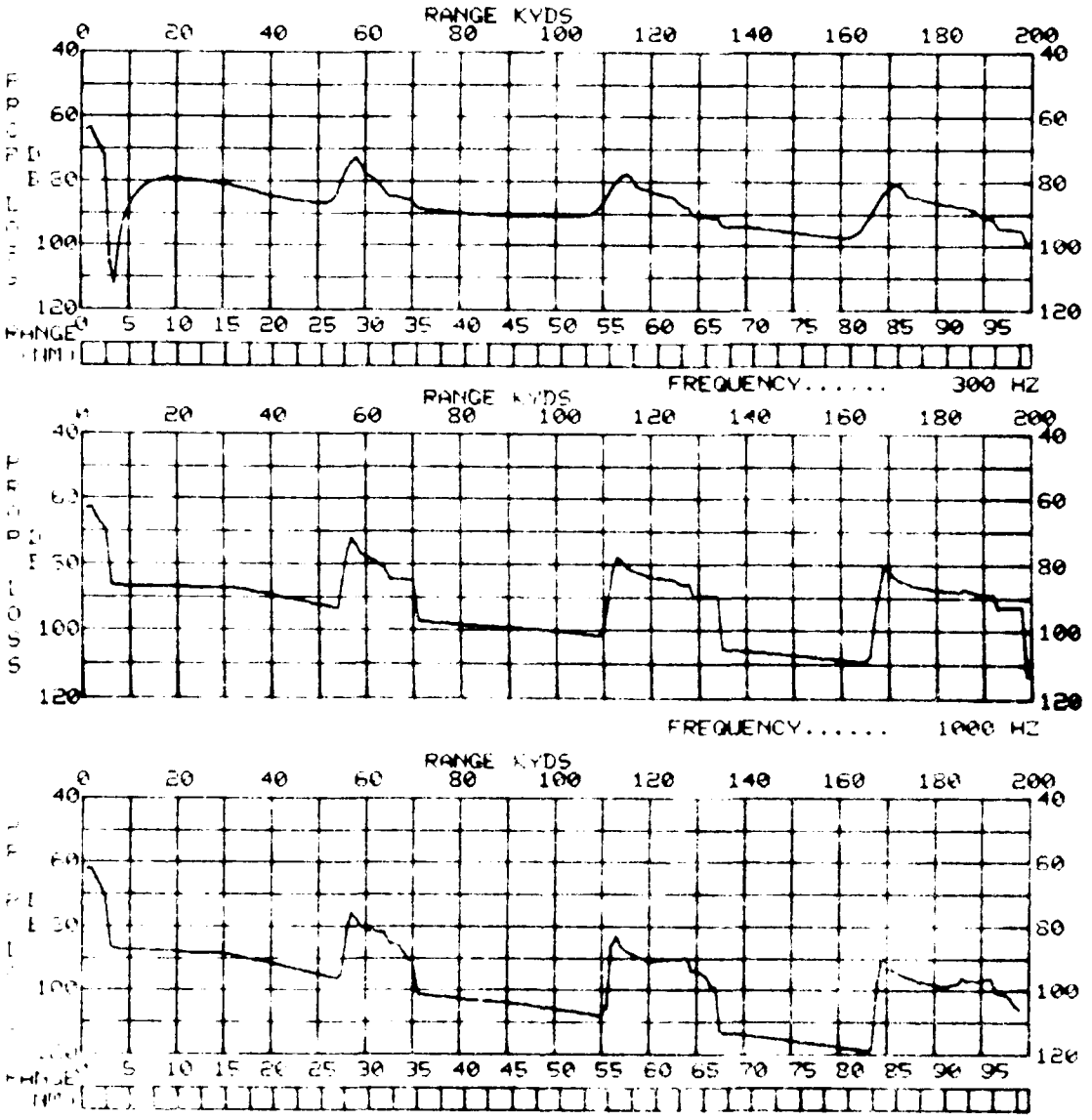

Figure 5. Propagation-loss curves of shallow source and shallow receiver applied to equations 1, 2, and 3.

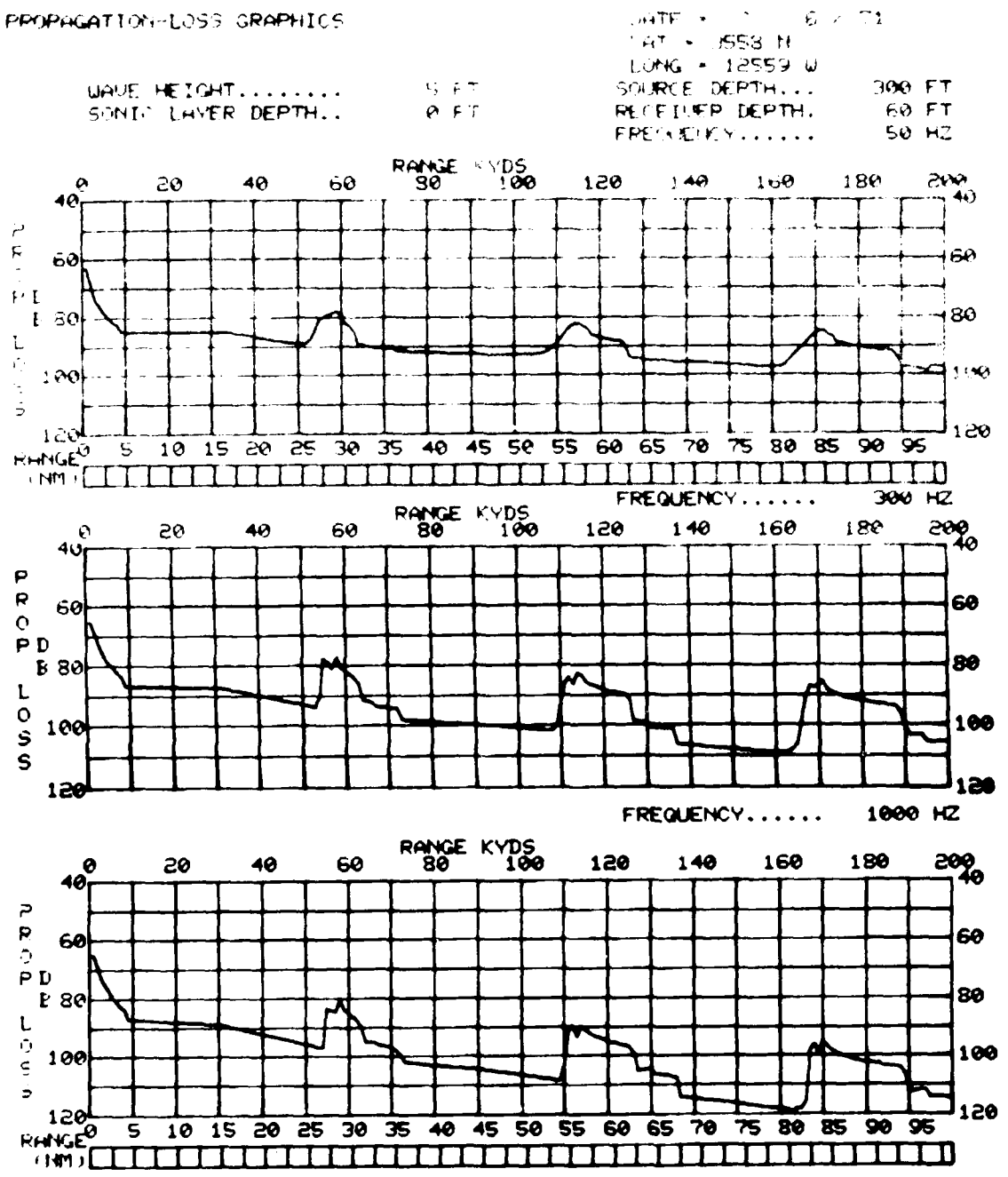

Figure B-2. Propagation loss curves at a shallow receiver depth and deep source depth for scenarios 1, 2, and 3.

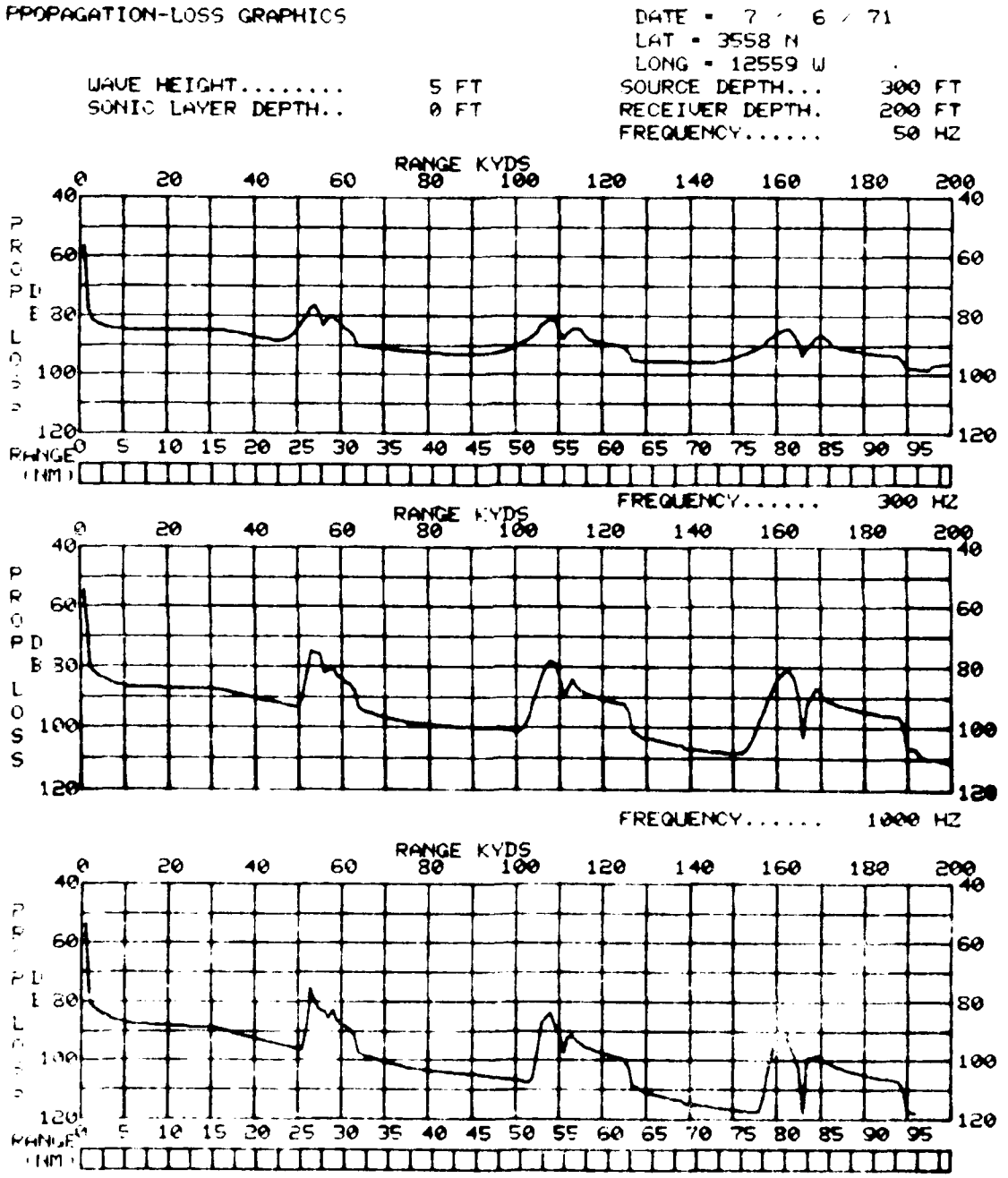

Figure B-1. Propagation-loss curves for deep source depth and deep receiver depth for scenarios 1, 2 and 3.

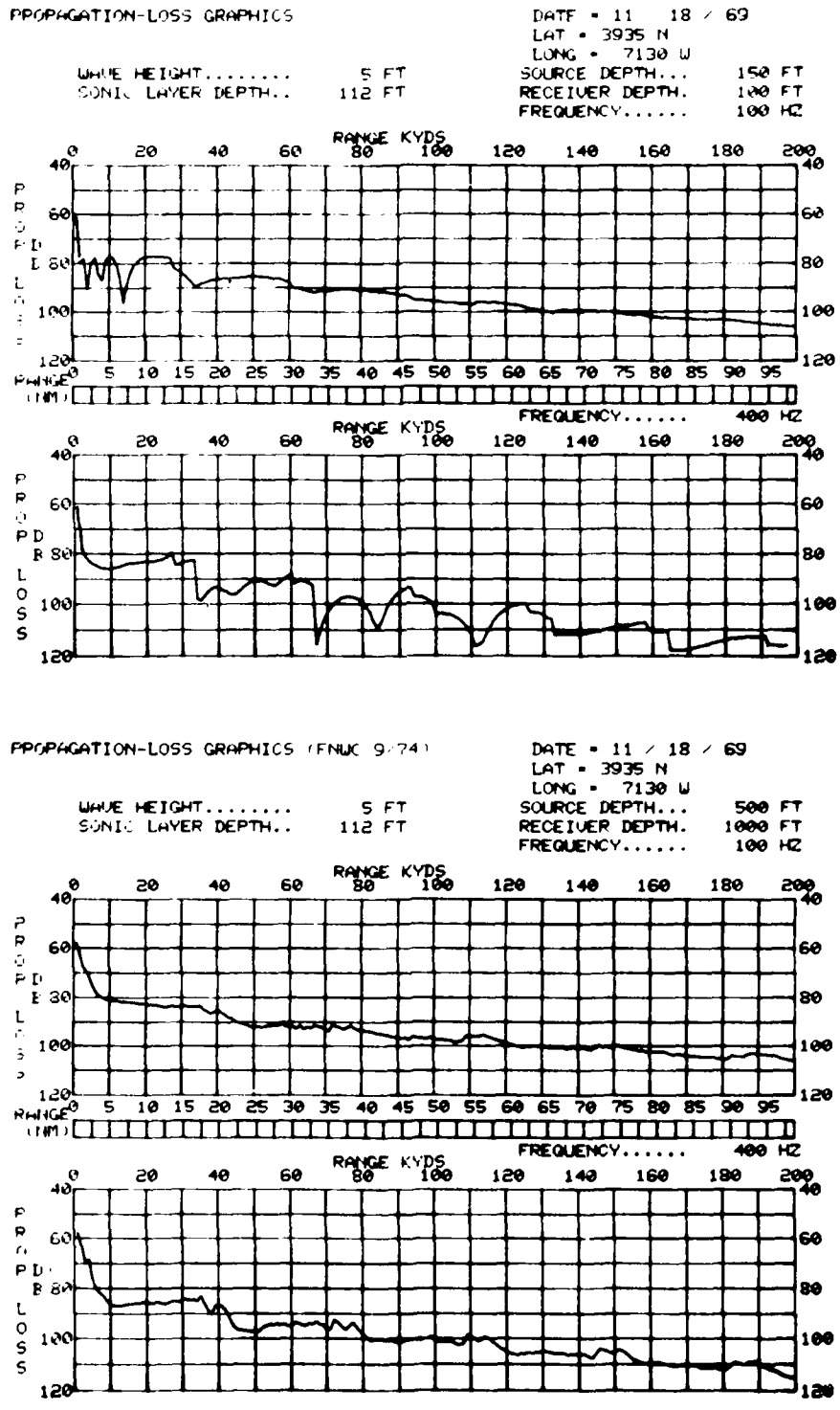

Figure B-4. Propagation loss curves exhibiting direct path sound transmission with no convergence zone used as input to the tactical models in scenario 4.

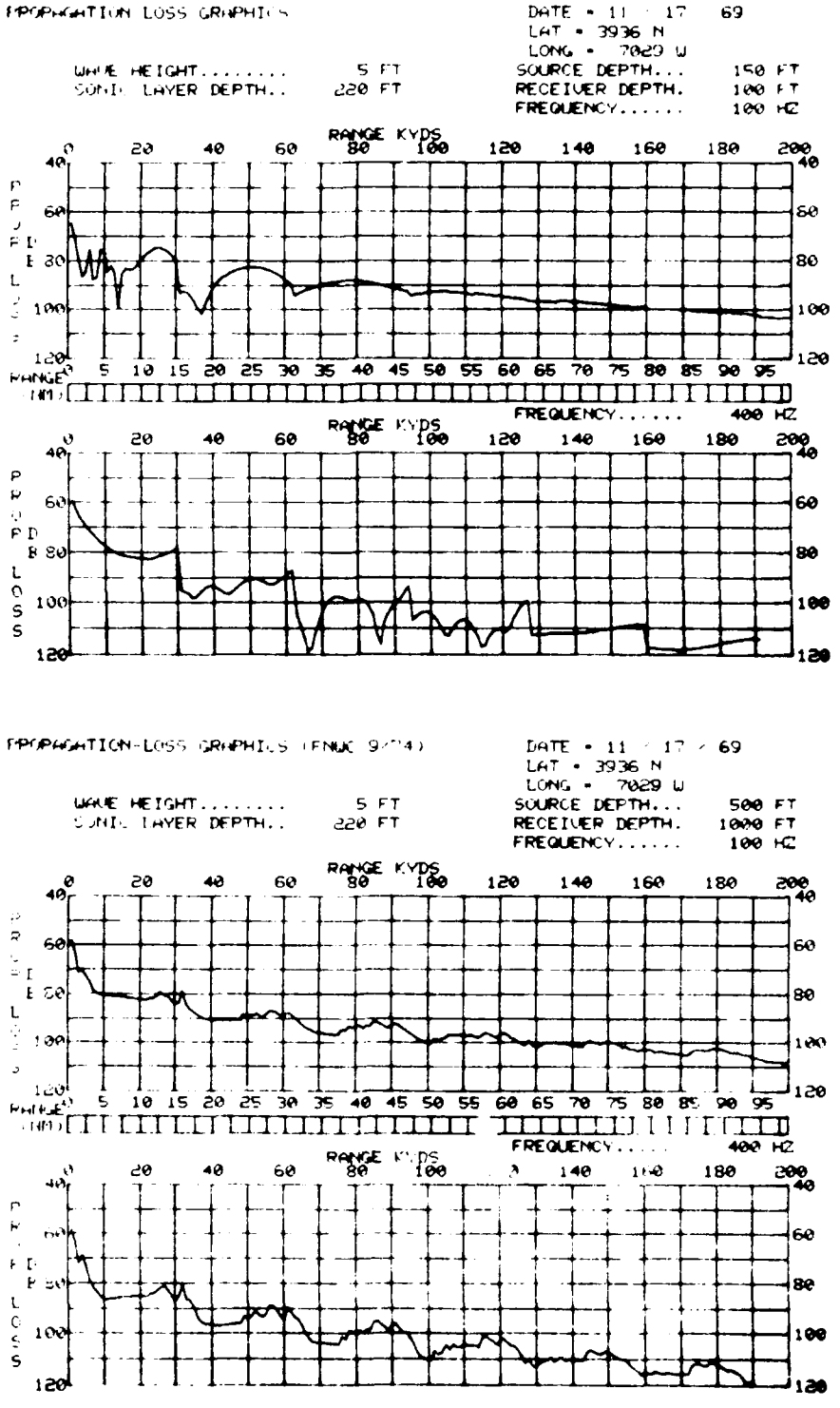

Figure B-5. Atlantic-path stream propagation loss curves exhibiting direct path sound transmission used as input to the tactical models in scenario 4.

APPENDIX C

OUTPUT VALUES

This appendix contains a summary of the computer runtime for each of the scenarios. It should be noted that the runtime for AZOI includes the calculation of P DE/NDT in addition to EPOD and CPOD. Also, AZOI includes pattern processing time. Runtime must be miltiplied by a factor of 60 when estimating minicomputer runtime. Therefore, the values can be considered in hours rather than minutes when making minicomputer runtime estimates.

Also in this appendix are the original data generated by the programs (Figures C-1 through C-62). The data are presented in graphical form. The original data were reduced to single EPOD and CPOD indicator values for the purposes of program comparison in this report. The method for obtaining the indicator values is shown in Figures C-63, C-64, C-65. The derived indicator values for each FOM, frequency and depth combination are listed in the tables in the appendix. These values were averaged to obtain values for analysis in the text of this report.

Table C-1. Runtime Using
The Univac 1108 Computer

	CPU Time	I/O Time	Total Time
Scenario 1			
TASDA	31.7 min	1.5 min	33.2 min
AZOI	180.3 min	.3 min	180.6 min
SPAM	110.0 min	1.5 min	111.5 min
Scenario 2			
TASDA	17.0 min	1.2 min	18.2 min
AZOI	13.0 min	.3 min	13.3 min
SPAM	23.3 min	0.9 min	24.2 min
Scenario 3			
TASDA	6.6 min	1.3 min	7.9 min
AZOI	14.0 min	.3 min	14.3 min
SPAM	12.1 min	.9 min	13.0 min
Scenario 4			
TASDA	3.8 min	3.2 min	7.0 min
AZOI	12.7 min	.3 min	13.0 min
SPAM	11.6 min	.7 min	12.3 min

The output used to construct graphs of the original data was obtained from computer listings of set time intervals for each model. TASDA outputs CPOD values in increments of 1/6 of an hour. Time Late is a direct input for TASDA. The user specifies Target speed, and Distance Travelled by target while aircraft is on station. Time on station is calculated using these variables.

AZOI outputs CPOD values in increments of time specified by the user. For the three scenarios, the increment was set to 10 min or 1/6 of an hour. If execution will not terminate before the end of the Time On Station. Runtime values are shown in Table C-1. AZOI outputs only Expected Probability of Detection (EPOD) for the Last Run Case. Therefore, only one value is obtained instead of a series of steadily increasing values.

SPAM outputs CPOD values in increments of 1/10 of an hour or every 6 minutes. SPAM will terminate output when the CPOD values settle out to a maximum value before the end of the Time On station period. Output values for VDLOS were not included.

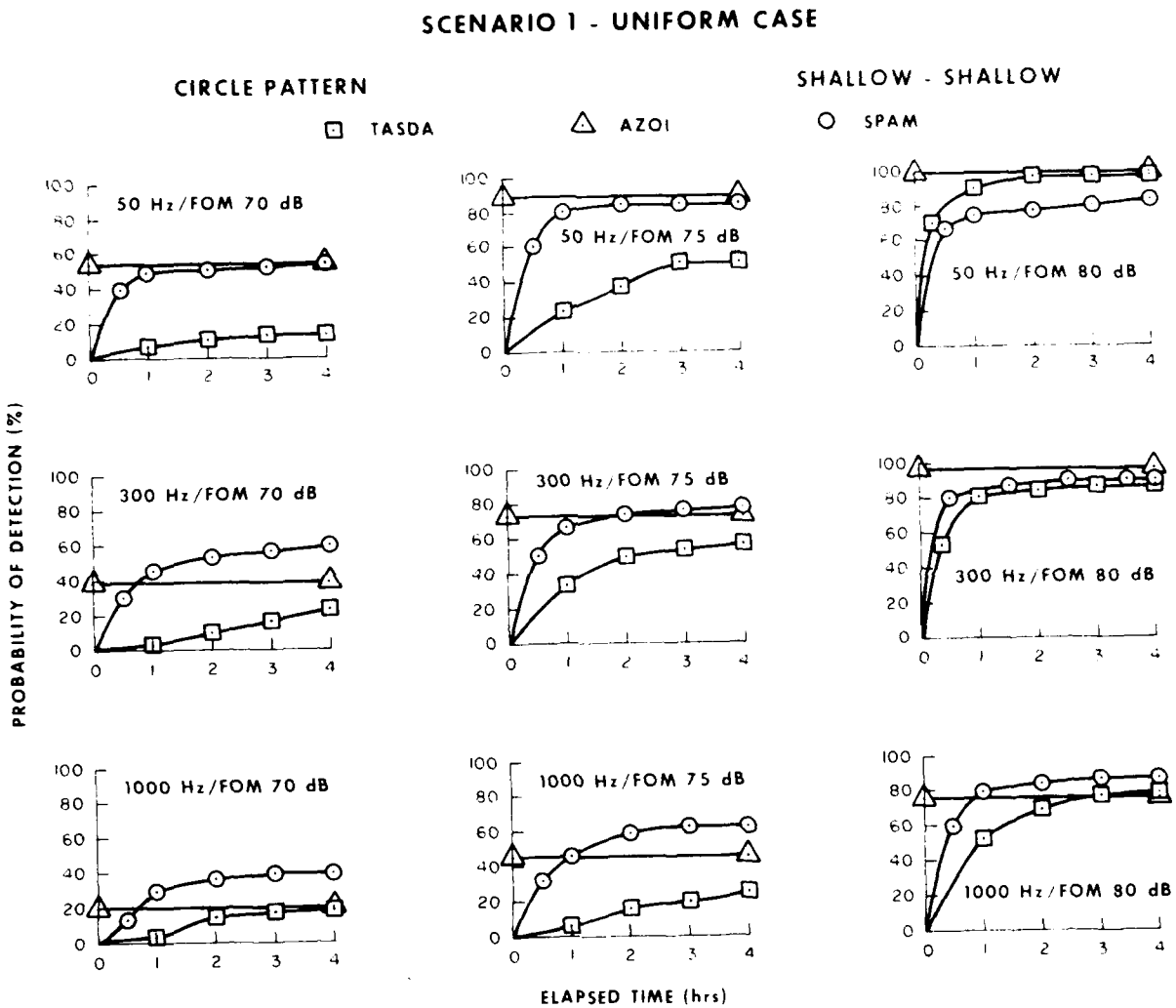

Figure C 1. Comparison of TASDA, AZOI and SPAM with a uniform initial target location at 30 minutes time late with a shallow target and a shallow receiver in scenario 1 using the circle pattern.

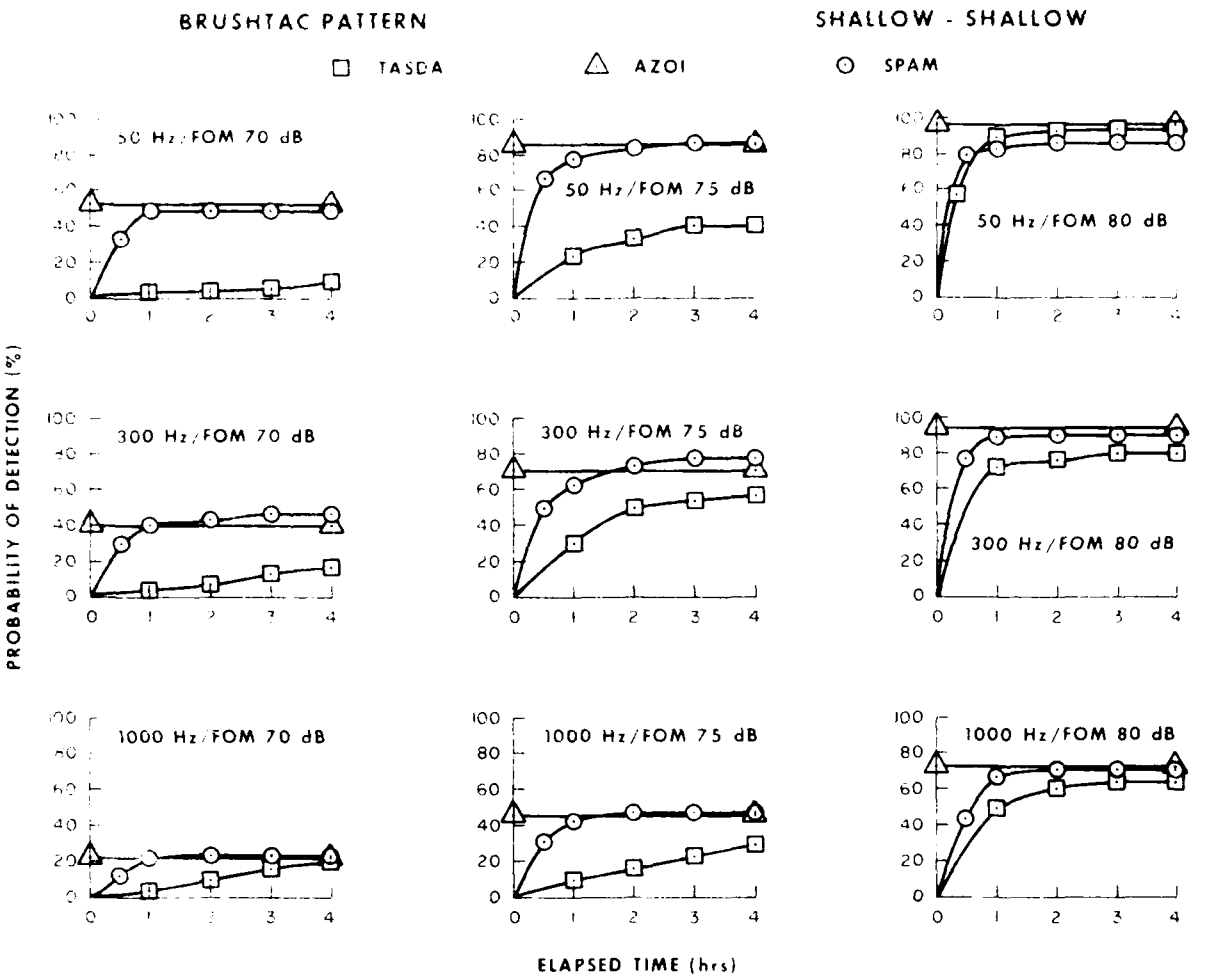

Figure C-2. Comparison of TASDA, AZOI and SPAM with a uniform initial target location at 30 minutes time late with a shallow target and a shallow receiver in scenario 1 using the brushtac pattern.

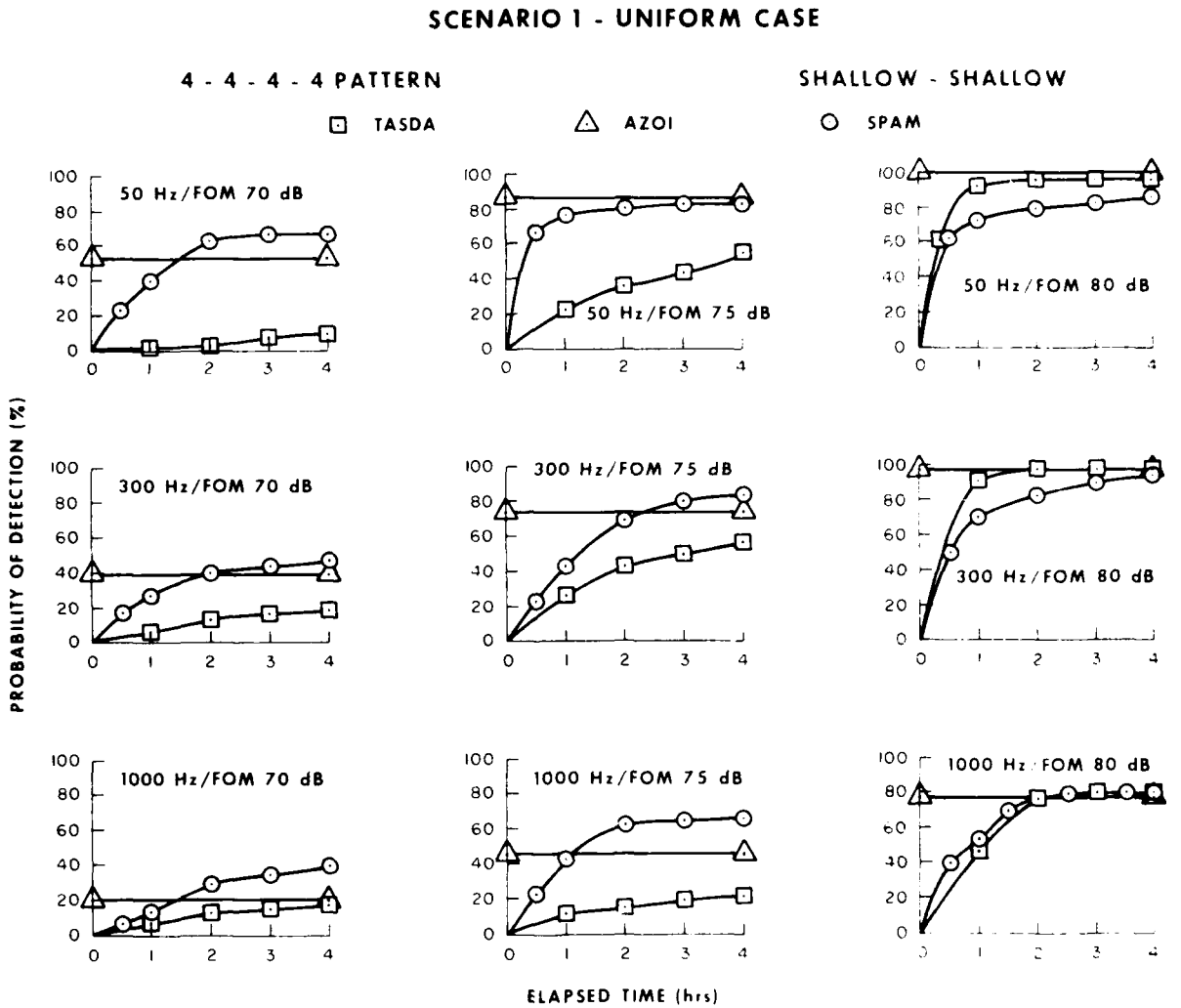

Figure C 3. Comparison of TASDA, AZOI and SPAM with a uniform initial target location at 30 minutes time late with a shallow target and a shallow receiver in scenario 1 using the 4 4 4 4 pattern.

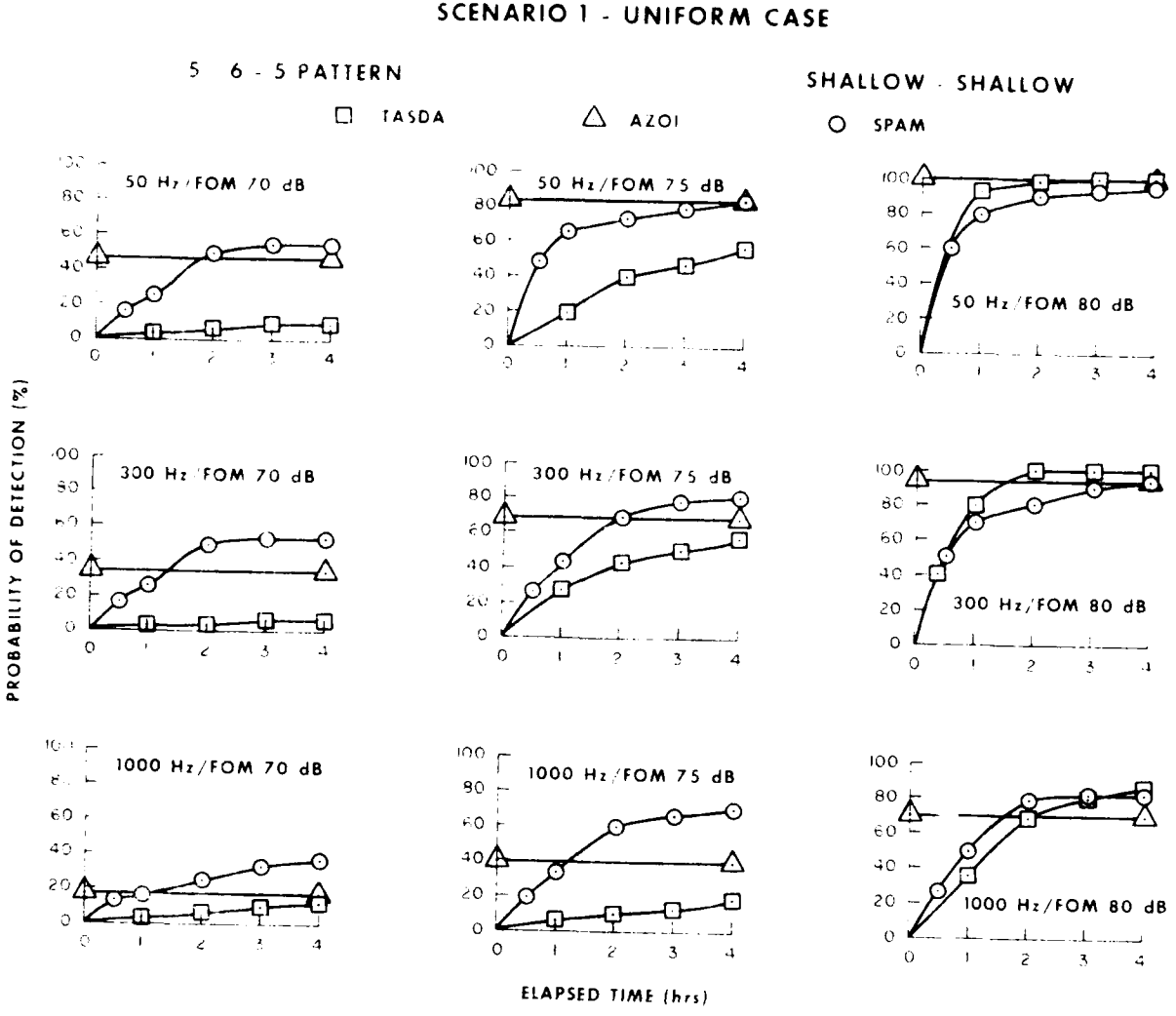

Figure C-4. Comparison of TASDA, AZOI and SPAM with a uniform initial target location at 30 minutes time late with a shallow target and a shallow receiver in scenario 1 using the 5 6 5 pattern.

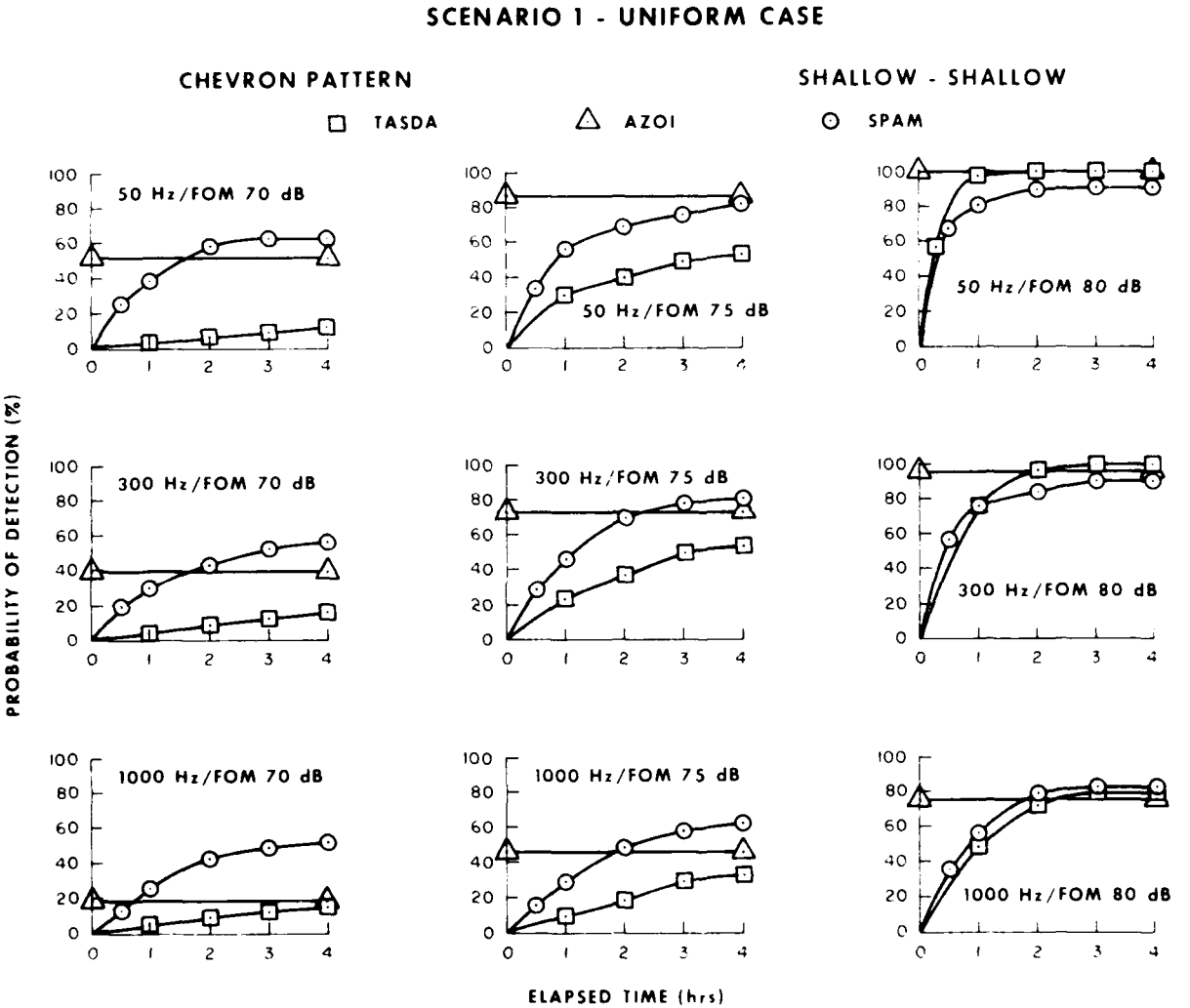

Figure C 5. Comparison of TASDA, AZOI and SPAM with a uniform initial target location at 30 minutes time late with a shallow target and a shallow receiver in scenario 1 using the chevron pattern.

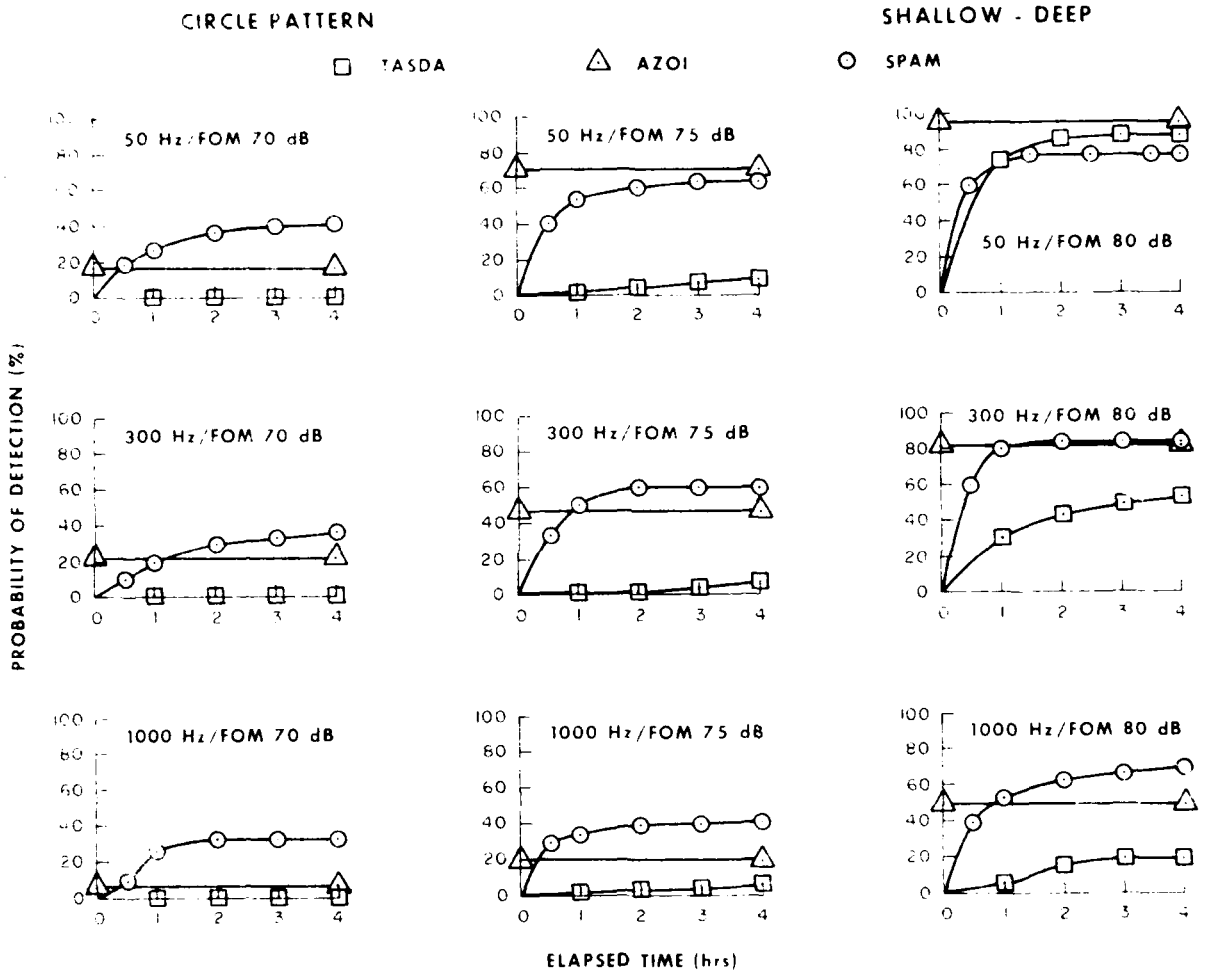

Figure C-6. Comparison of TASDA, AZOI and SPAM with [illegible] target location at 30 minutes time late with a [illegible] target receiver combination in scenario 1 [illegible]

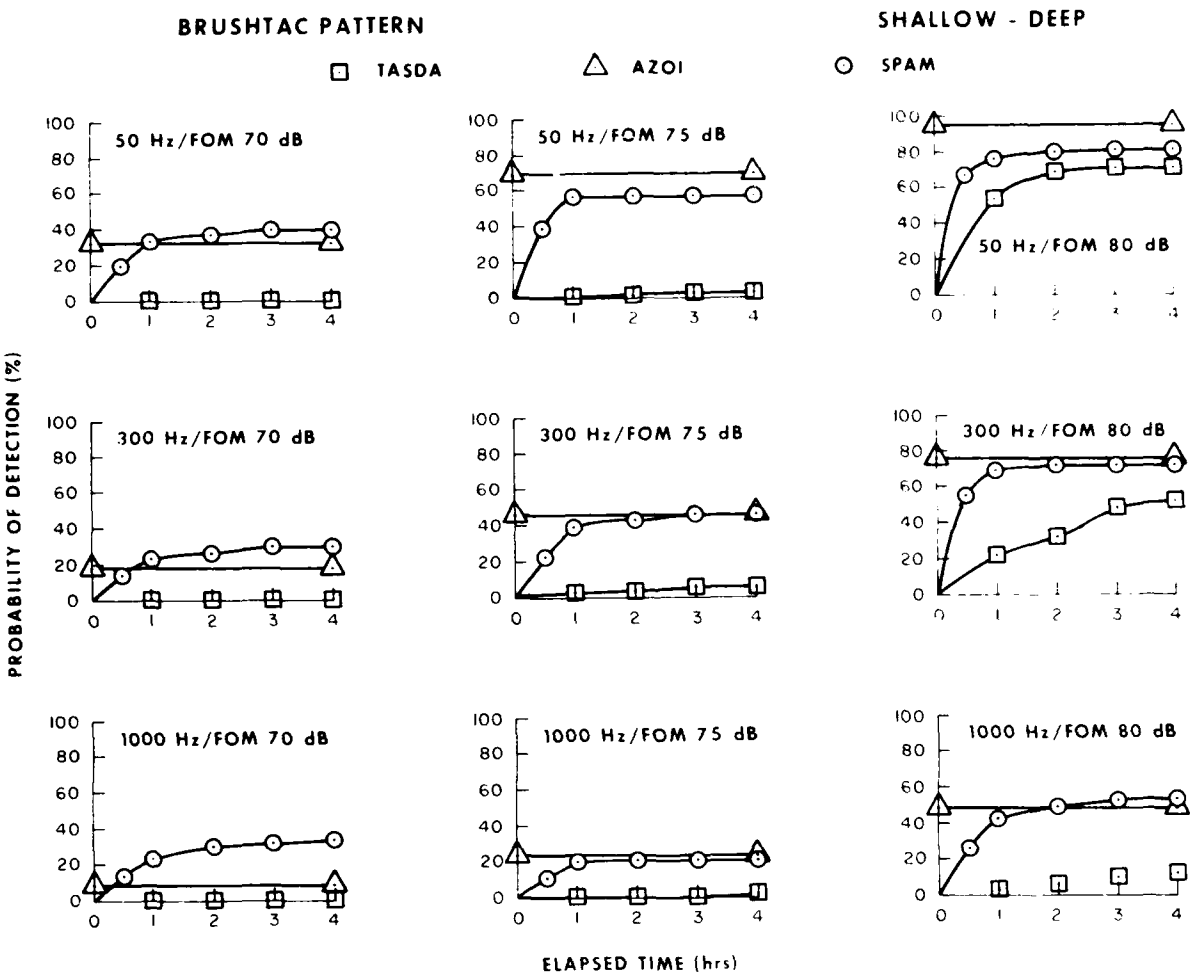

Figure C 7. Comparison of TASDA, AZOI and SPAM with a uniform initial target location at 30 minutes time late with a shallow deep target receiver combination in scenario 1 using the brushtac pattern.

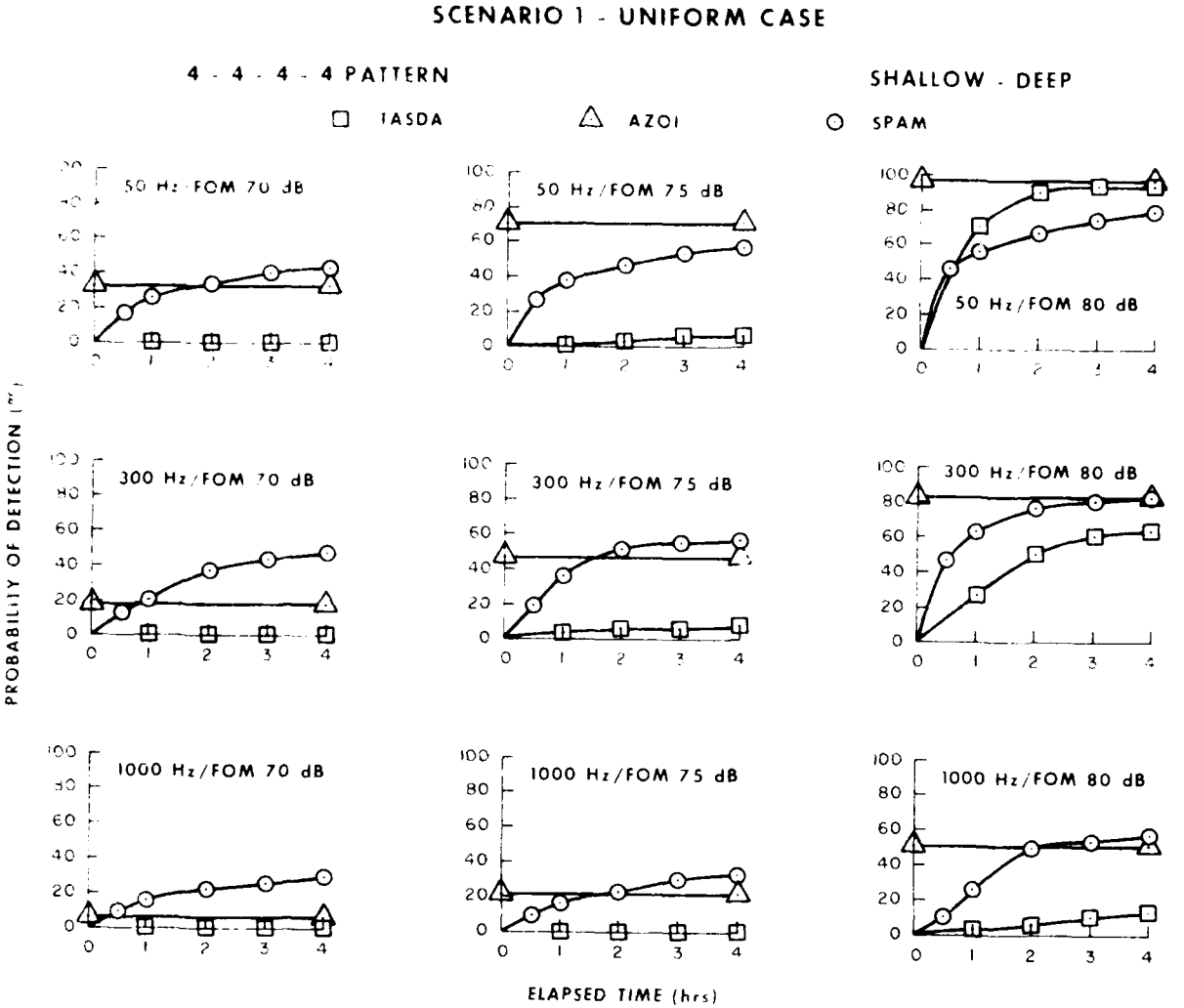

Figure C 8. Comparison of TASDA, AZOI and SPAM with a uniform initial target location at 30 minutes time late with a shallow deep target receiver combination in scenario 1 using the 4 4 4 4 pattern.

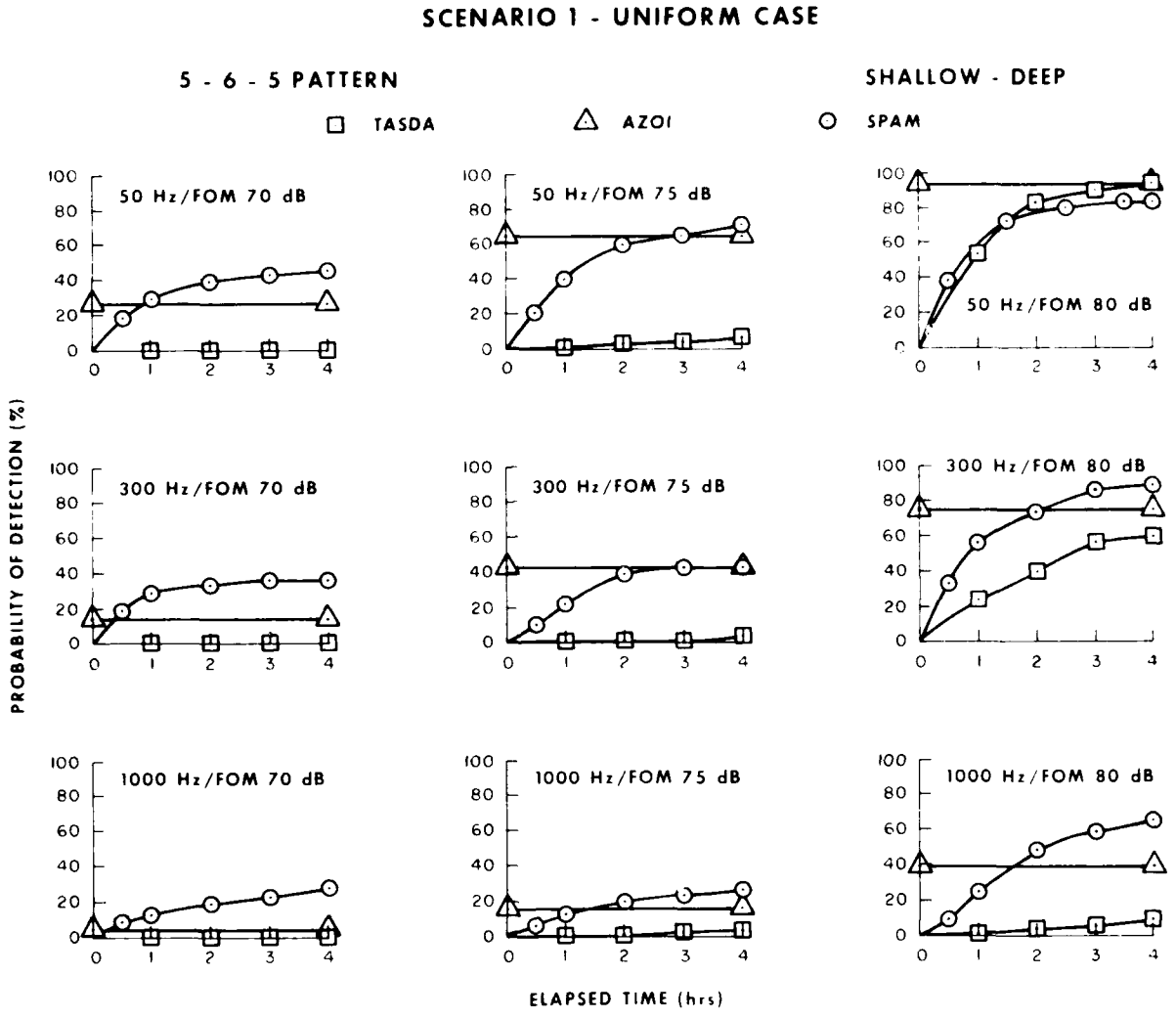

Figure C 9. Comparison of TASDA, AZOI and SPAM with a uniform initial target location at 30 minutes time late with a shallow deep target receiver combination in scenario 1 using the 5 6 5 pattern.

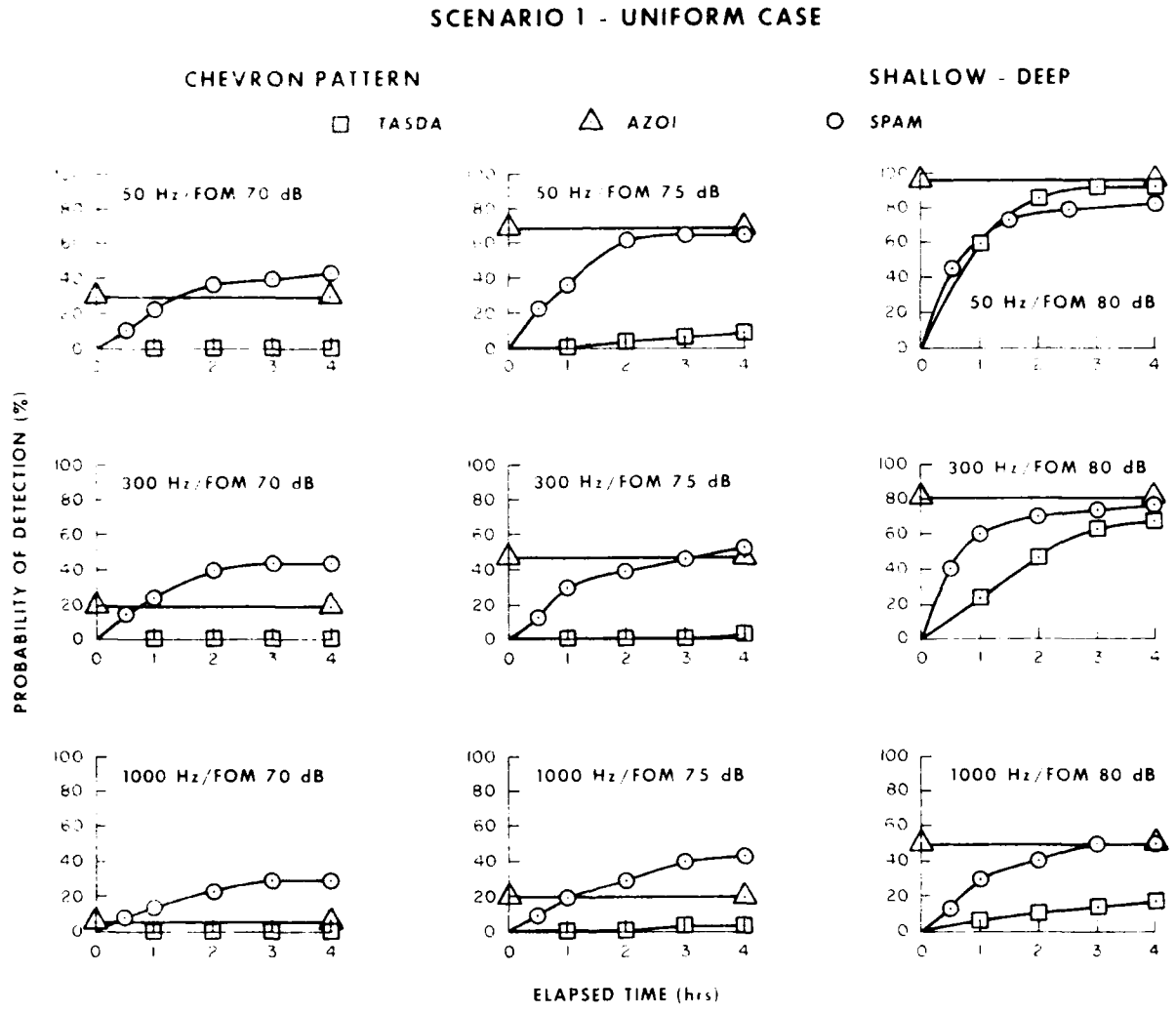

Figure C-10. Comparison of TASDA, AZOI and SPAM with a uniform initial target location at 30 minutes time late with a shallow deep target receiver combination in scenario 1 using the chevron pattern.

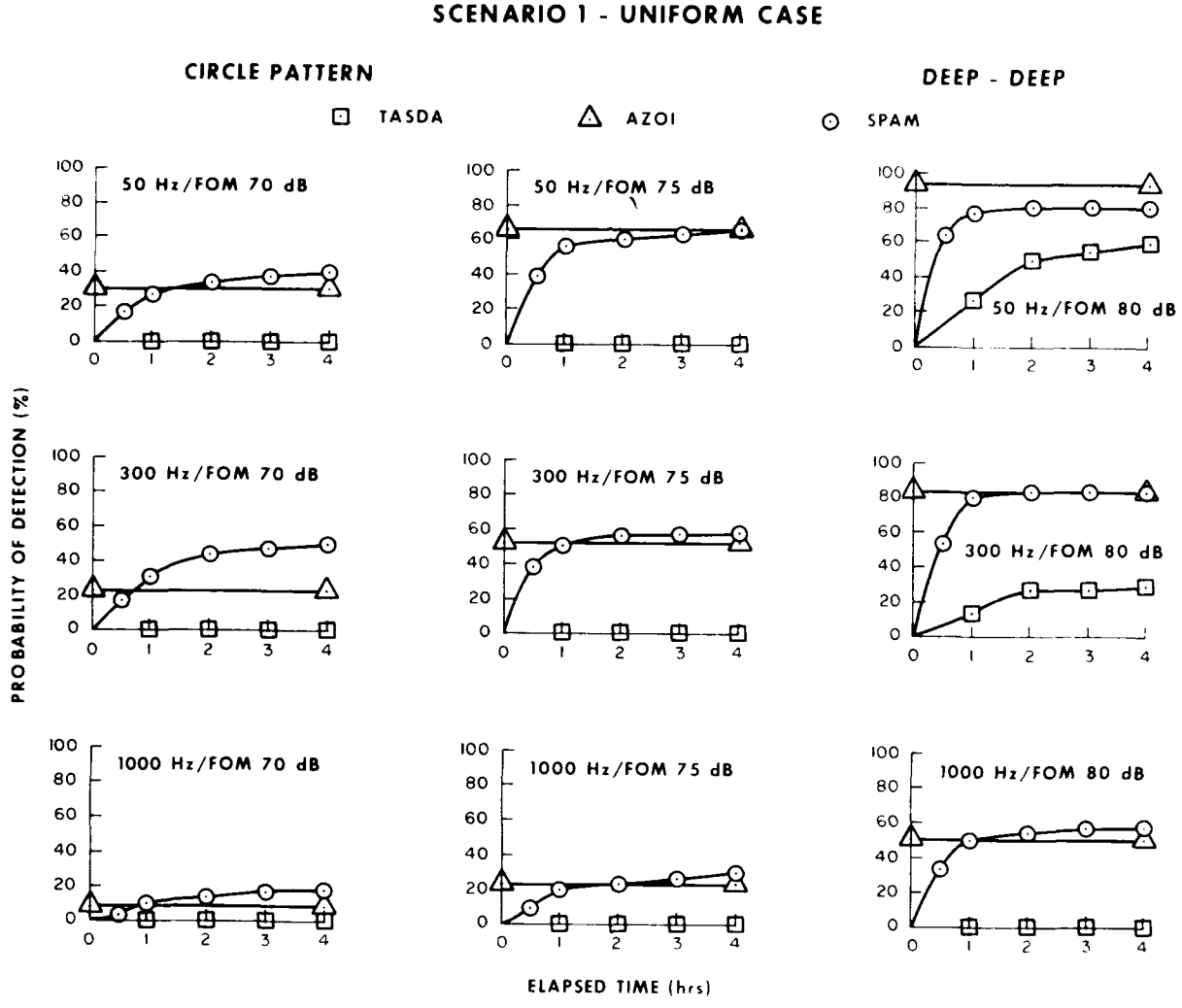

Figure C 11. Comparison of TASDA, AZOI and SPAM with a uniform initial target location at 30 minutes time late with a deep target and a deep receiver in scenario 1 using the circle pattern.

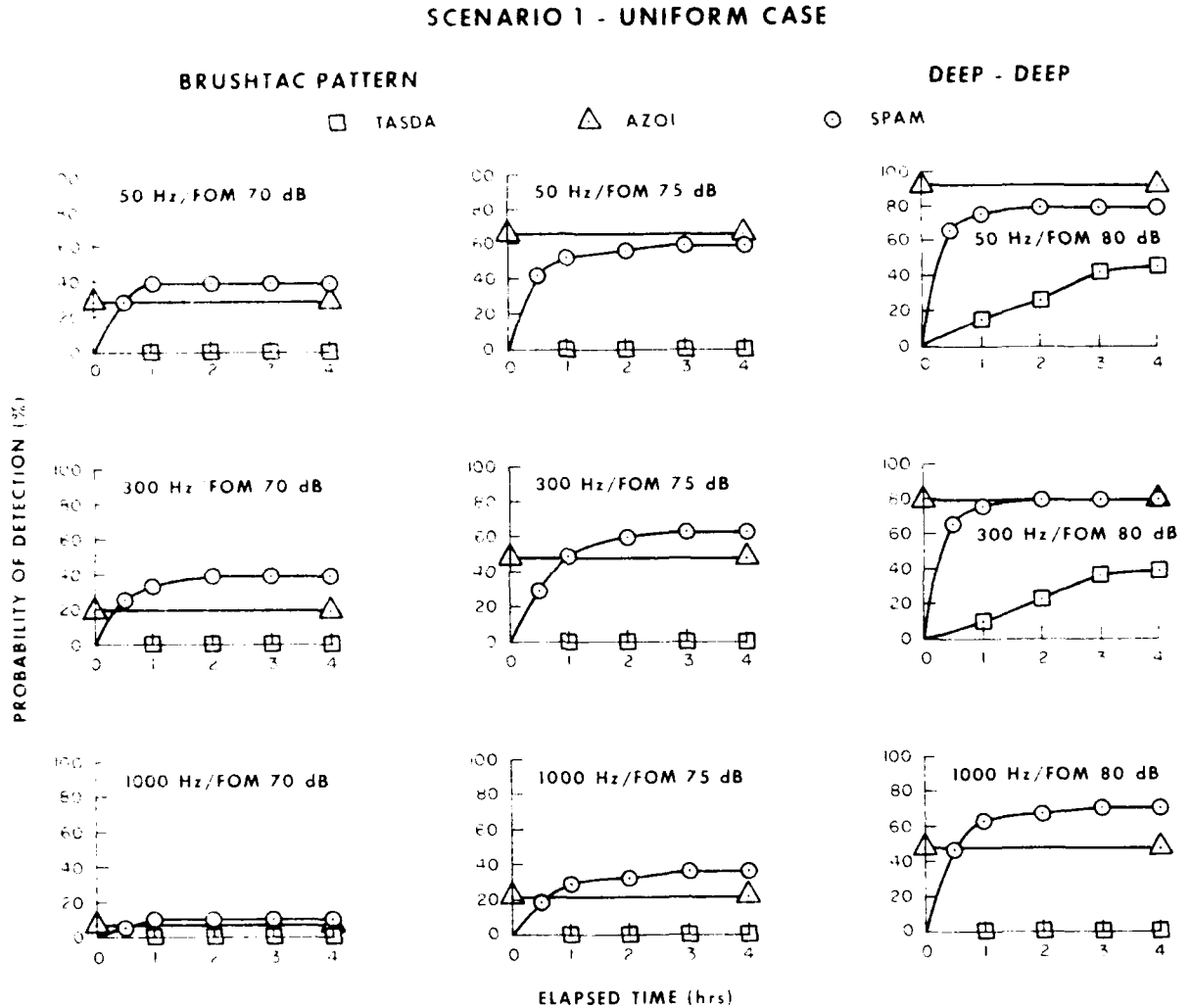

Figure C-12. Comparison of TASDA, AZOI and SPAM with a uniform initial target location of 30 minutes time late with a deep target and a deep receiver in scenario 1 using the brushtac pattern.

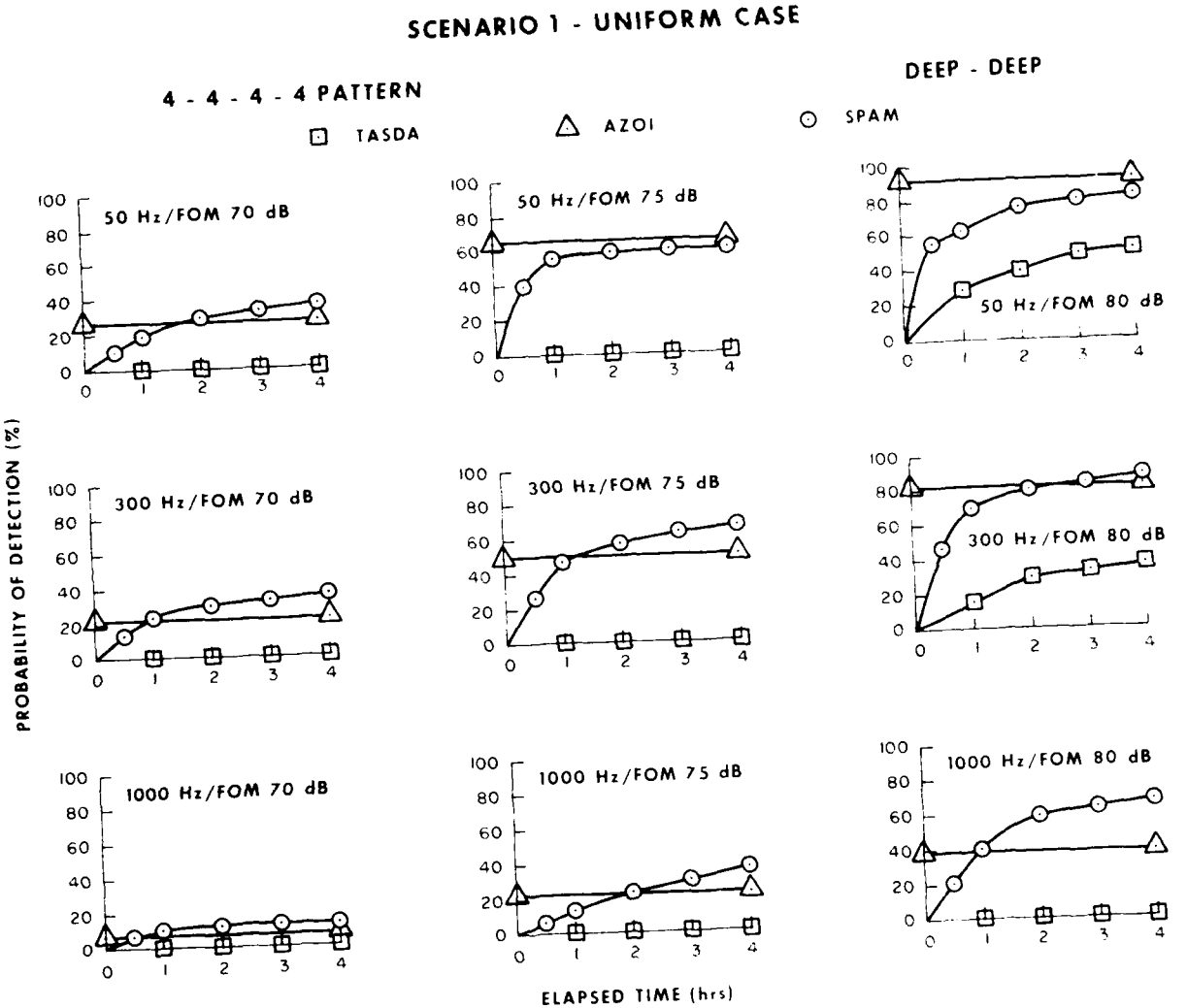

Figure C 13. Comparison of TASDA, AZOI and SPAM with a uniform initial target location at 30 minutes time late with a deep target and a deep receiver in scenario 1 using the 4 4 4 4 pattern.

SCENARIO 1 - UNIFORM CASE

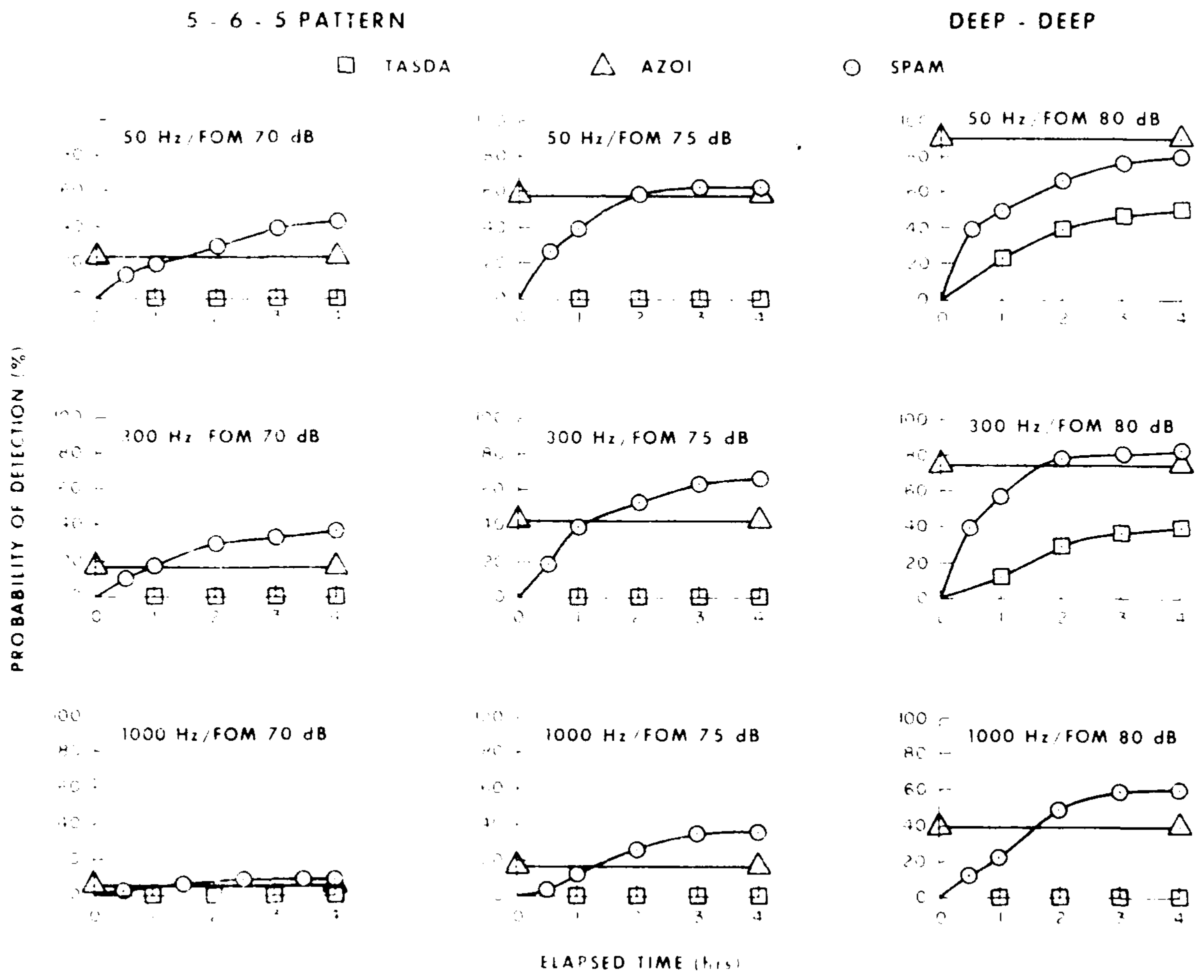

Figure C-[illegible] TASDA, AZOI and SPAM with a uniform initial [illegible] of 30 minutes time late with a deep target and [illegible] scenario 1 using the 5-6-5 pattern.

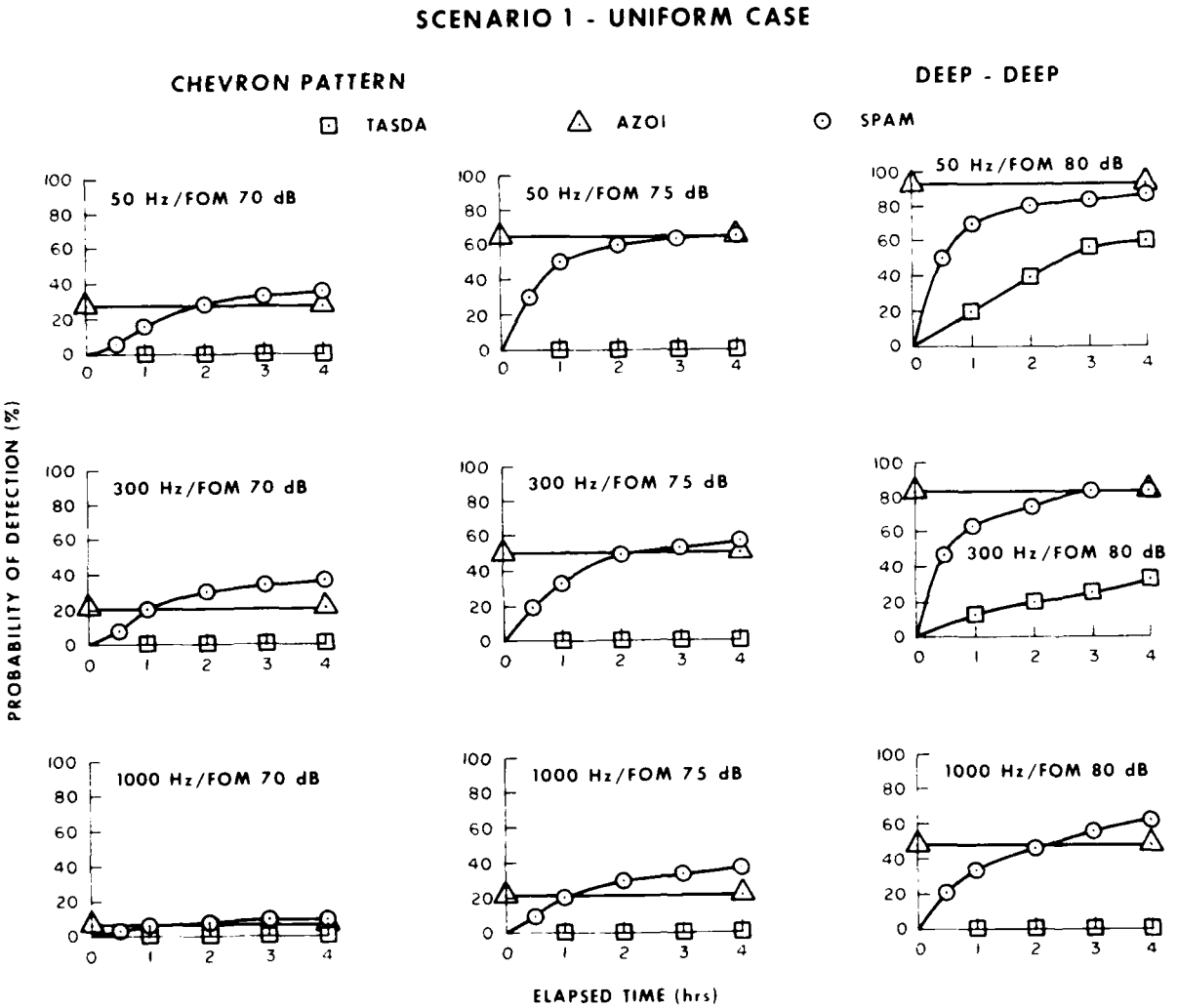

Figure C 15. Comparison of TASDA, AZOI and SPAM with a uniform initial target location at 30 minutes time late with a deep target and a deep receiver in scenario 1 using the chevron pattern.

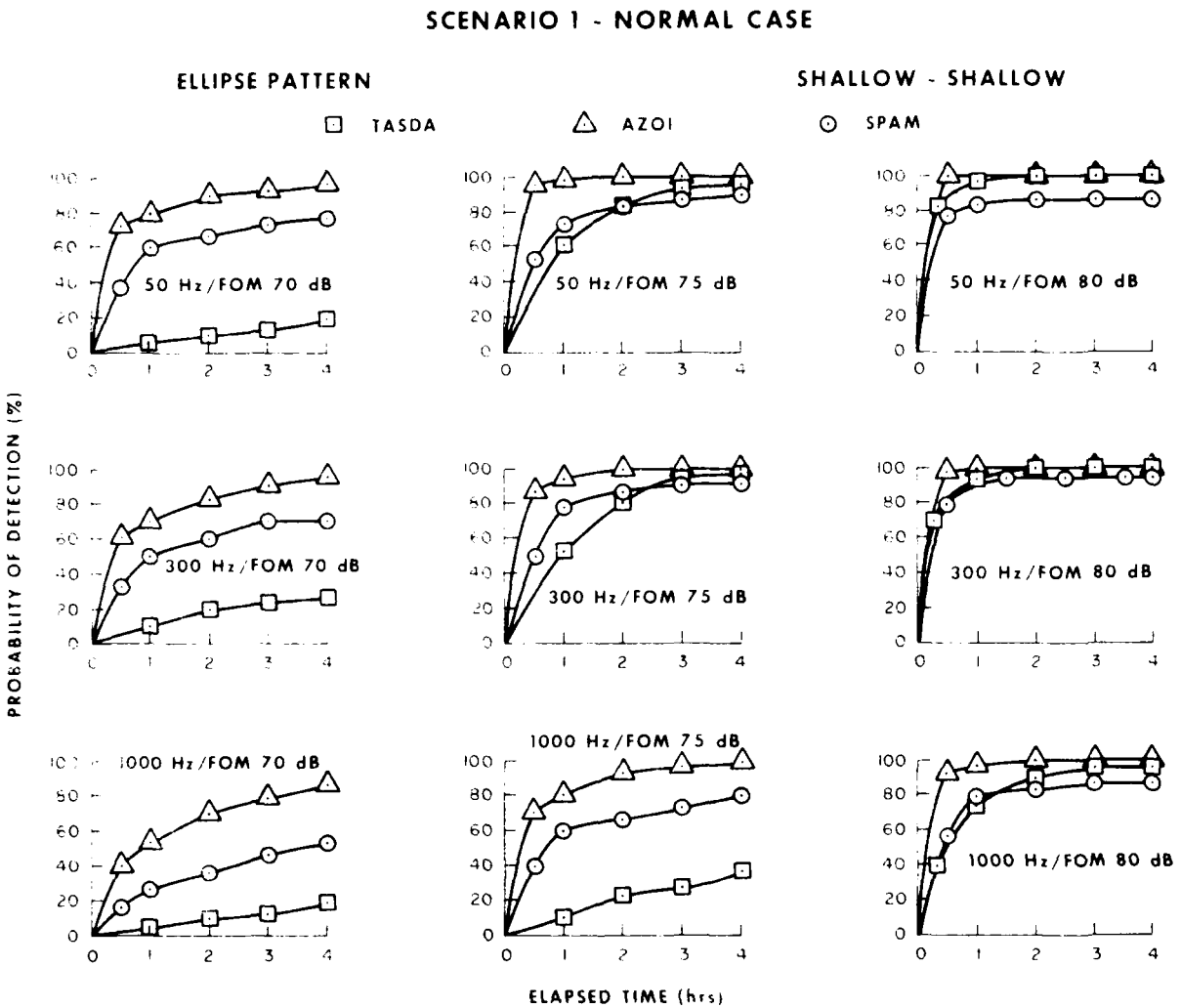

Figure C 16. Comparison of TASDA, AZOI and SPAM with a normal initial target location at 30 minutes time late with a shallow target and a shallow receiver in scenario 1 using the ellipse pattern.

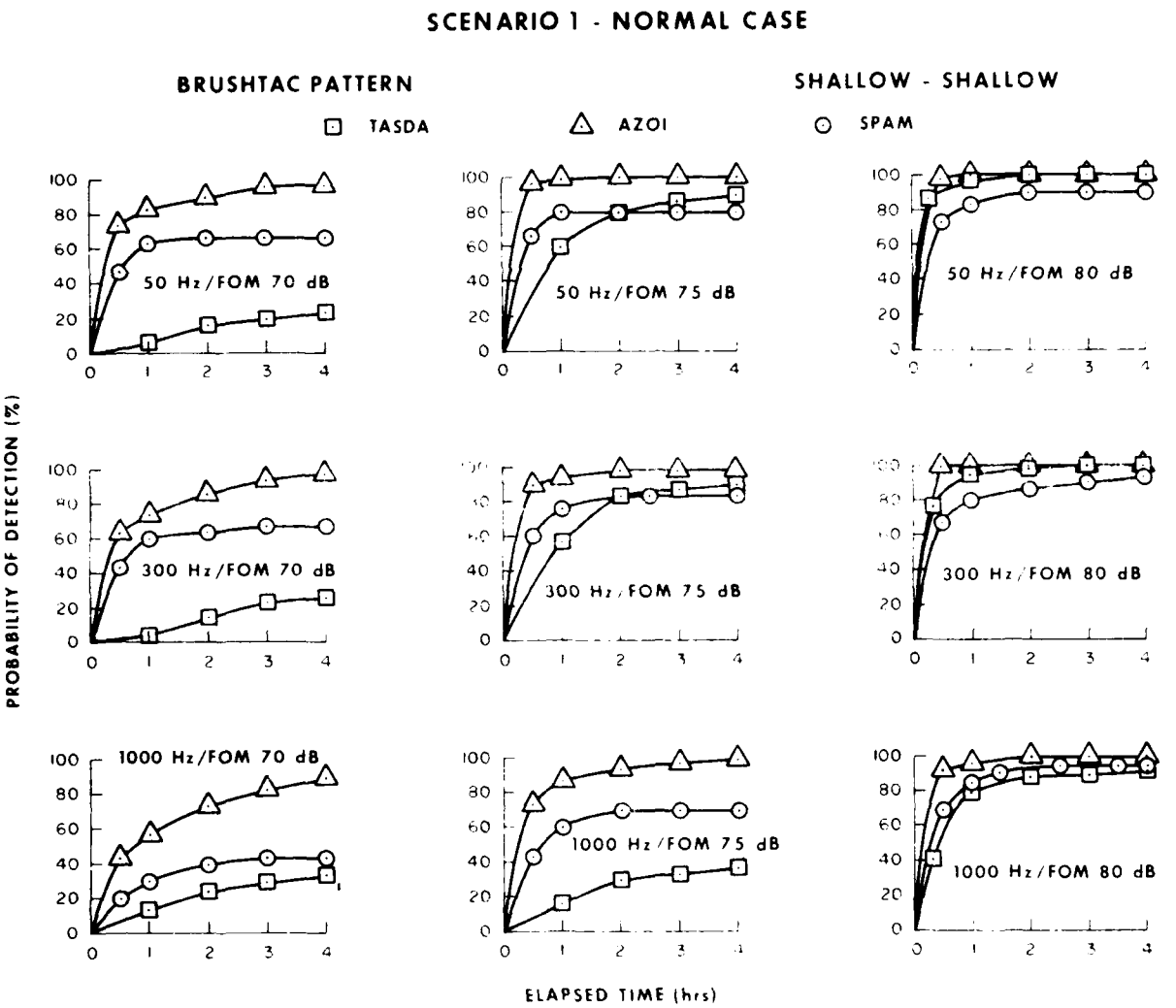

Figure C 17. Comparison of TASDA, AZOI and SPAM with a uniform initial target location at 30 minutes for Late with a deep target and a deep receiver in scenario 1 using the brushtac pattern.

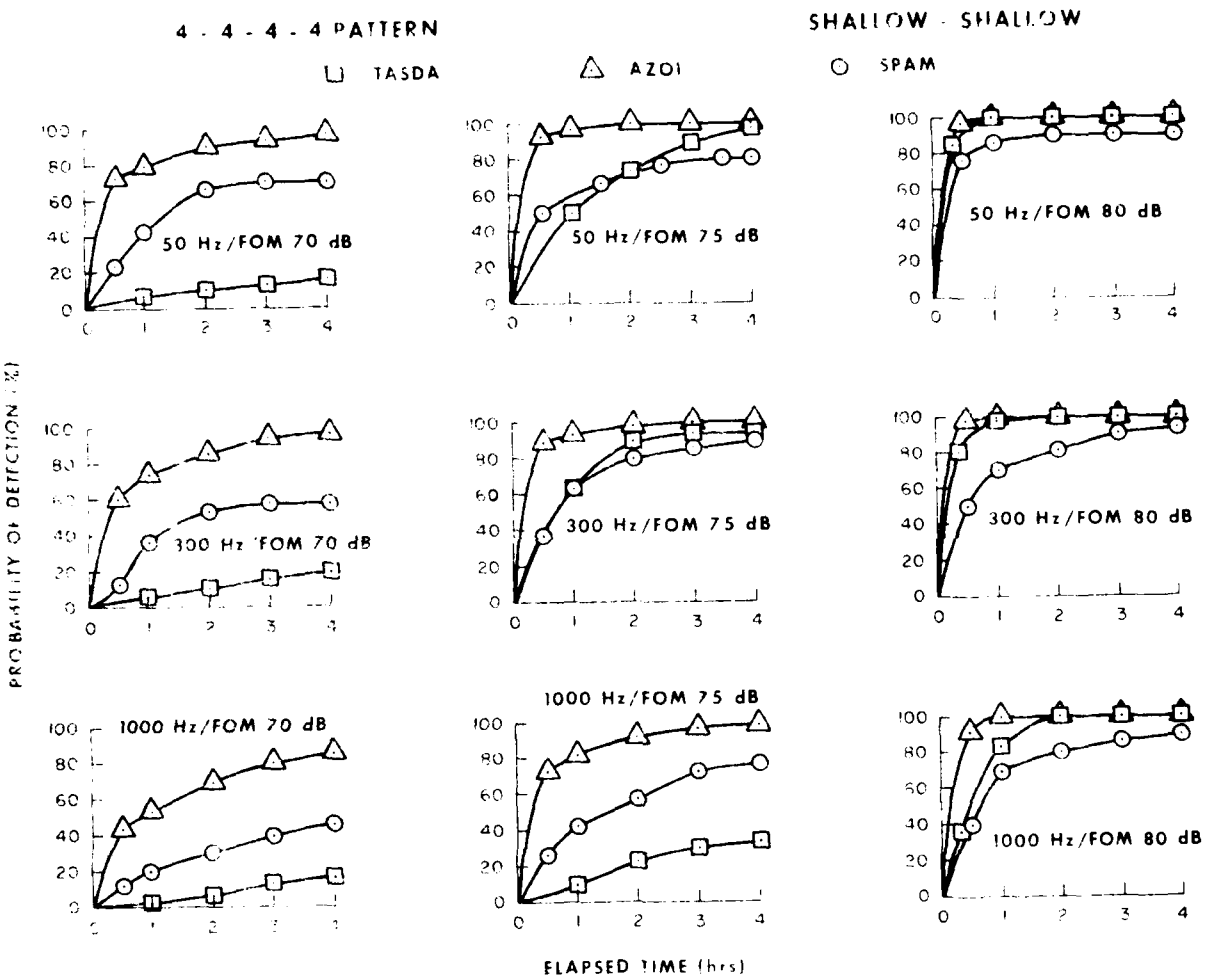

Figure C18. Comparison of TASDA, AZOI and SPAM with a normal initial target location at 30 minutes time late with a shallow target and a shallow receiver in scenario I using the 4 - 4 - 4 - 4 pattern.

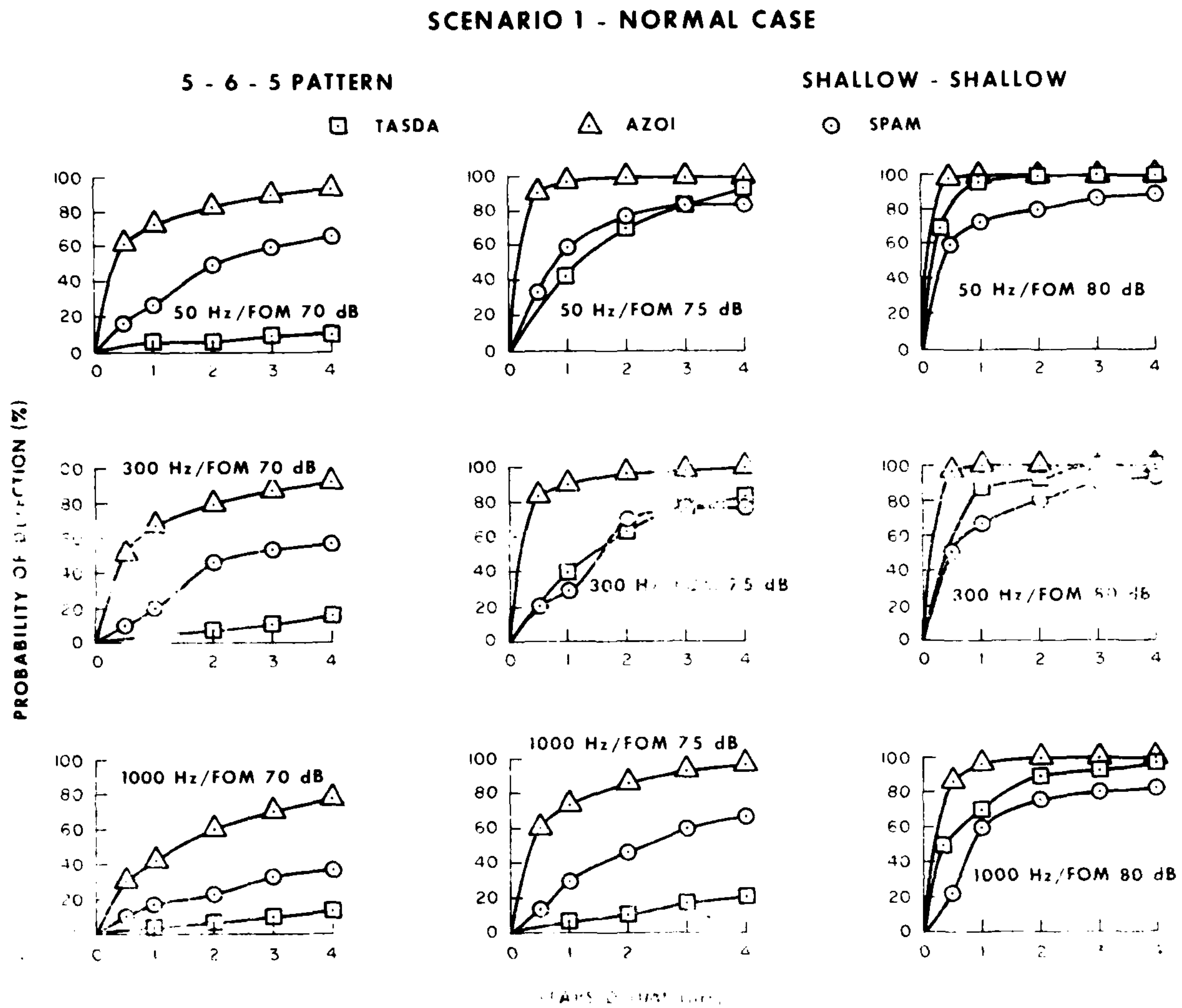

Figure C-19. Comparison of TASDA, AZOI and SPAM with a [illegible] [illegible] [illegible] 1 30 minutes time late with a shallow [illegible] [illegible] receiver in scenario 1 using the 5-6-5 pattern.

SCENARIO 1 - NORMAL CASE

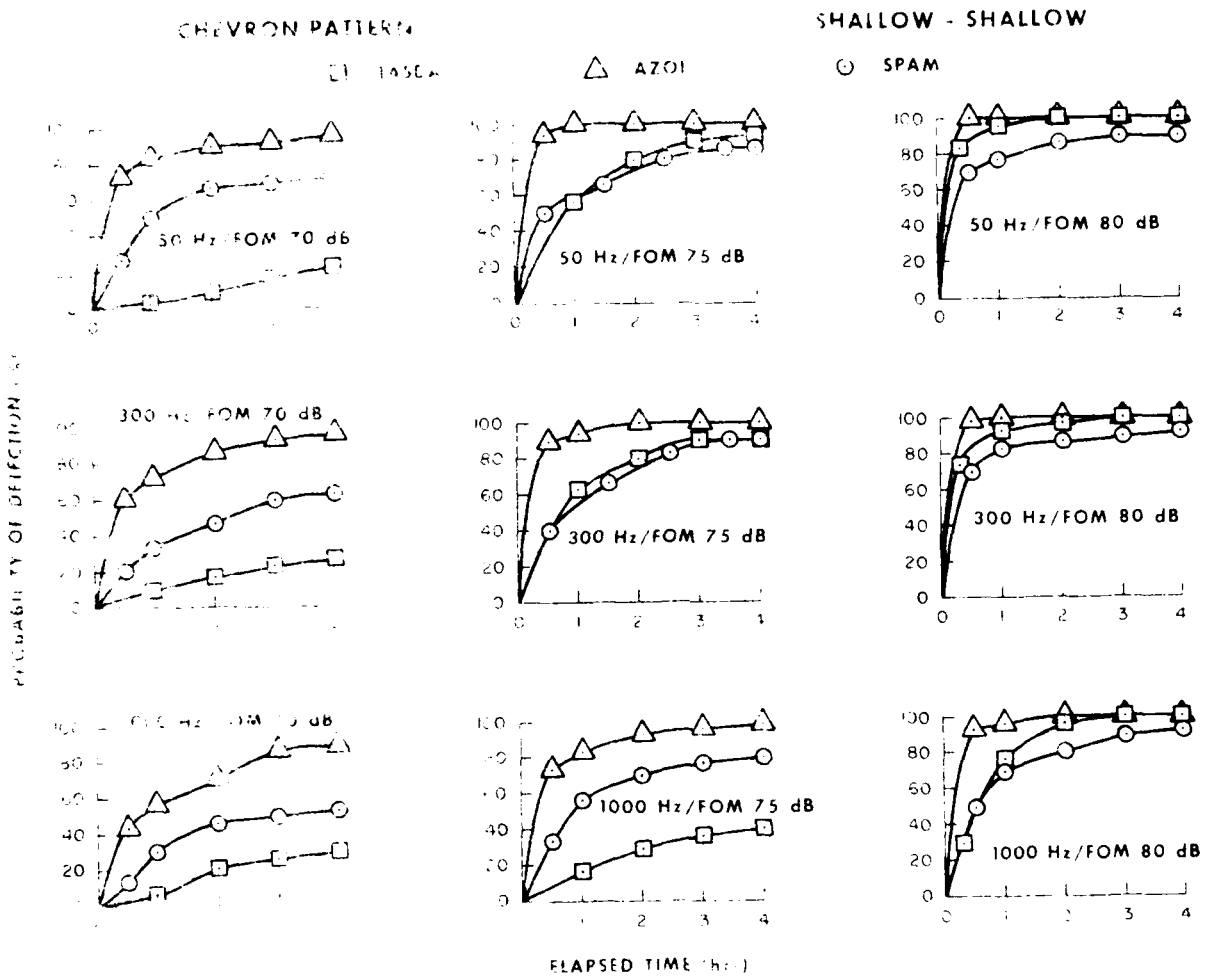

Figure [illegible] ASDA, AZOI and SPAM with normal initial [illegible]

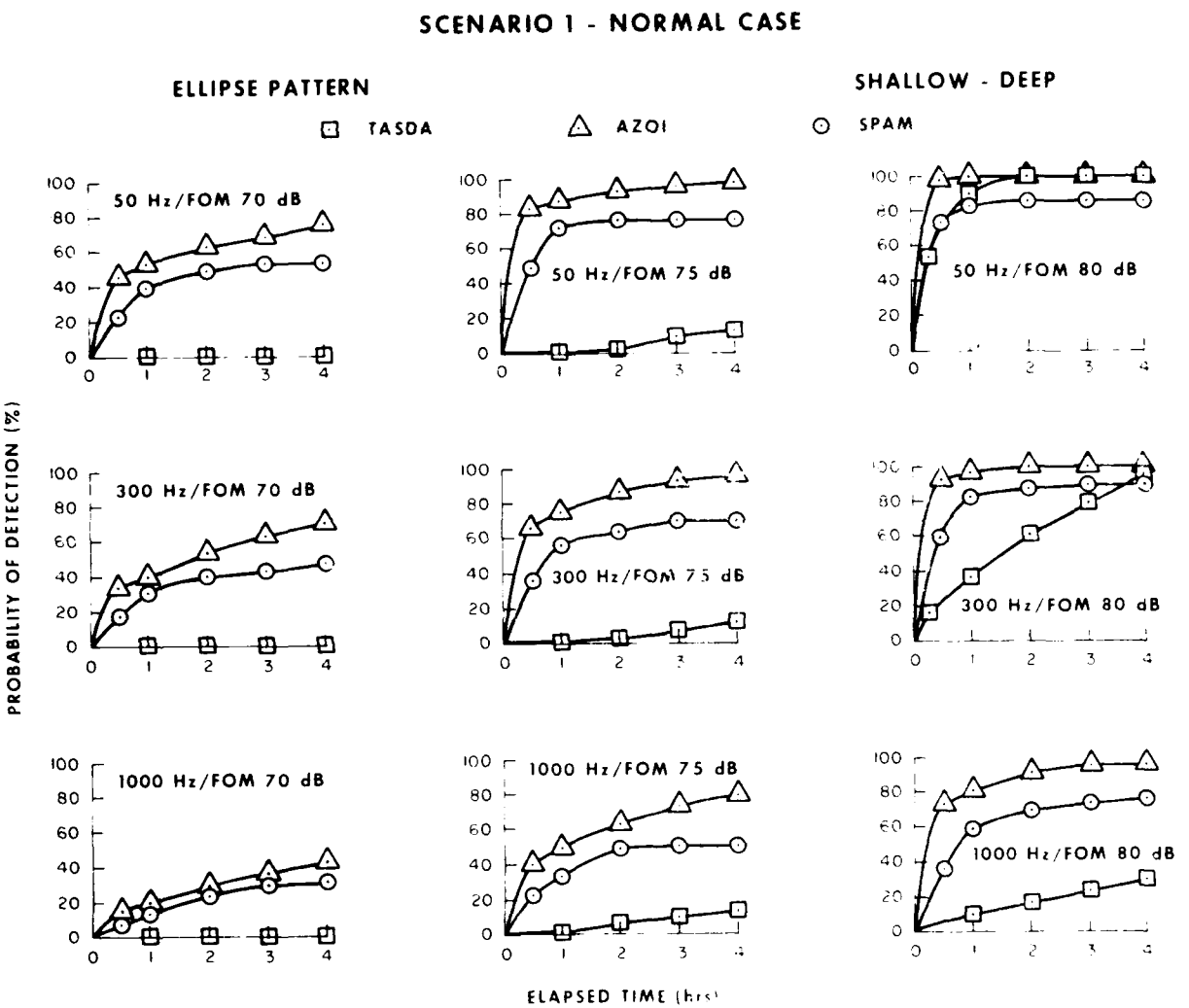

Figure C 21. Comparison of TASDA, AZOI and SPAM with a range of initial target location at 30 minutes time late with a shallow deep target receiver combination in scenario 1 using the ellipse patter

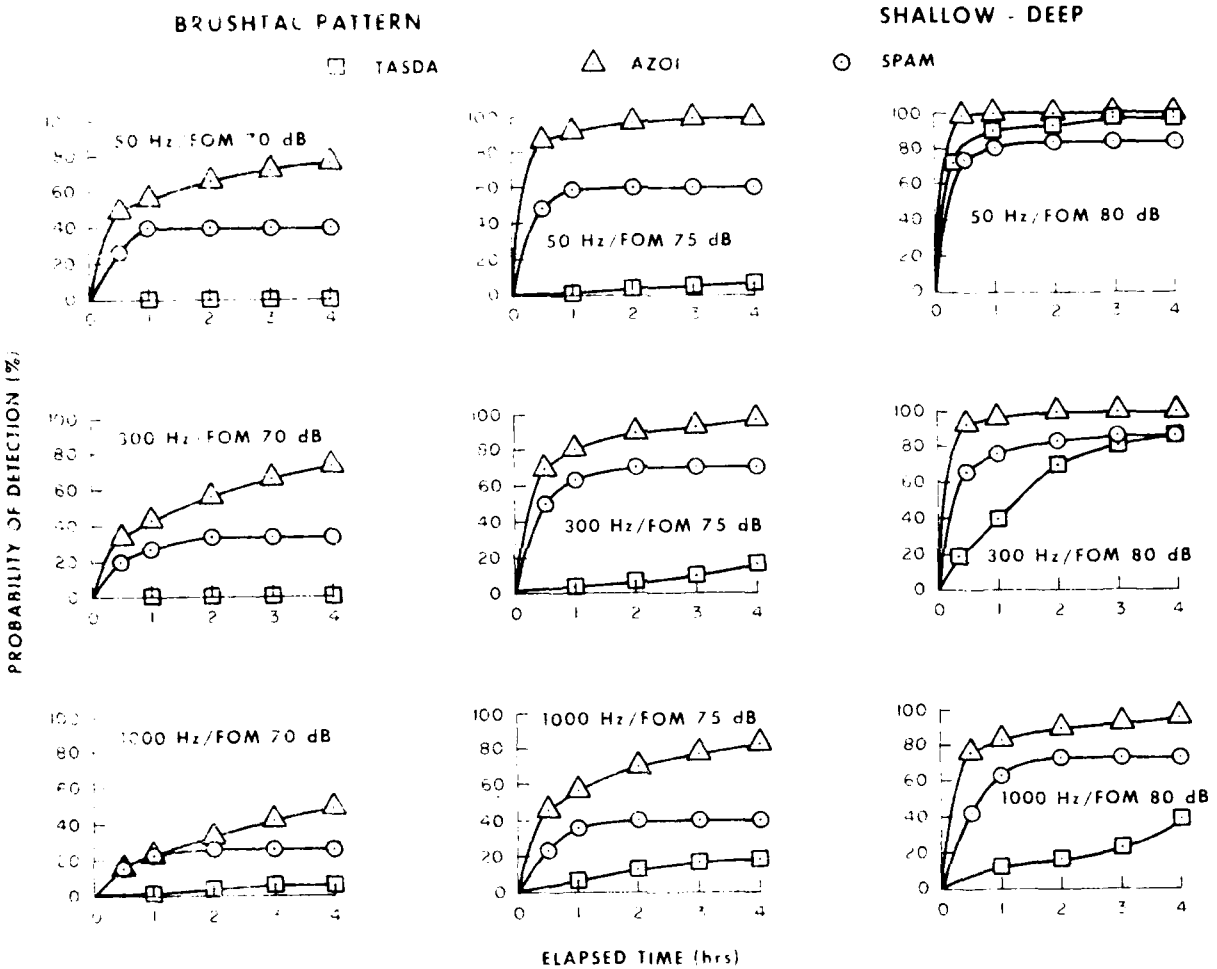

Figure [illegible] 22. Comparison of TASDA, AZOI and SPAM with a normal initial target location at 30 minutes time late with a shallow deep target receiver combination in scenario 1 using the brushtac pattern.

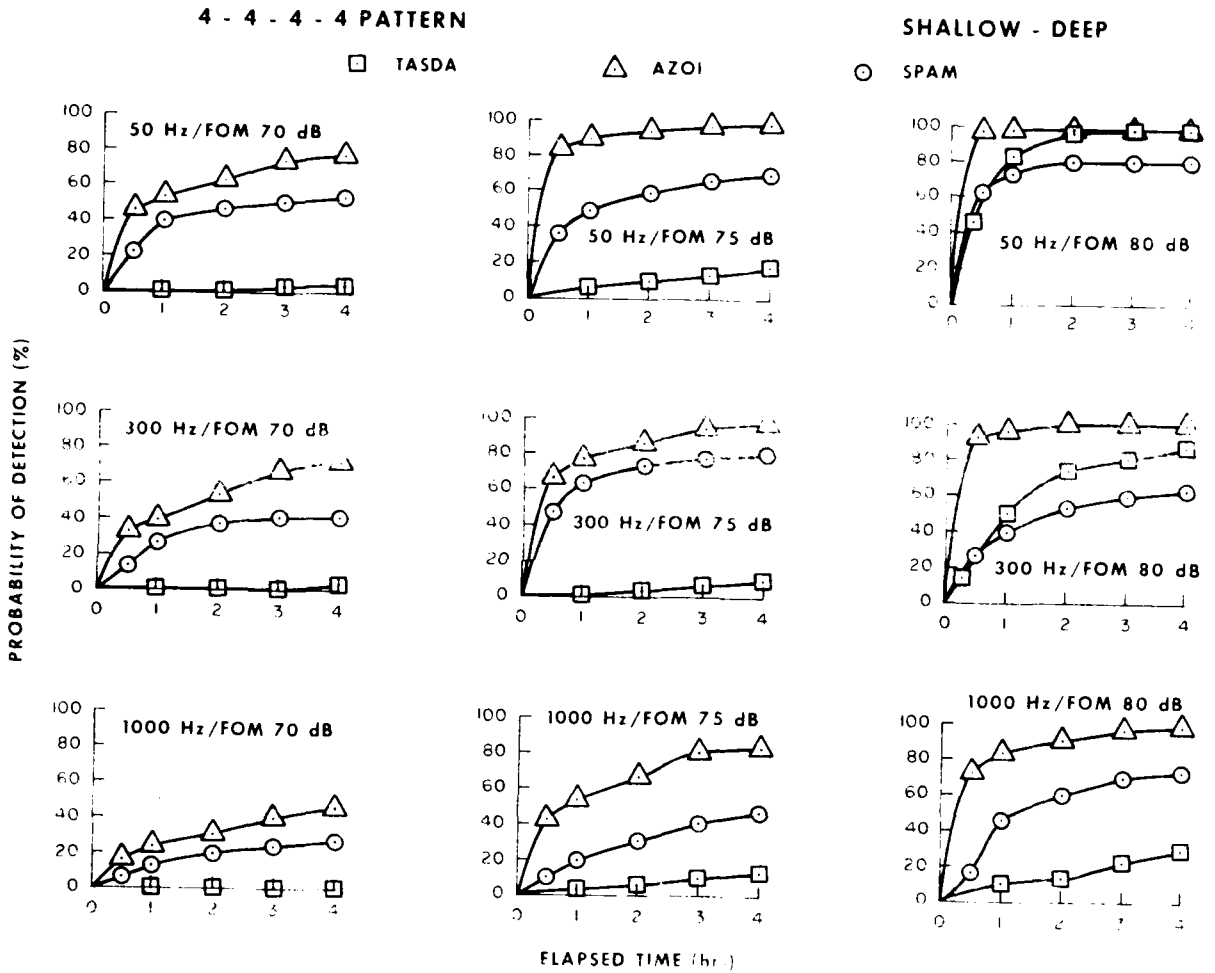

Figure 23. Comparison of TASDA, AZOI and SPAM with a normal initial target location at 30 minute time late with a shallow-deep target receiver combination in scenario 1

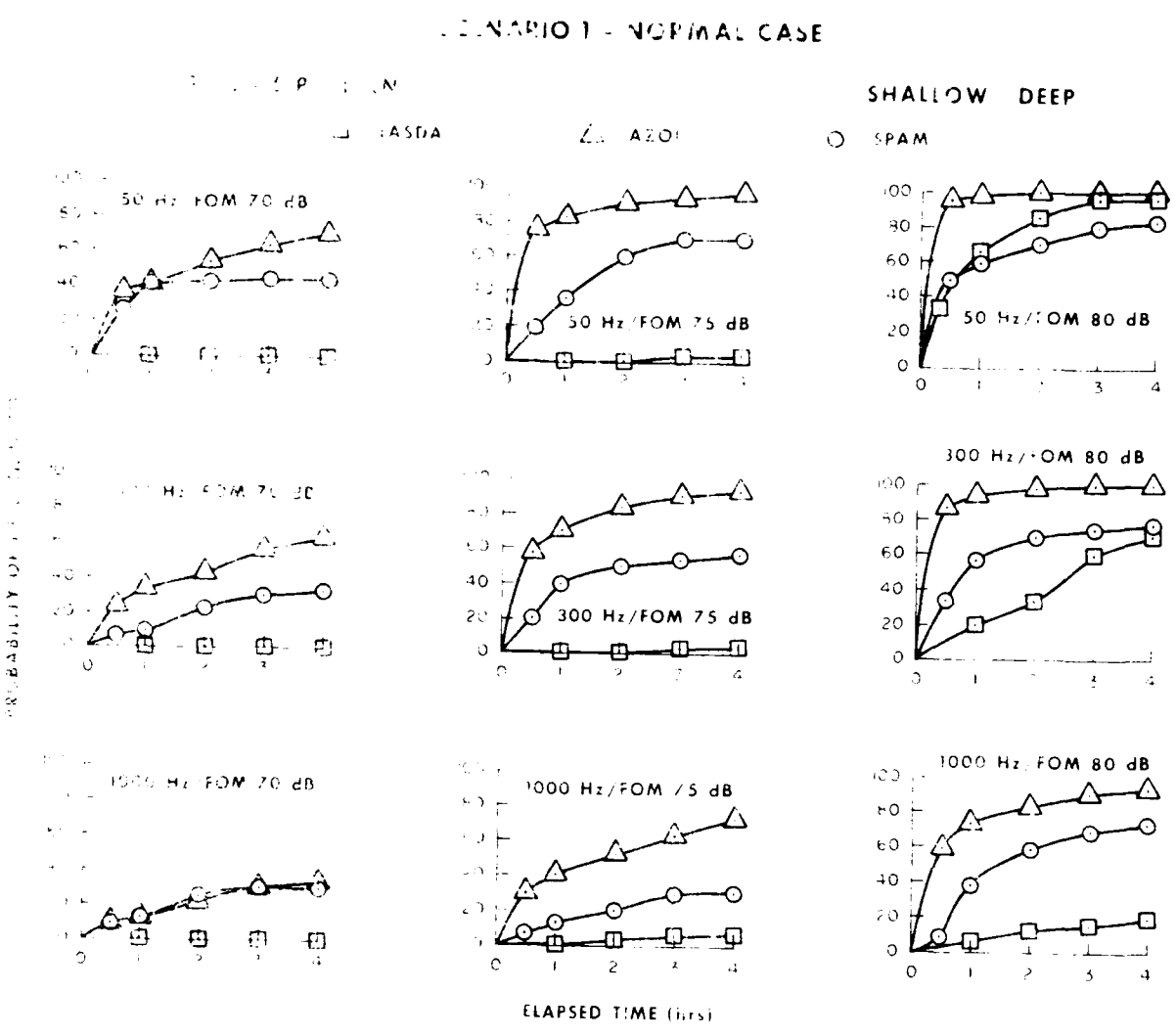

[illegible] of TASDA, AZOI and SPAM with a normal initial location at 30 minutes time late with a shallow deep receiver combination in Scenario 1 using the 5/6 s pattern.

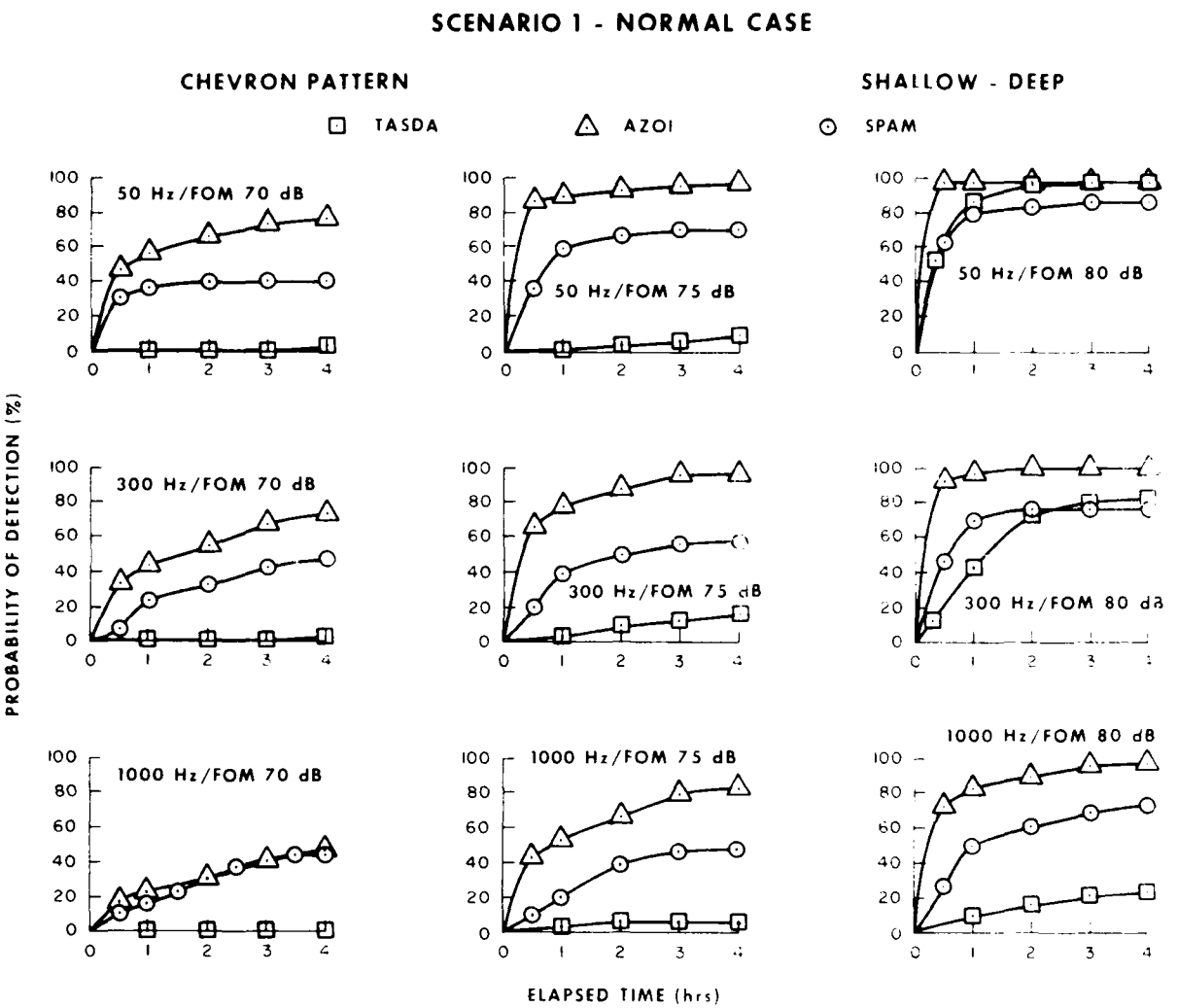

Figure C 25. Comparison of TASDA, AZOI and SPAM with a normal initial target location at 30 minutes time late with a shallow deep target receiver combination in scenario 1 using the chevron pat

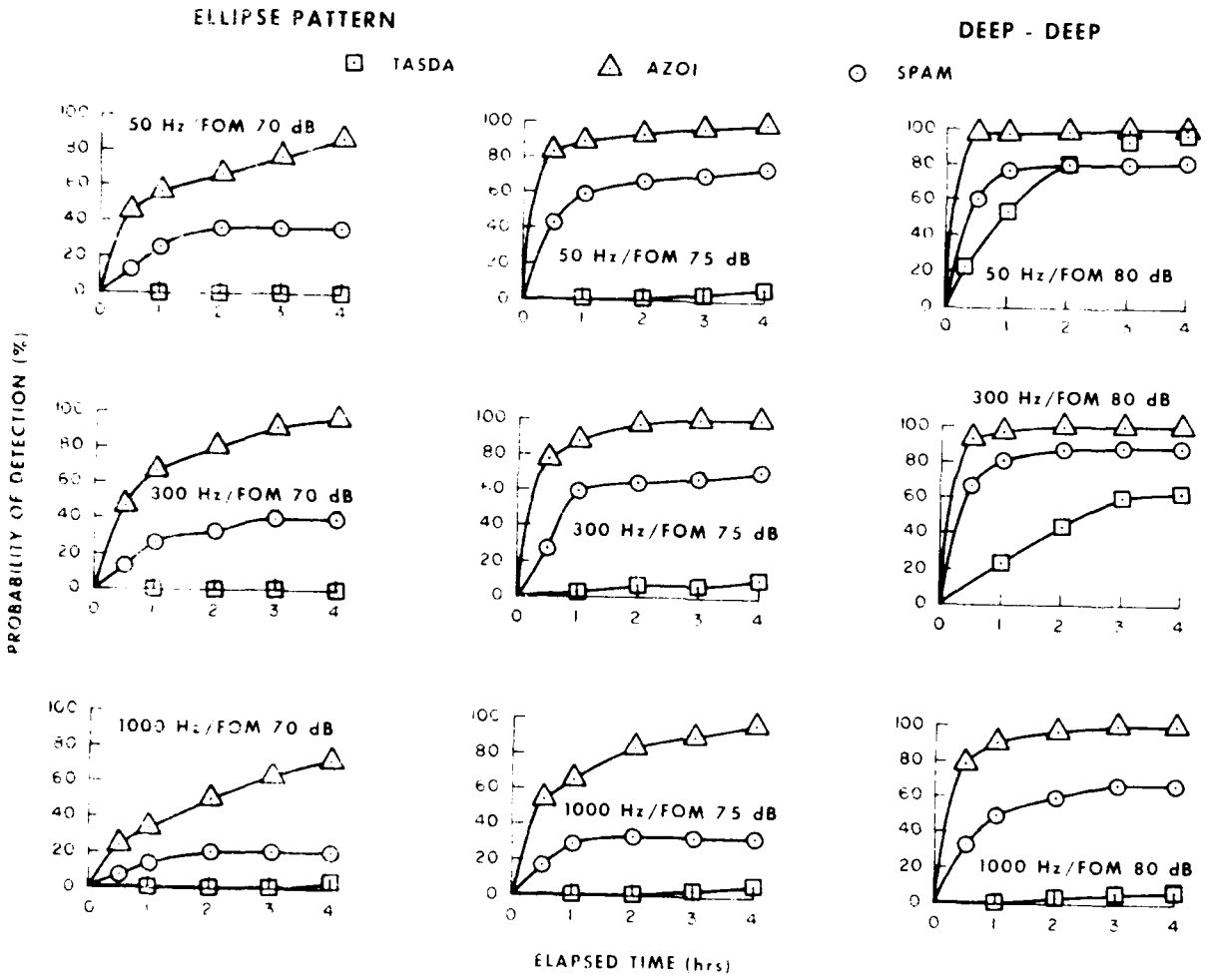

Figure C-26. Comparison of TASDA, AZOI and SPAM with a normal initial target location at 30 minutes late with a deep barrier and a [illegible] coverage under the ellipse pattern.

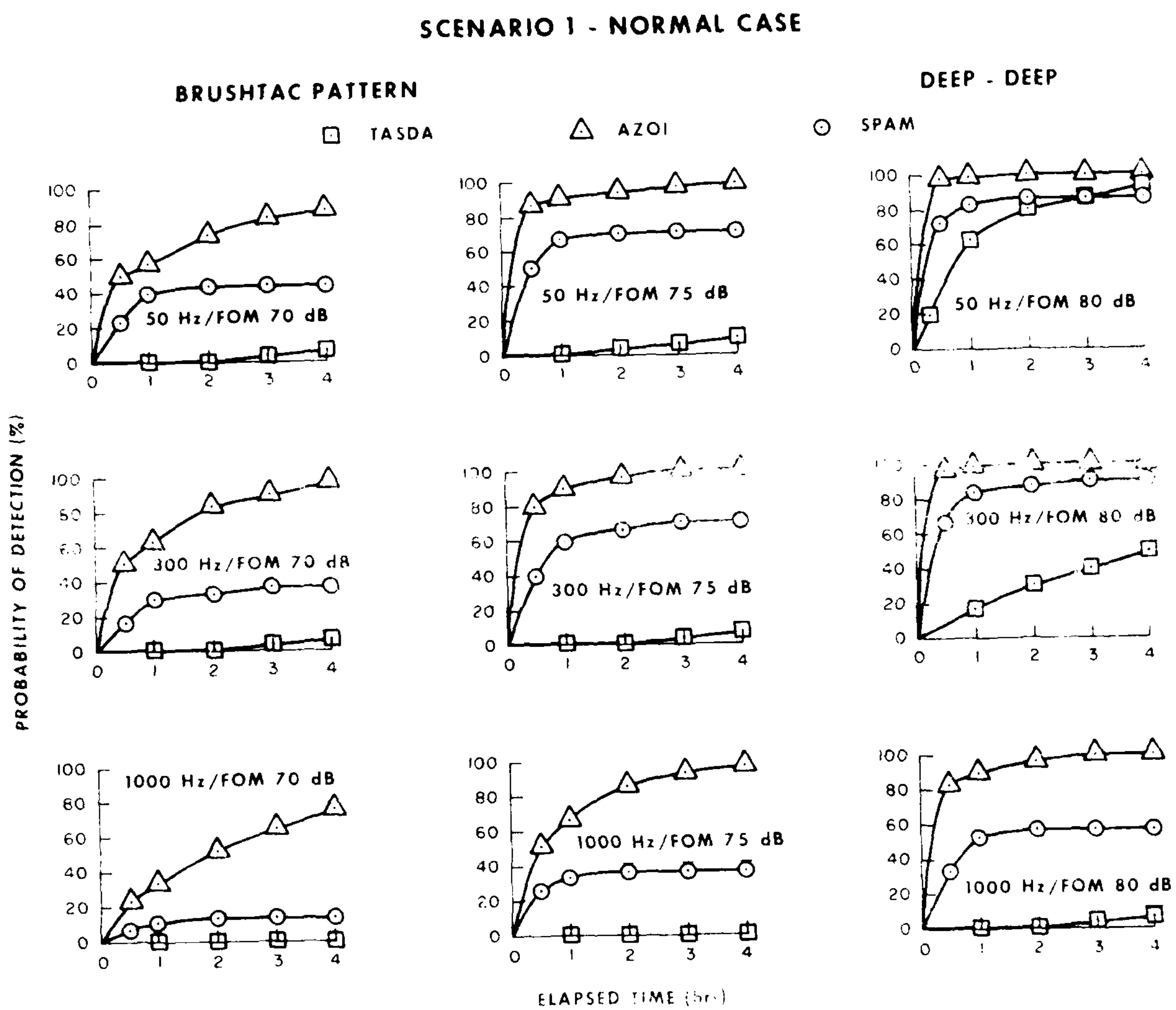

Figure C-2[illegible] Comparison of TASDA, AZOI, [illegible] SPAM [illegible] target location at 30 minutes [illegible] a deep target and a deep receiver in scenario [illegible] using the brushtac pattern.

[illegible] NORMAL CASE

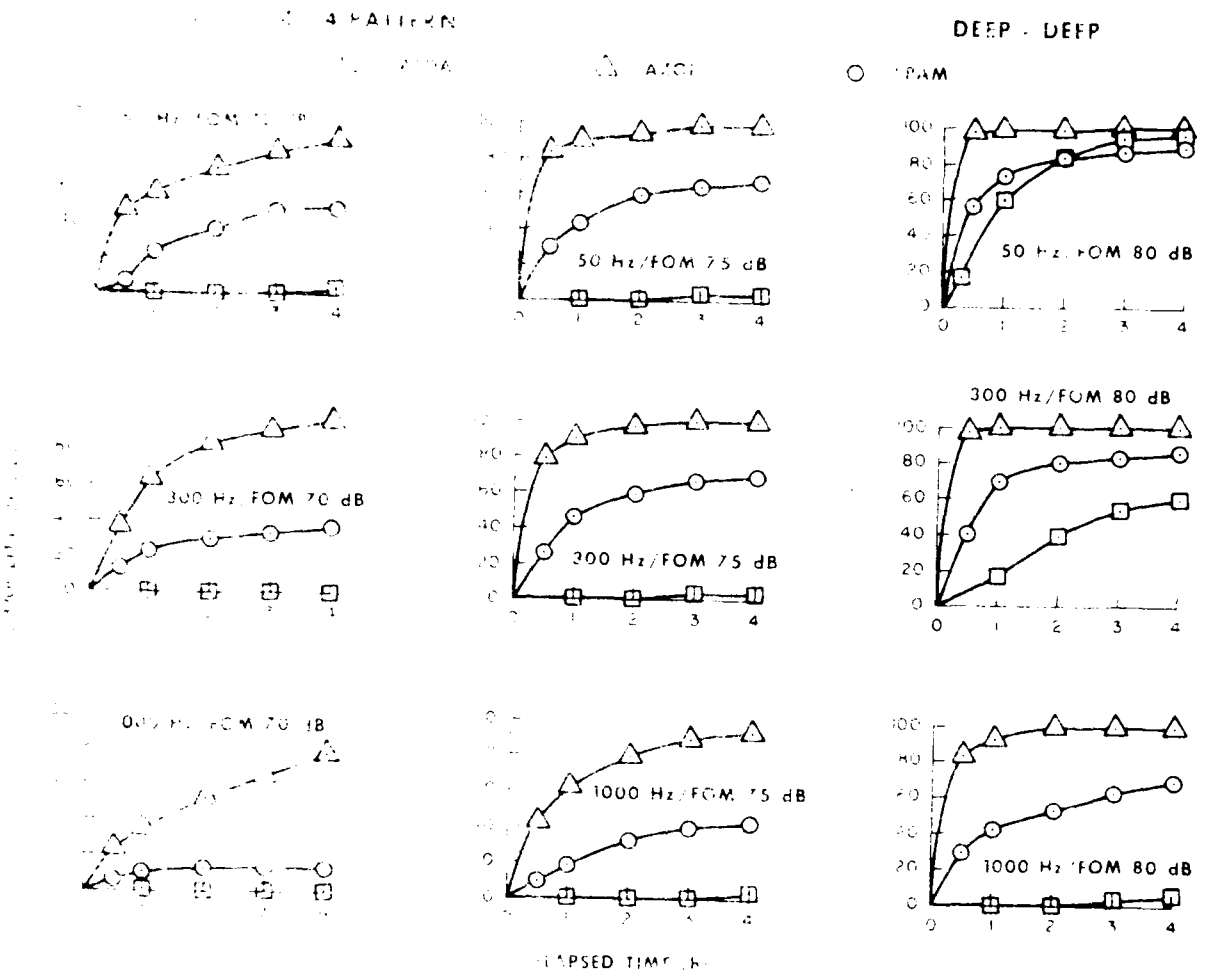
DEEP - DEEP
50 Hz/FOM 75 dB
50 Hz/FOM 80 dB
300 Hz/FOM 80 dB
300 Hz/FOM 75 dB
1000 Hz/FOM 75 dB
1000 Hz/FOM 80 dB

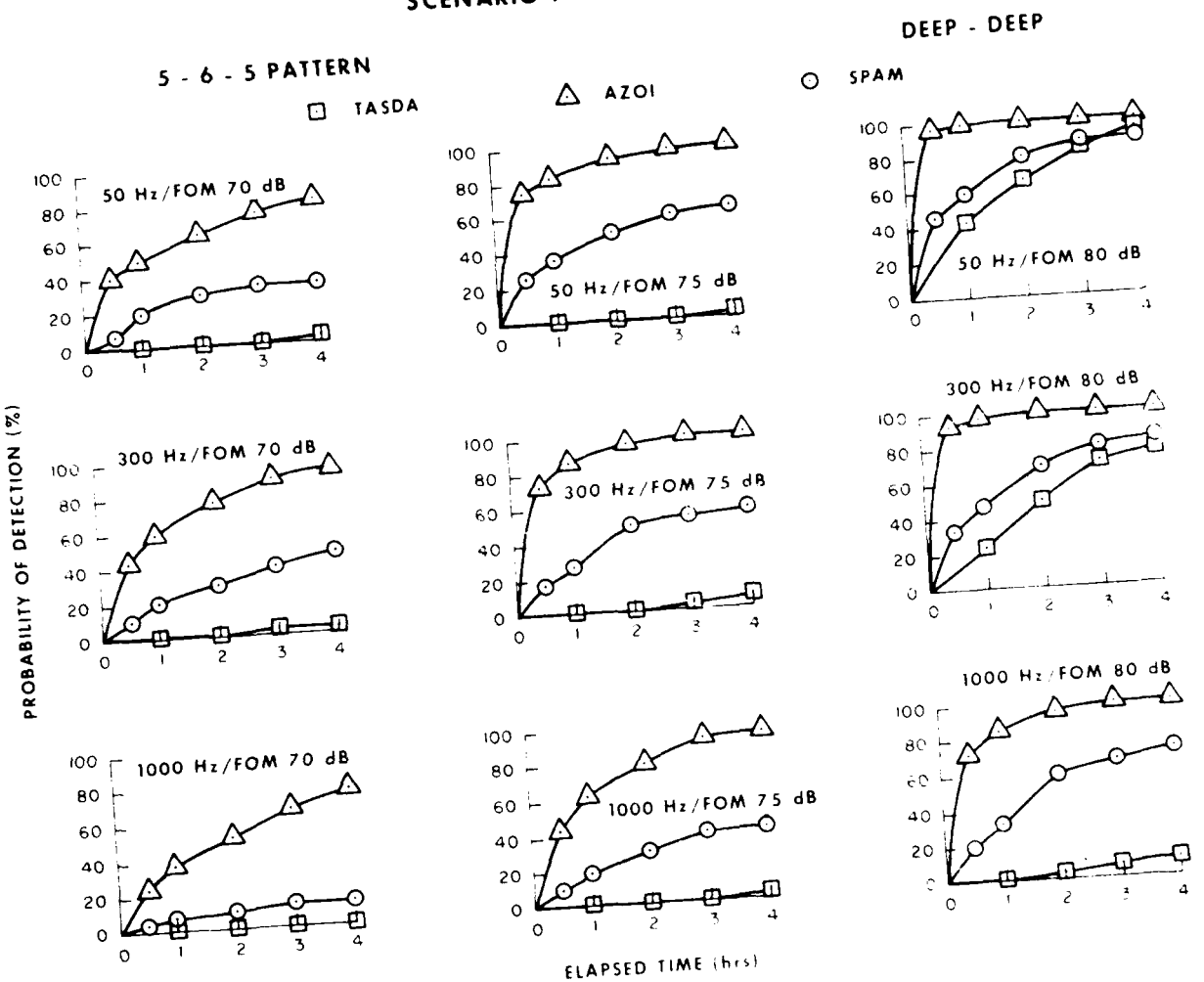

Figure C 29. Comparison of TASDA, AZO[illegible] AJ[illegible] initial target location at 30 minute[illegible] and a deep receiver in scenario 1 using the 5 - 6 - 5 pattern.

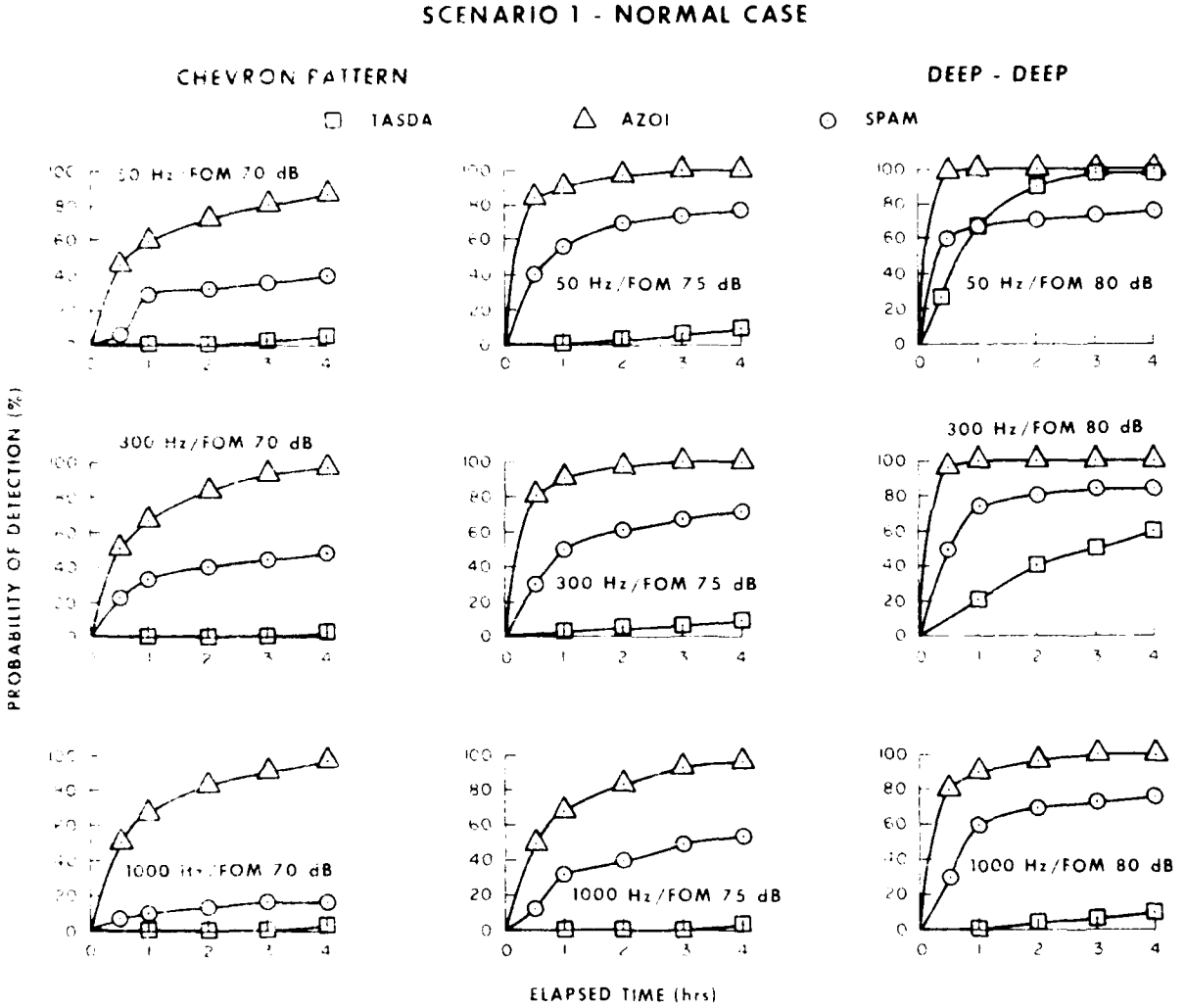

Figure C-30. Comparison of TASDA, AZOI and SPAM with a normal initial target location at 30 minutes time late with a deep target ... a deep receiver in scenario 1 using the chevron pattern.

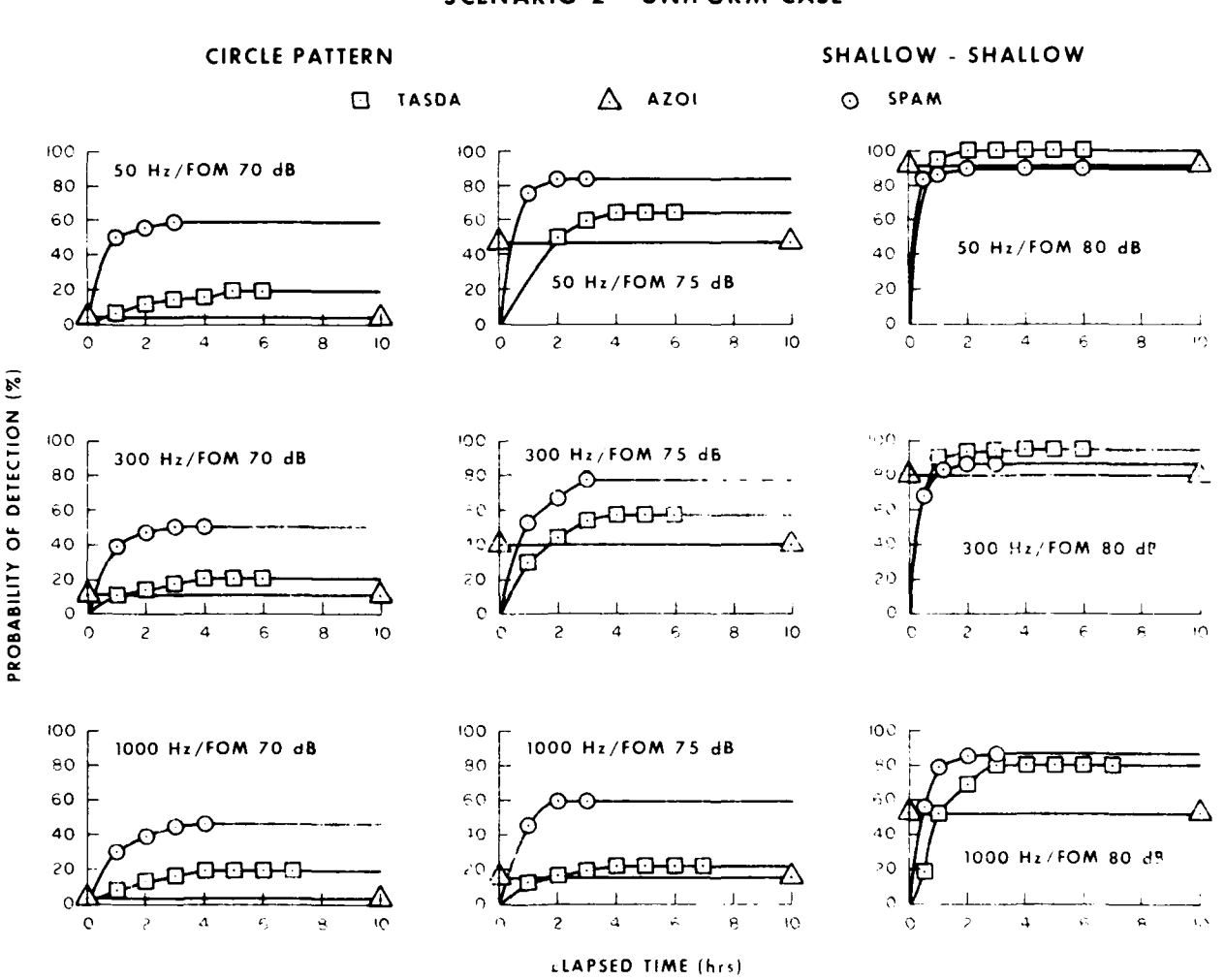

Figure C-31. [illegible] TASDA, AZOI [illegible] initial target location at one hour time late with a shallow target and a shallow receiver in scenario 2 using the circle pattern.

SCENARIO 2 - UNIFORM CASE

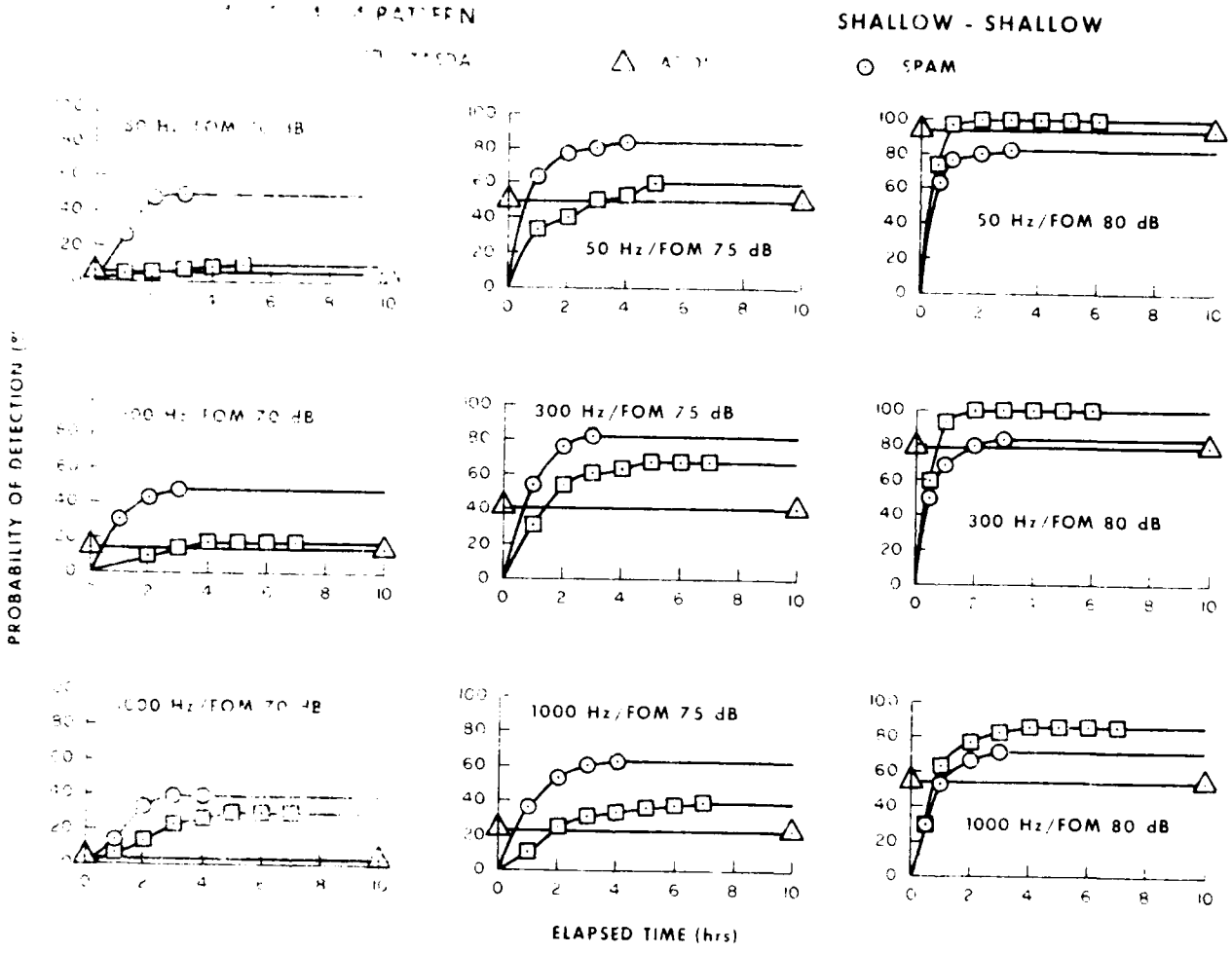

- Comparison of TASDA, AZOI and SPAM with a uniform initial target location at one hour time late with a shallow target and shallow receiver in scenario 2 using the 4 4 4 4 pattern.

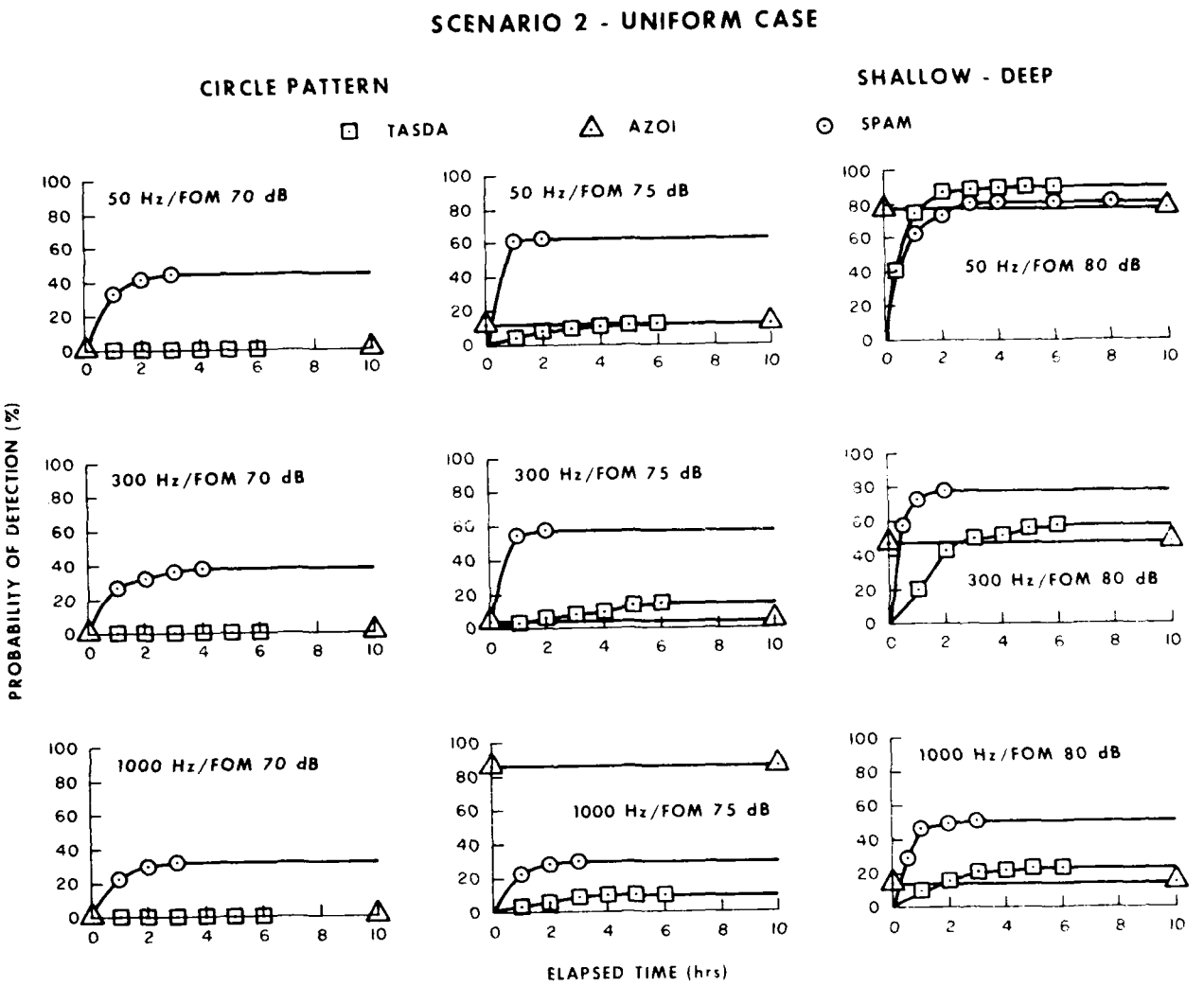

Figure C 33. Comparison of TASDA, AZOI and SPAM with a uniform initial target location at one hour time late with a shallow-deep target receiver combination in scenario 2 using the circle pattern.

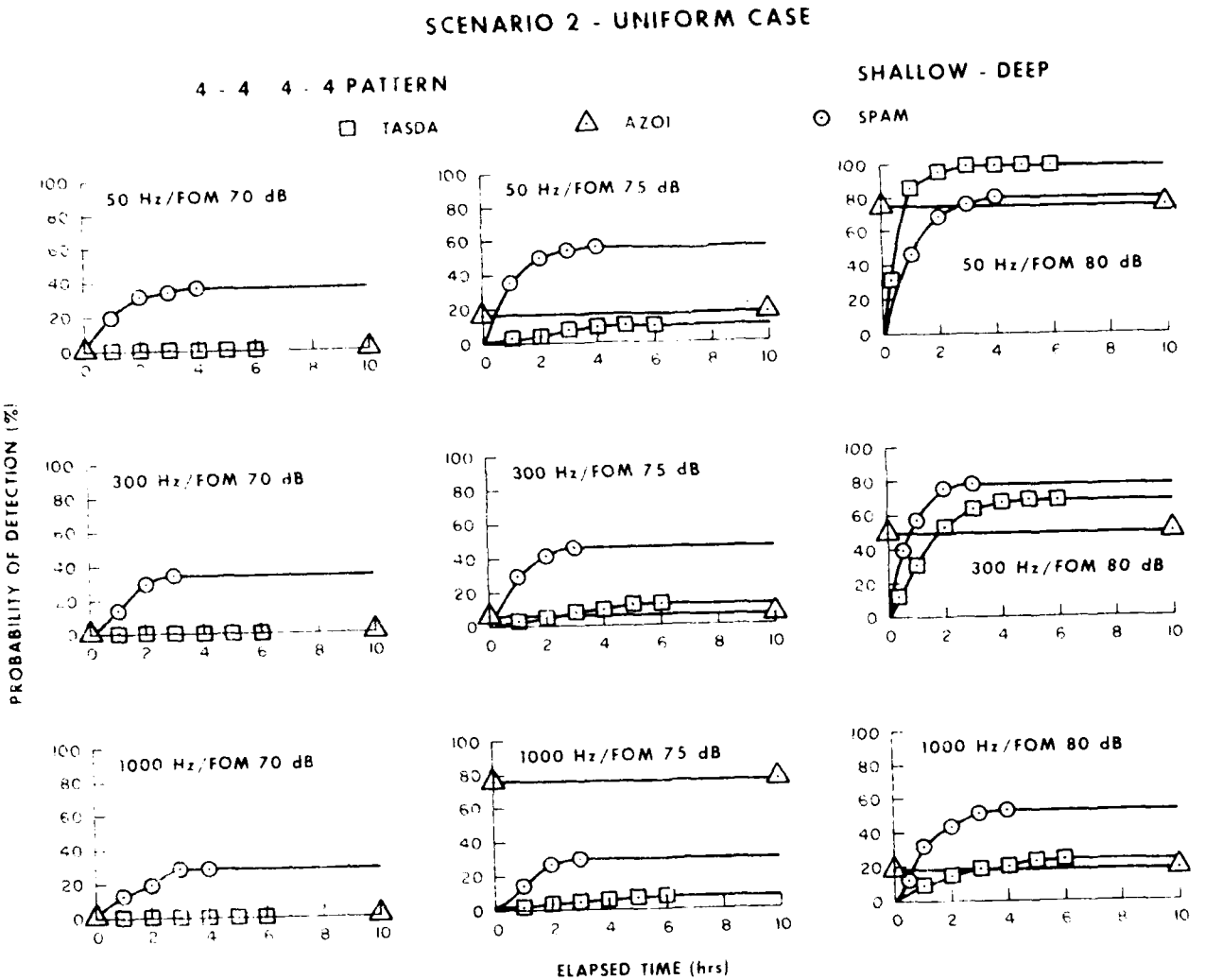

Figure C 34. Comparison of TASDA, AZOI and SPAM with a uniform initial target location at one hour time late with a shallow deep target receiver combination in scenario 2 using the 4 4 4 4 pattern.

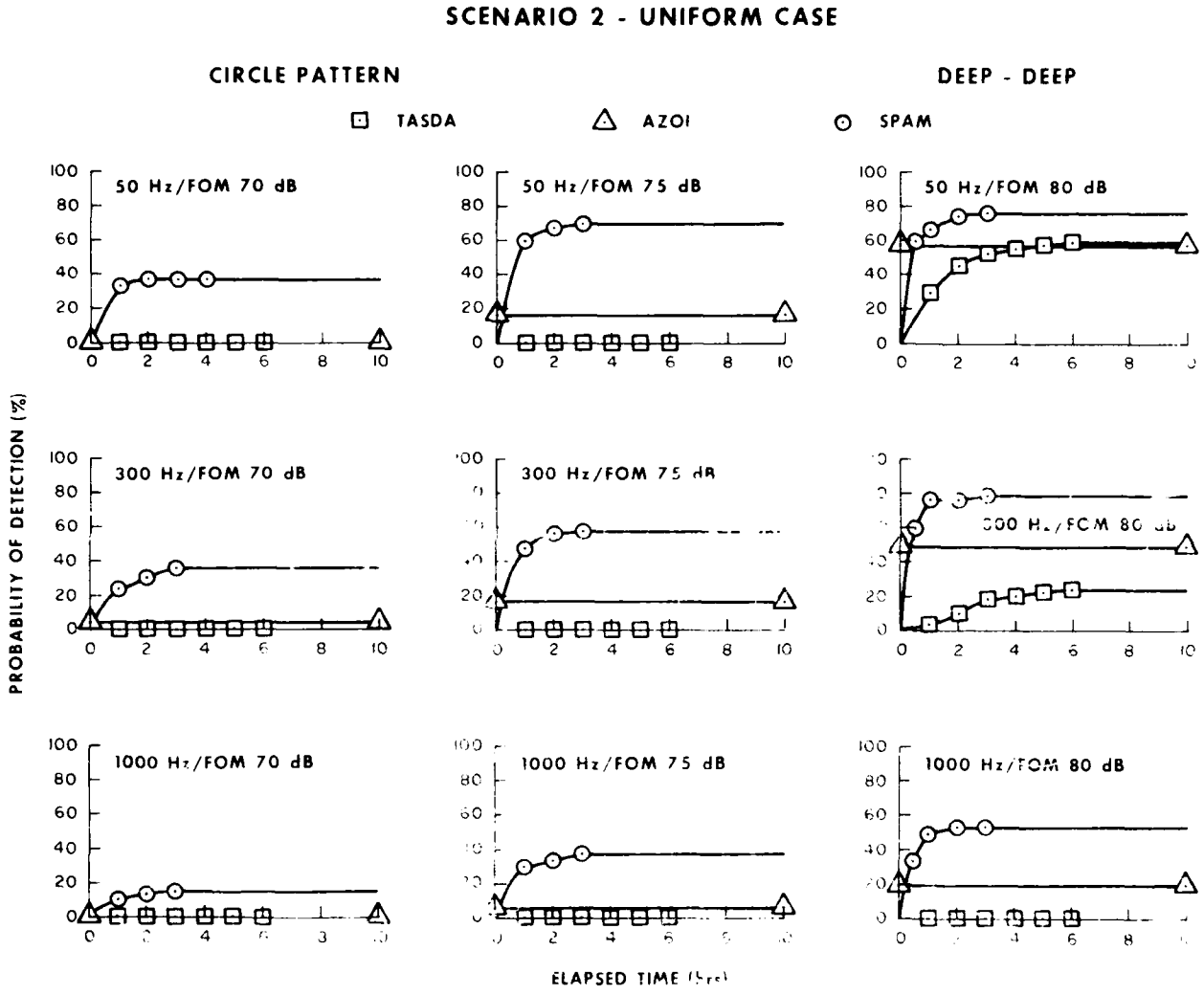

Figure C. 35. Comparison of TASDA, AZOI and SPAM with a uniform initial target location at one hour time late with a deep target and a deep receiver in scenario 2 with circle pattern

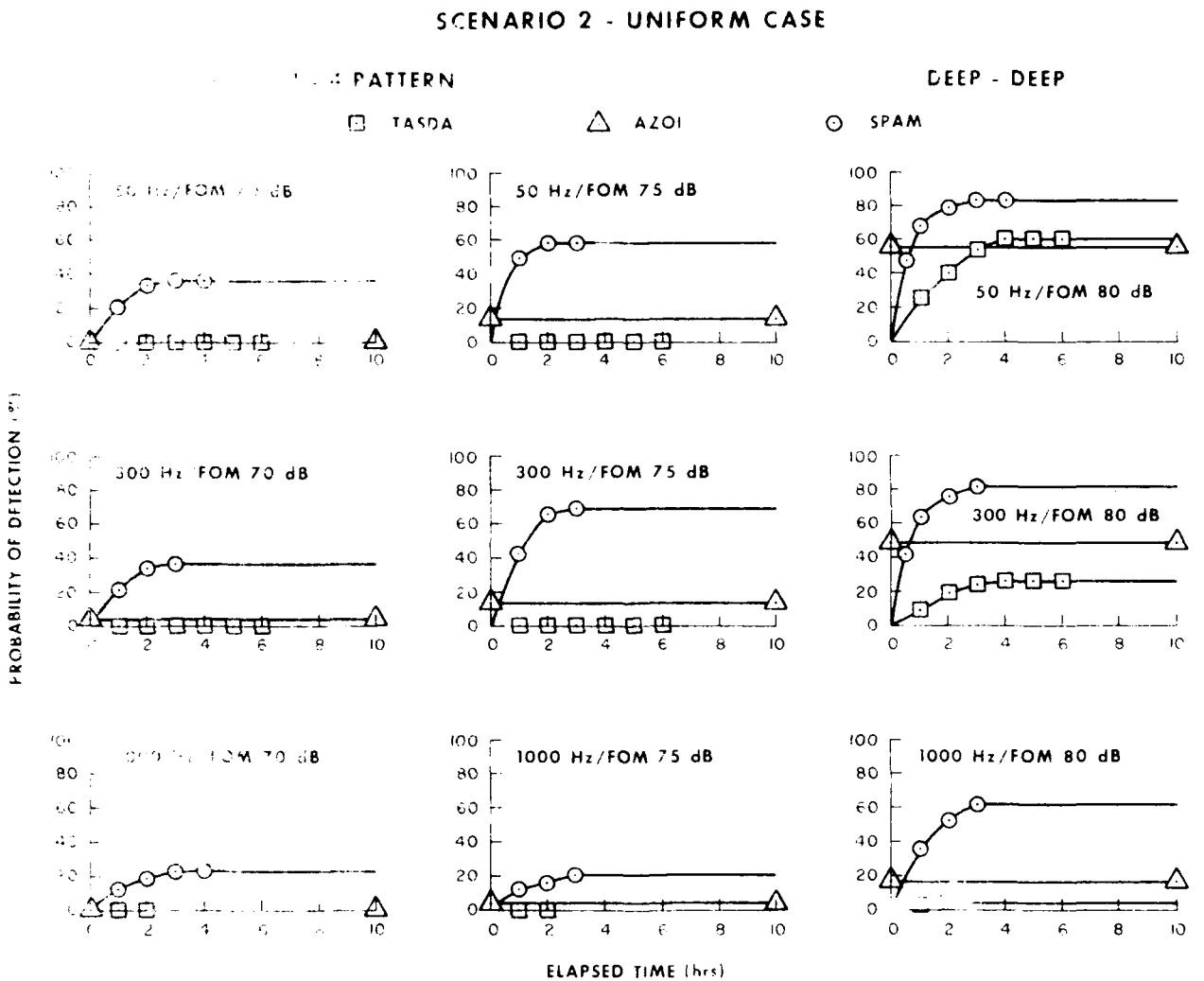

Figure 36. Comparison of TASDA, AZOI and SPAM with a uniform initial target location at one hour time late with a deep target and a deep receiver in scenario 2 using a [illegible] pattern.

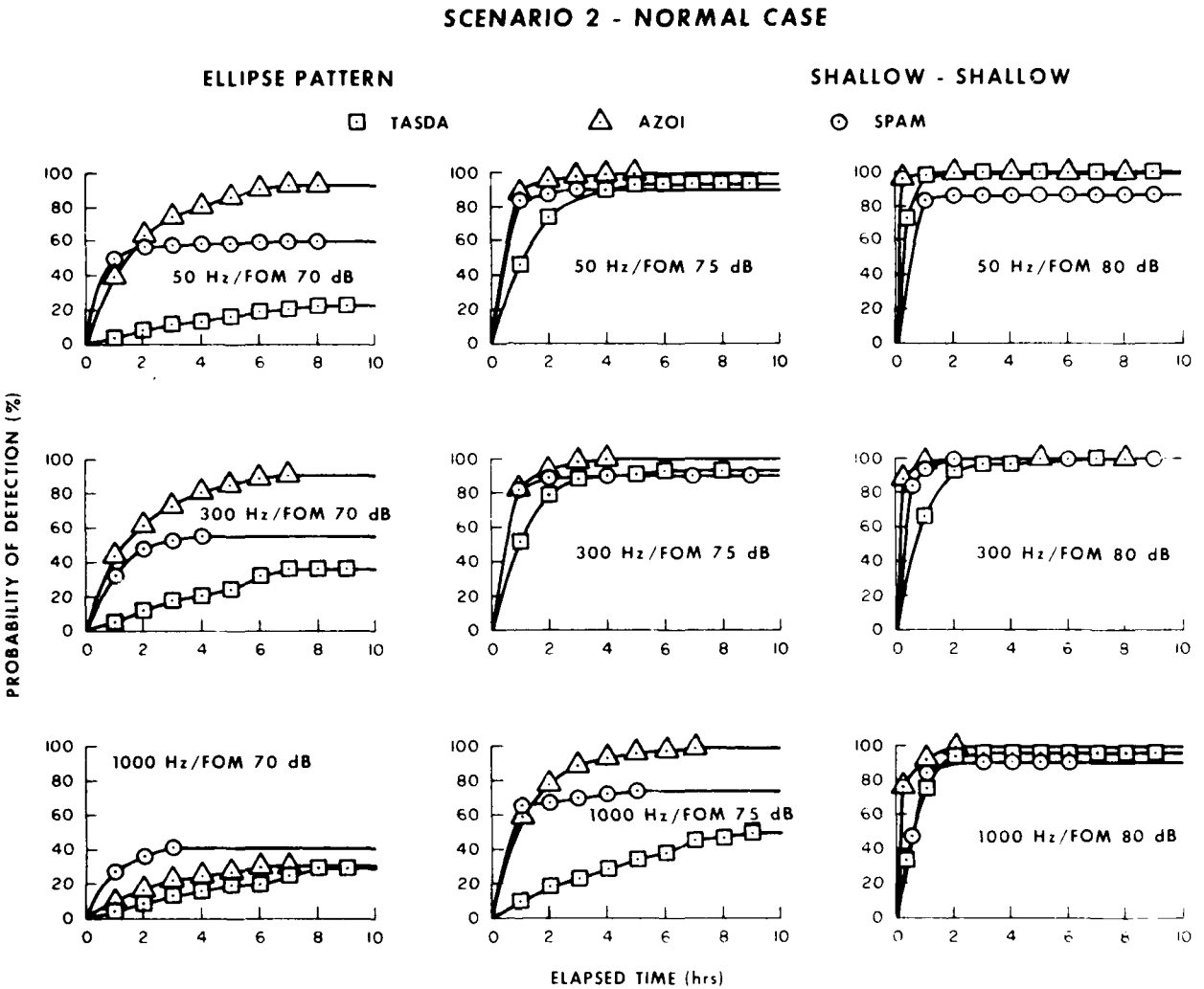

Figure C-37. Comparison of TASDA, AZOI and SPAM with a normal initial target location at one hour time late with a shallow target and a shallow receiver in scenario 2 using the ellipse pattern.

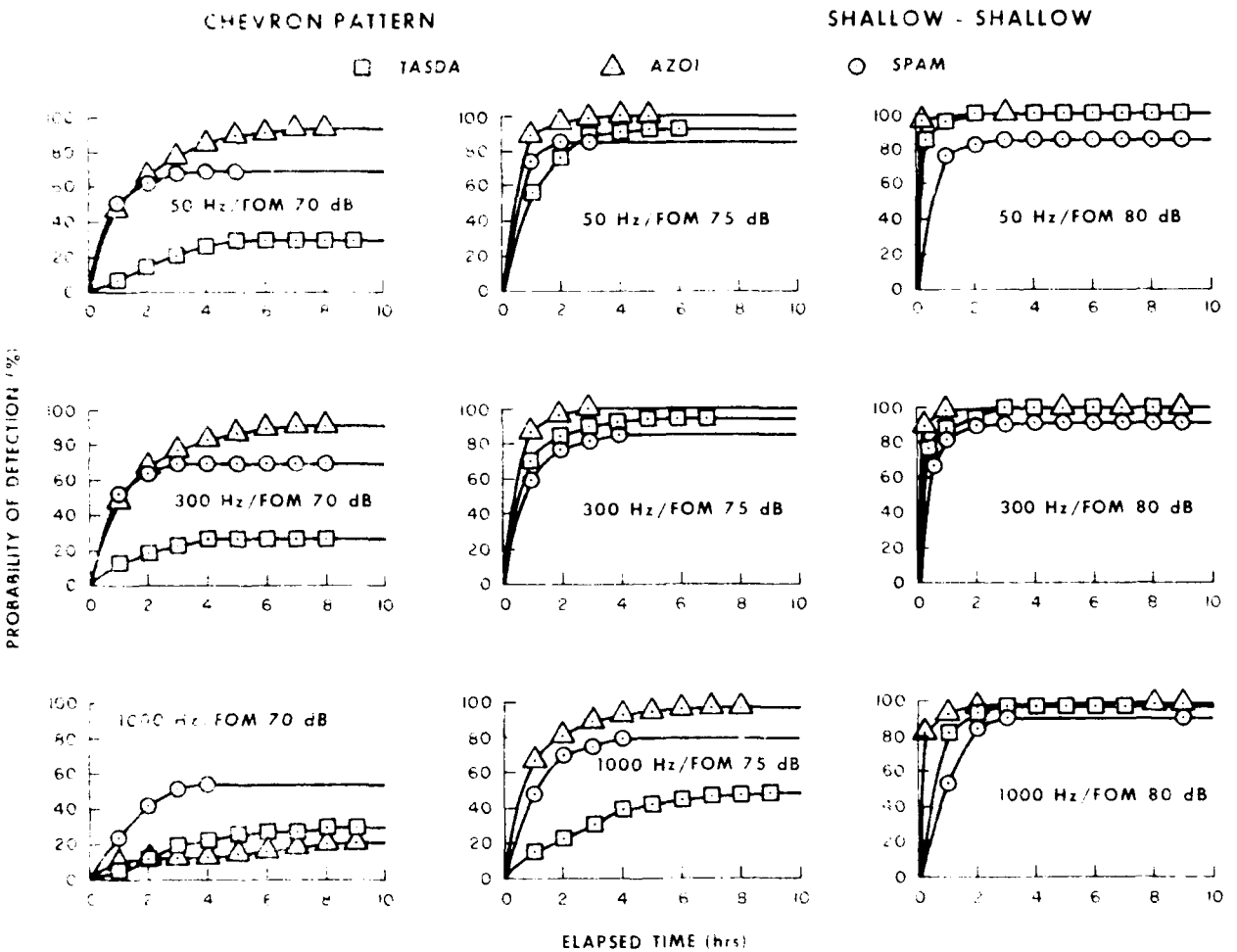

Figure 6-35. Comparison of TASDA, AZOI and SPAM with a normal initial target location at one hour time late with a shallow target and a shallow receiver in scenario 2 using the chevron pattern.

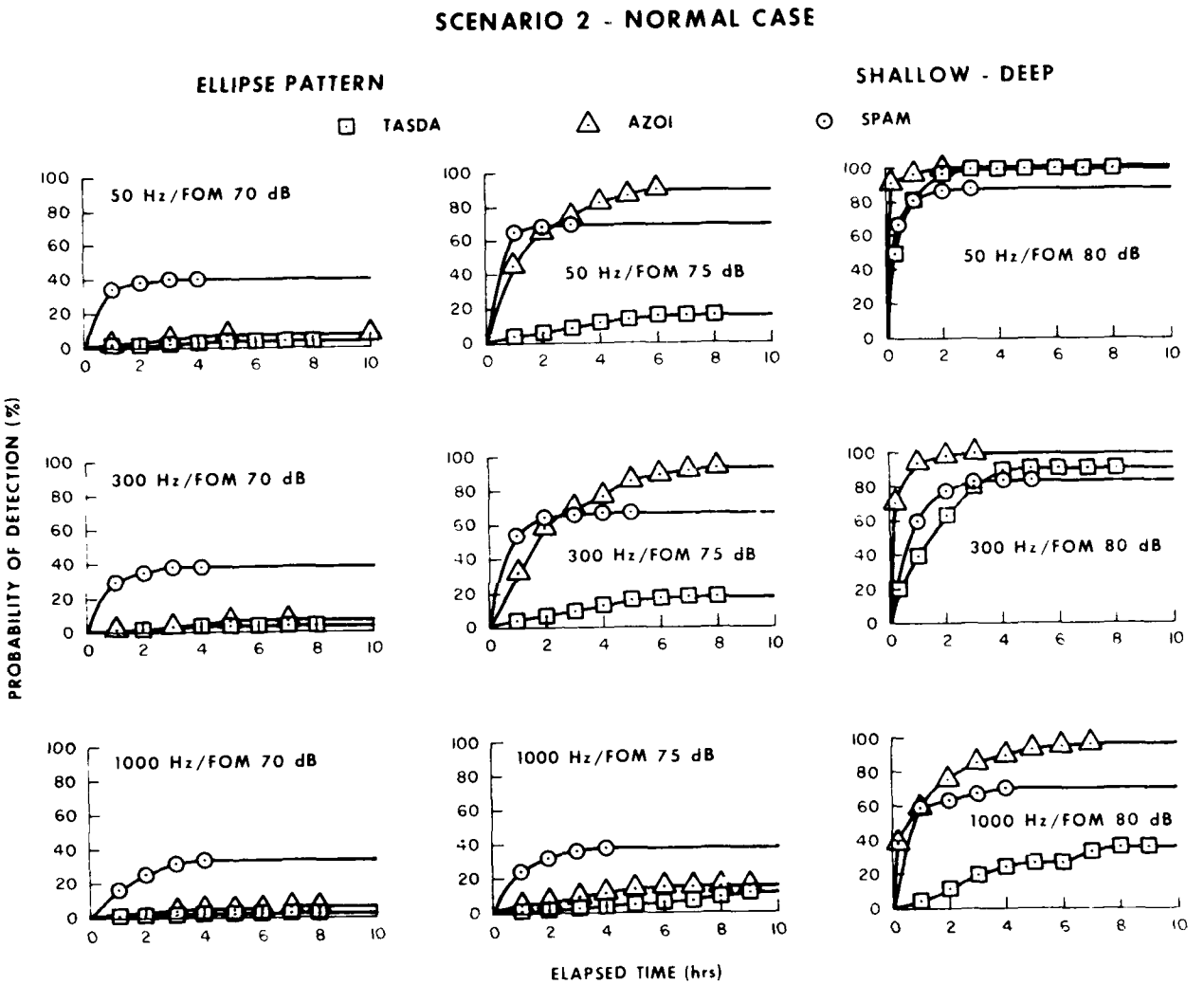

Figure C 39. Comparison of TASDA, AZOI and SPAM with a normal initial target location at one hour time late with a shallow deep target receiver combination in scenario 2 using the ellipse pattern.

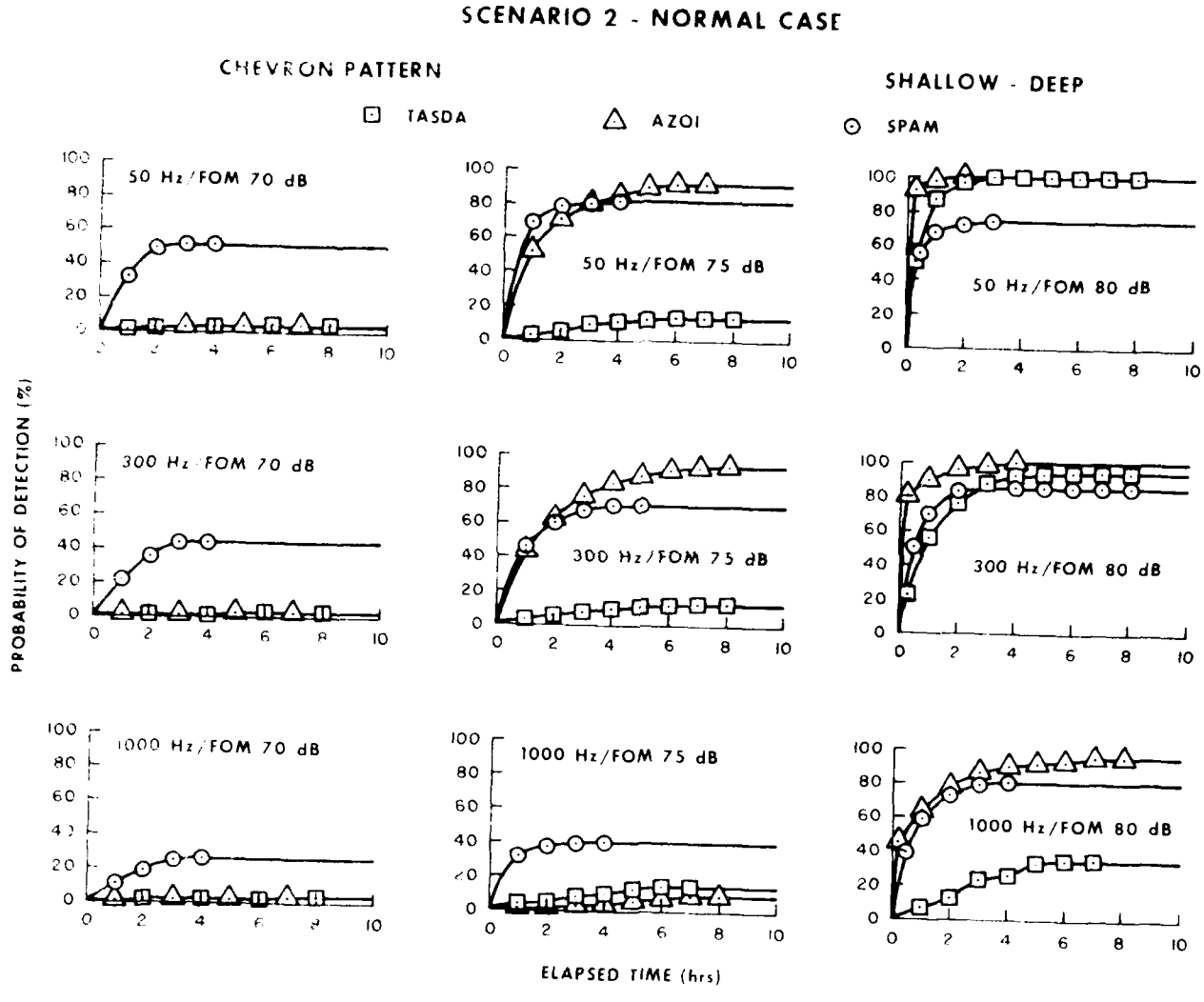

Figure C-40. Comparison of TASDA, AZOI and SPAM with a normal initial target location at one hour time late with a shallow deep target receiver combination in scenario 2 using the chevron pattern.

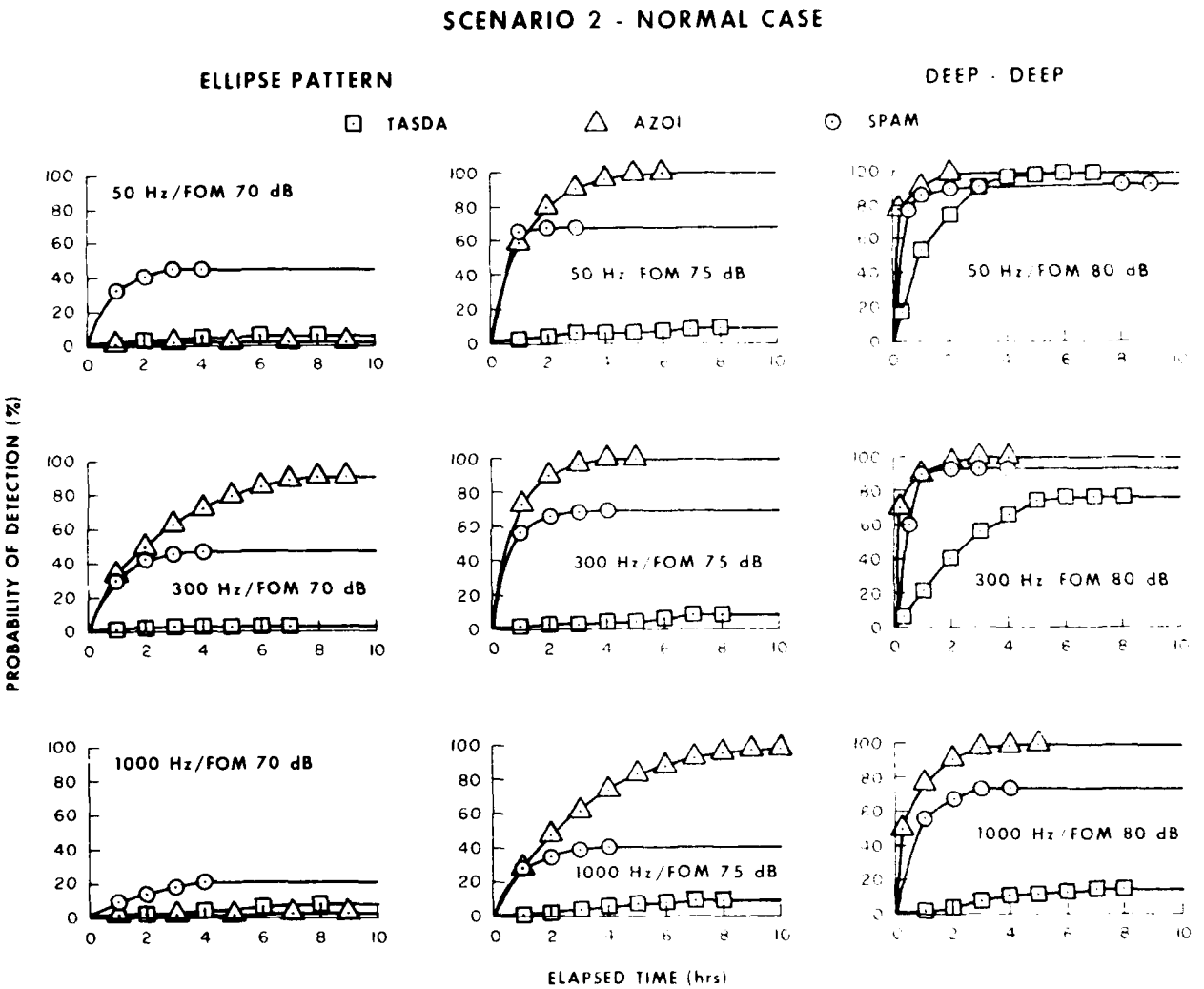

Figure C-41. Comparison of TASDA, AZOI and SPAM with a normal initial target location at one hour time late with a deep target and a deep receiver in scenario 2 using an ellipse pattern.

AD-A104 415 NAVAL OCEANOGRAPHIC OFFICE NSTL STATION MS F/G 11/1
ASSESSMENT OF TACTICAL SONOBUOY COMPUTER PROGRAMS FOR ENVIRONME--ETC(U)
FEB 81 L J FUSILLO
UNCLASSIFIED NOO-TR-260 NL

2 OF 3
AD-A104 415

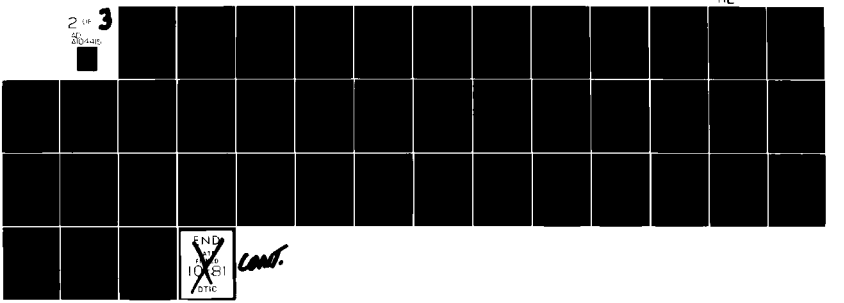

cont.

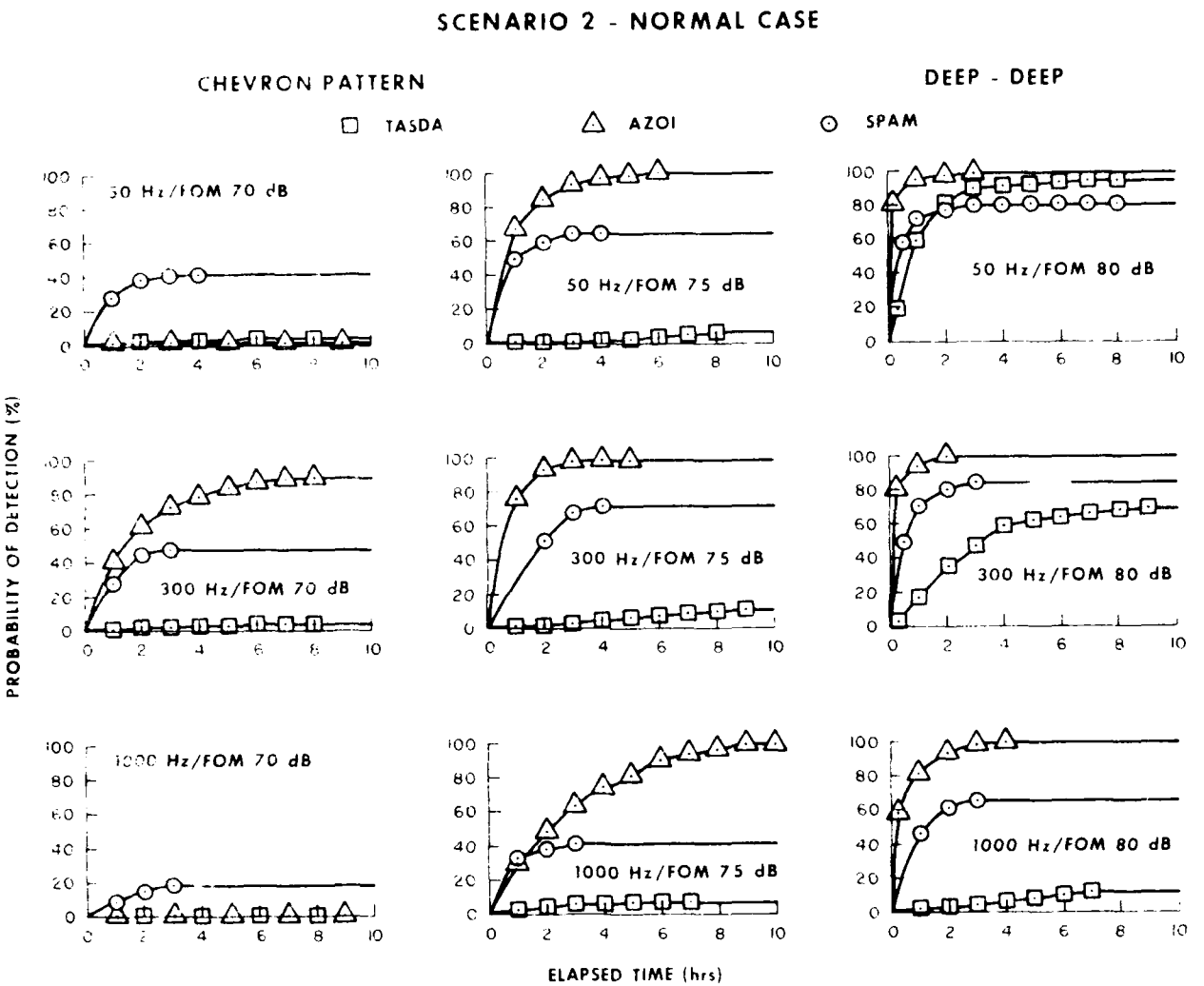

Figure C-12. Comparison of TASDA, AZOI and SPAM with a normal initial target location at one hour time late with a deep target and a deep receiver in scenario 2 using the chevron pattern.

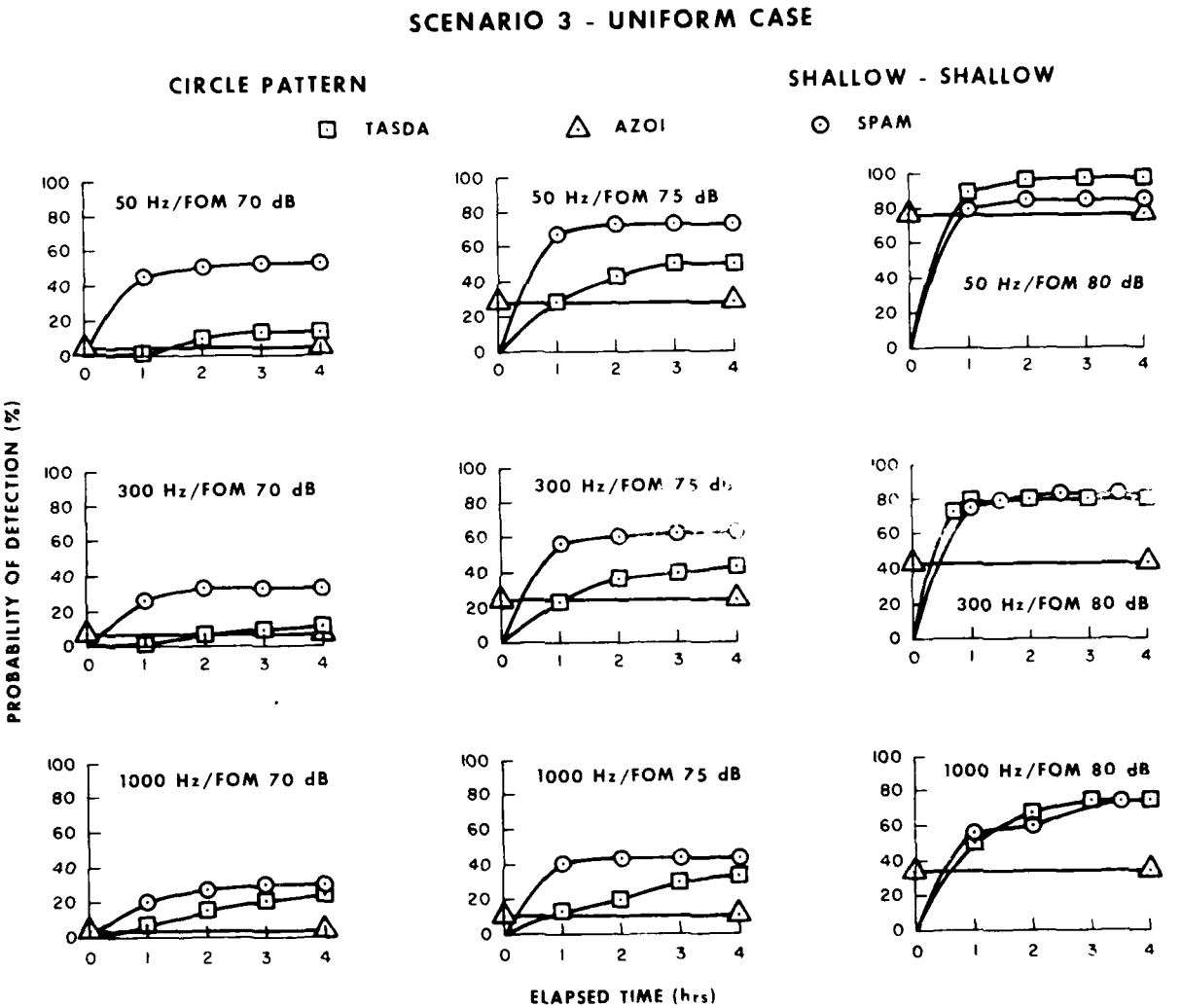

Figure C-43. Comparison of TASDA, AZOI and SPAM with a uniform initial target location at one hour time late with a shallow target and a shallow receiver in scenario 3 using the circle pattern.

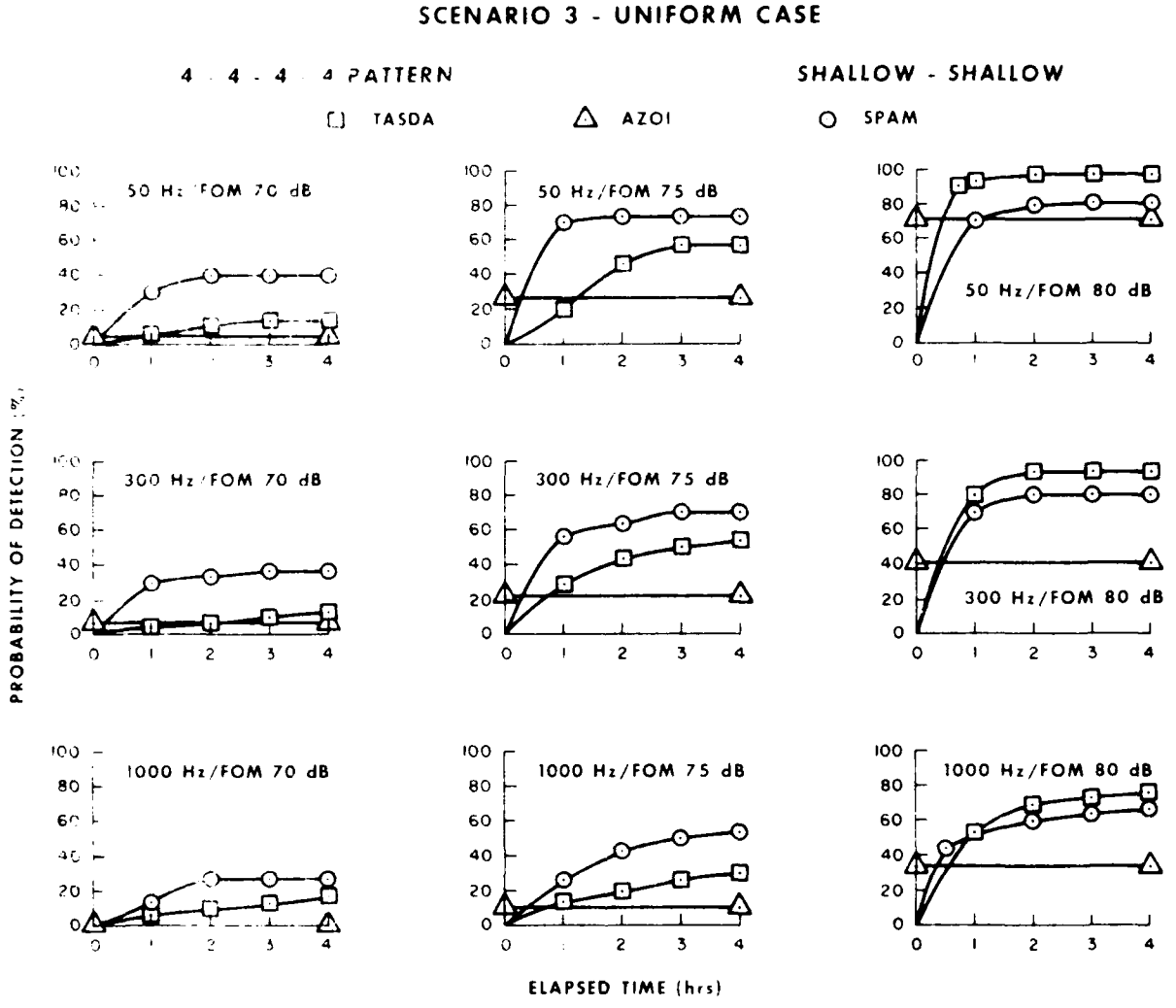

Figure 44. Comparison of TASDA, AZOI and SPAM with a uniform initial target location at one hour time late with a shallow target and a shallow receiver in scenario 3 using the 4 4 4 4 pattern.

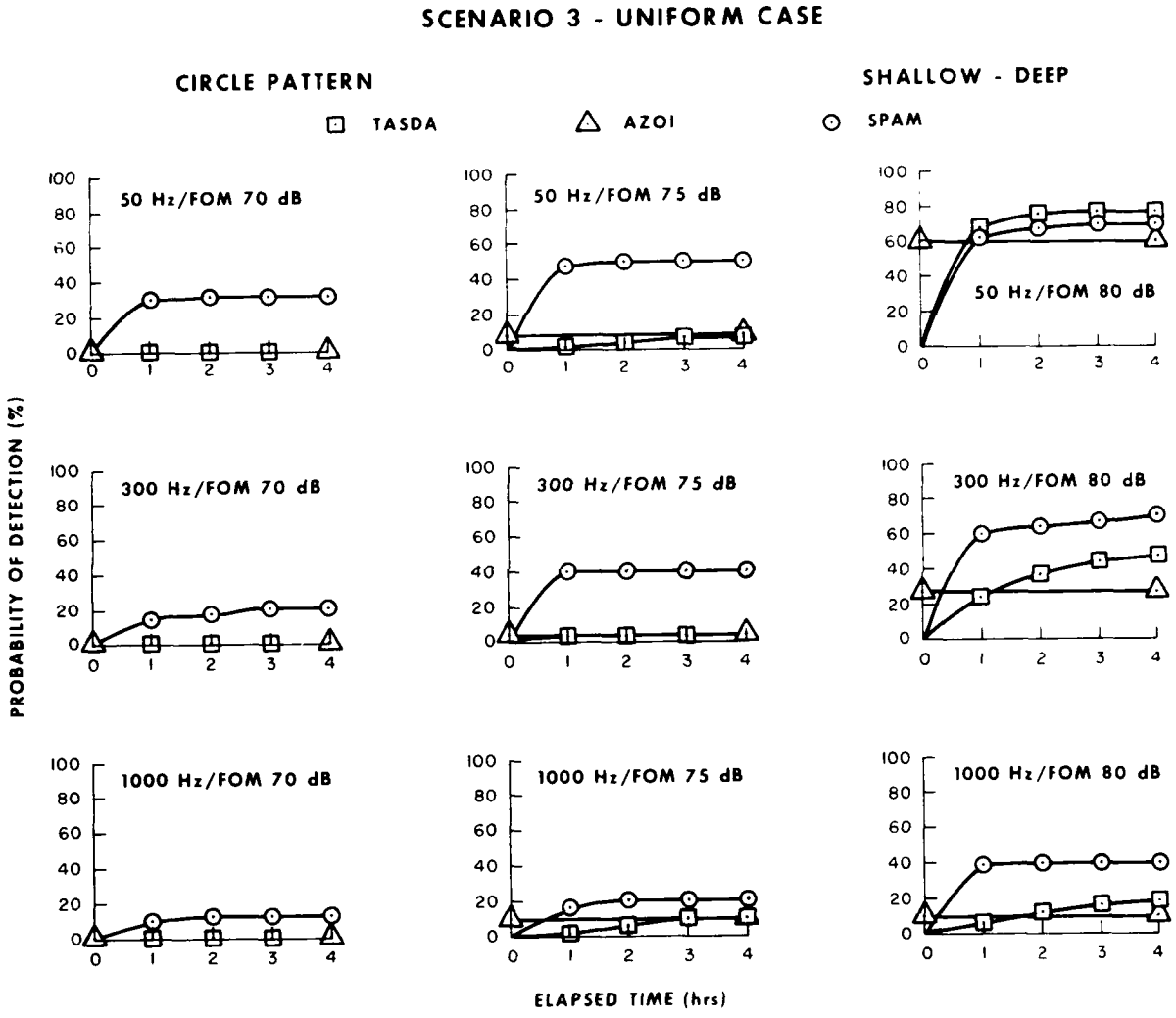

Figure C 45. Comparison of TASDA, AZOI and SPAM with a uniform initial target location at one hour time late with a shallow deep target receiver combination in scenario 3 using the circle pattern.

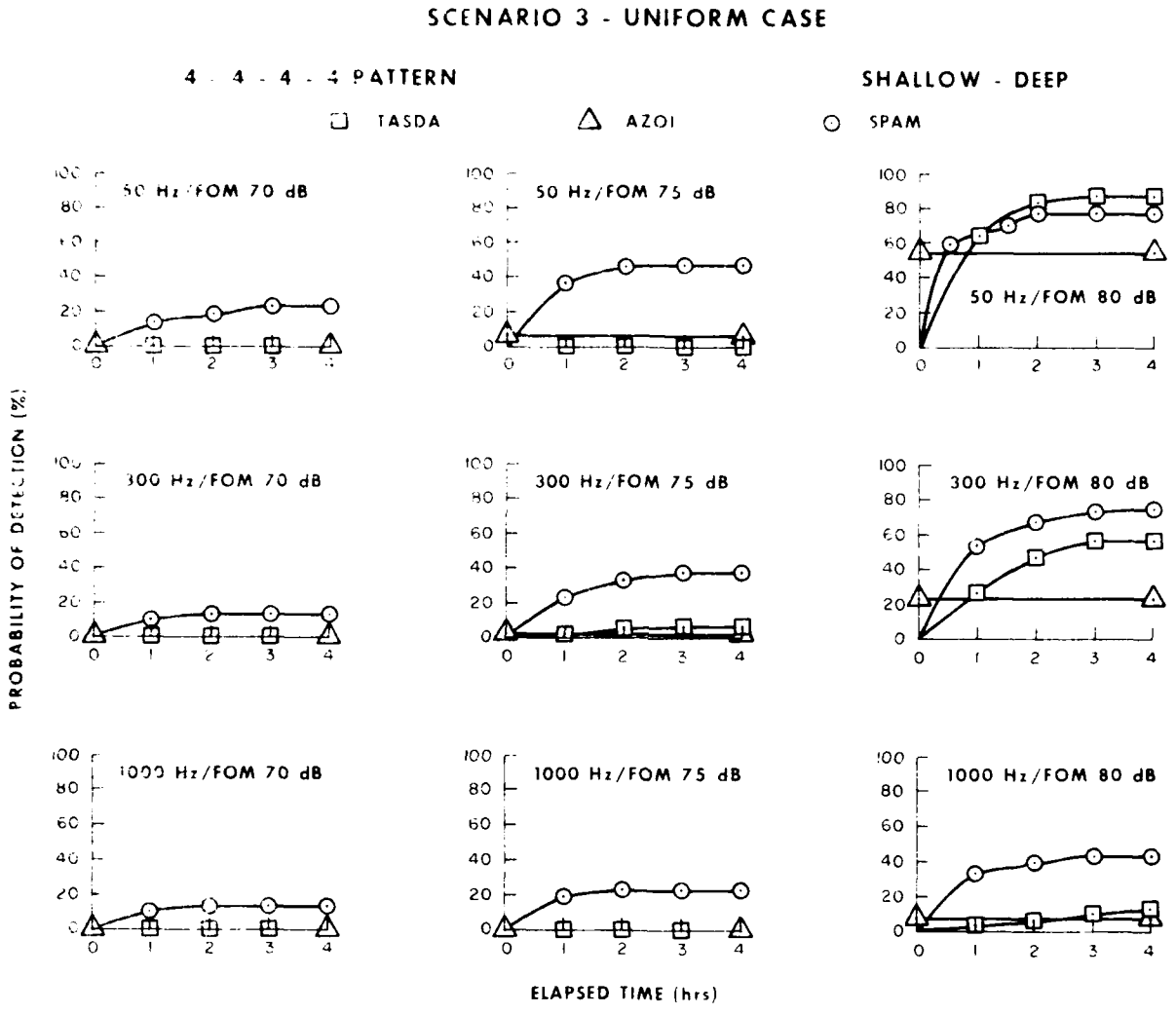

Figure C-46. Comparison of TASDA, AZOI and SPAM with a uniform initial target location at one hour time late with a shallow deep target receiver combination in scenario 3 using the 4 4 4 4 pattern.

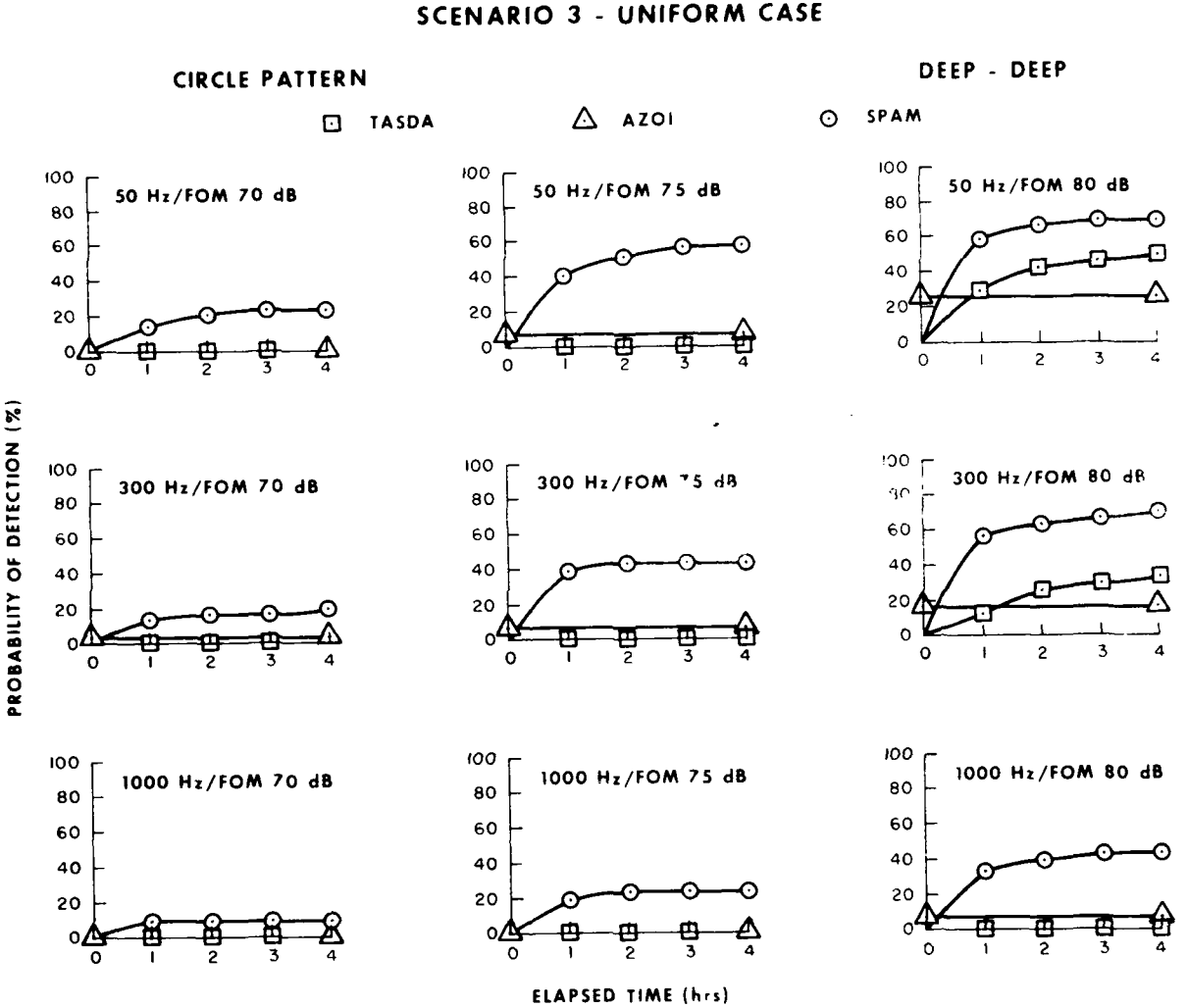

Figure C 47. Comparison of TASDA, AZOI and SPAM with a uniform initial target location at one hour time late with a deep target and a deep receiver in scenario 3 using a circle pattern.

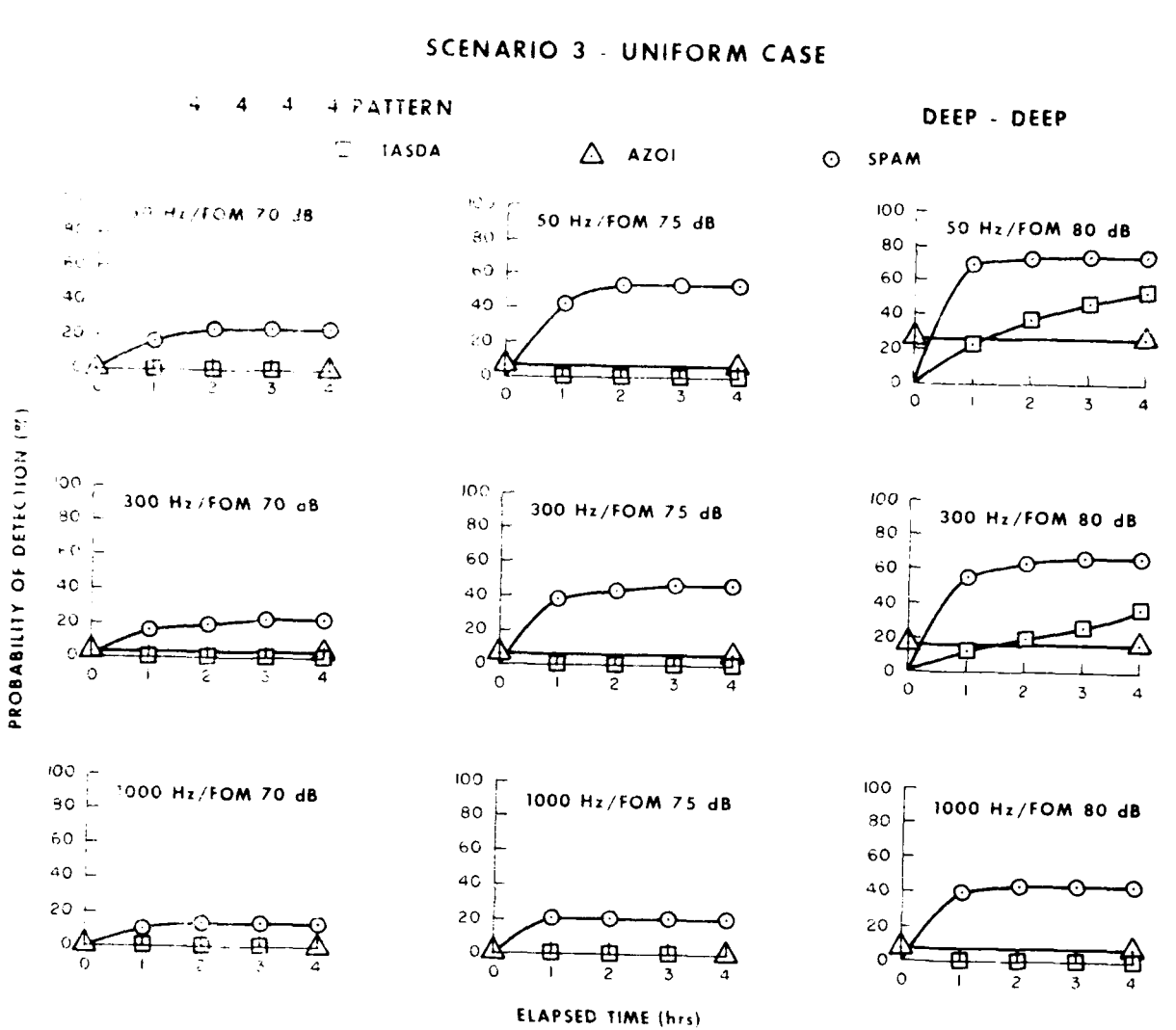

Figure C-48. Comparison of TASDA, AZOI and SPAM with a uniform initial location at one hour time late with a deep target and a deep receiver in scenario 3 using a 4 4 4 4 pattern.

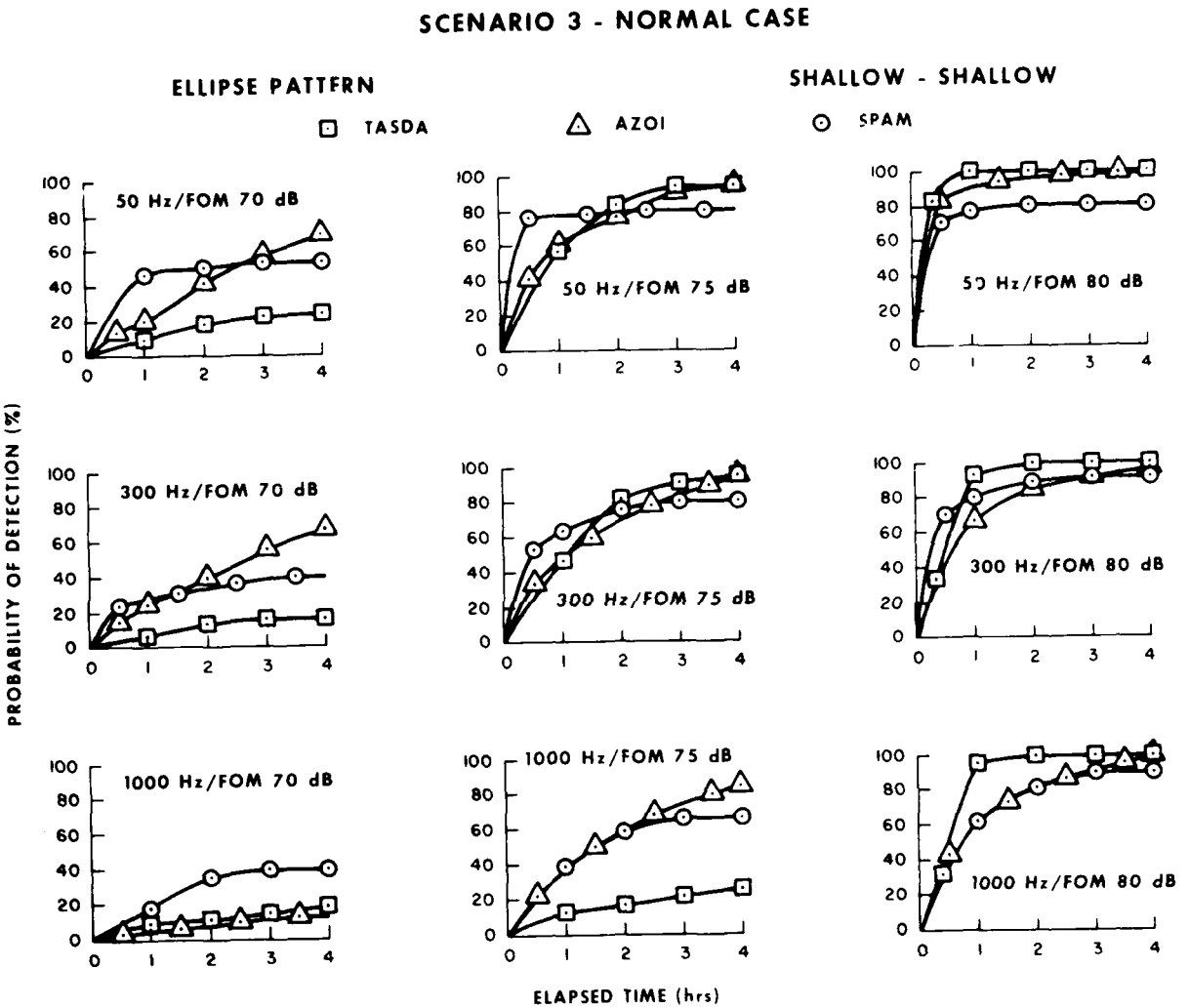

Figure C-49. Comparison of TASDA, AZOI and SPAM with a normal initial target location at one hour time late with a shallow target and a shallow receiver in scenario 3 using the ellipse pattern.

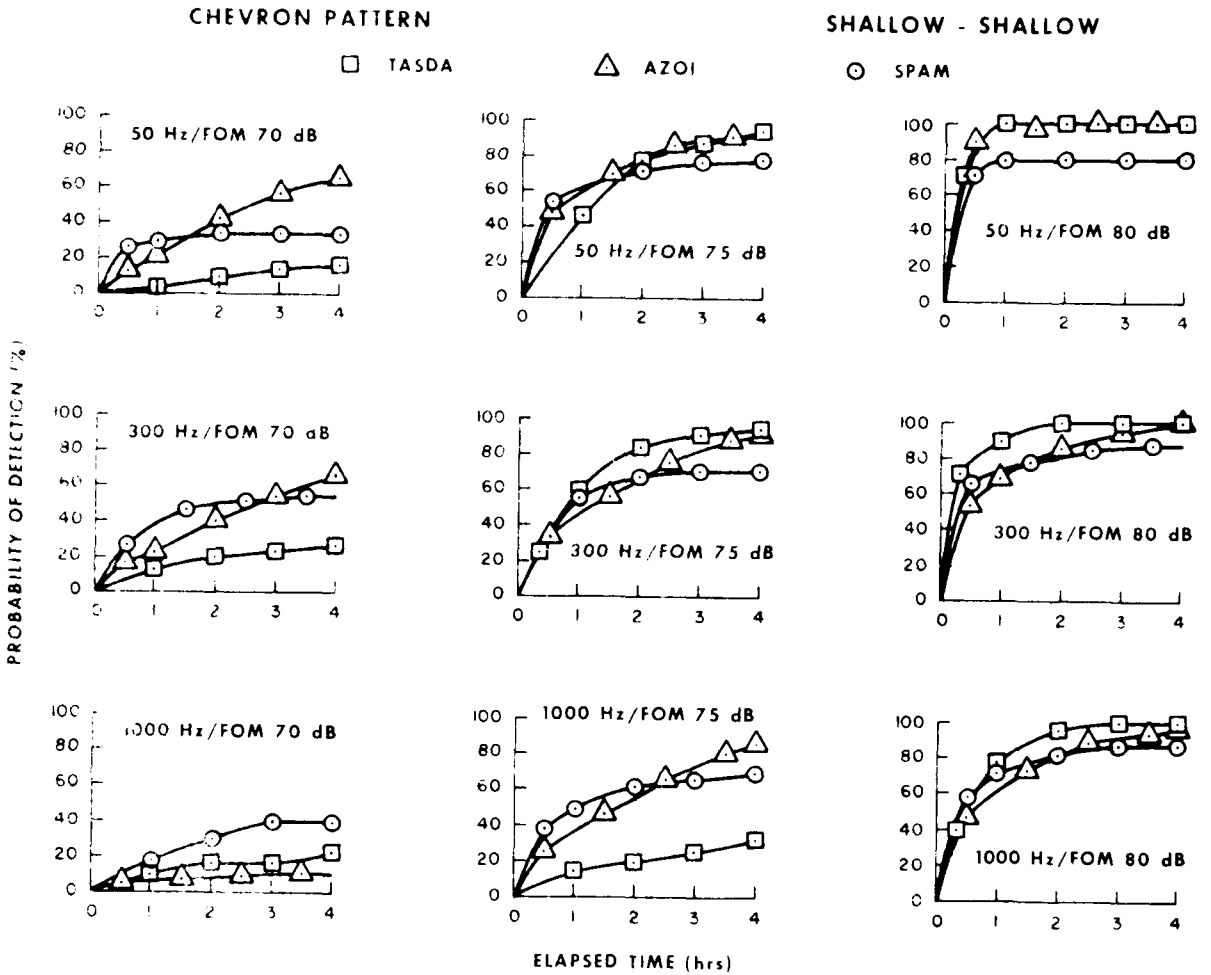

Figure C-50. Comparison of TASDA, AZOI and SPAM with a normal initial target location at one hour time late with a shallow target and a shallow receiver in scenario 3 using the chevron pattern.

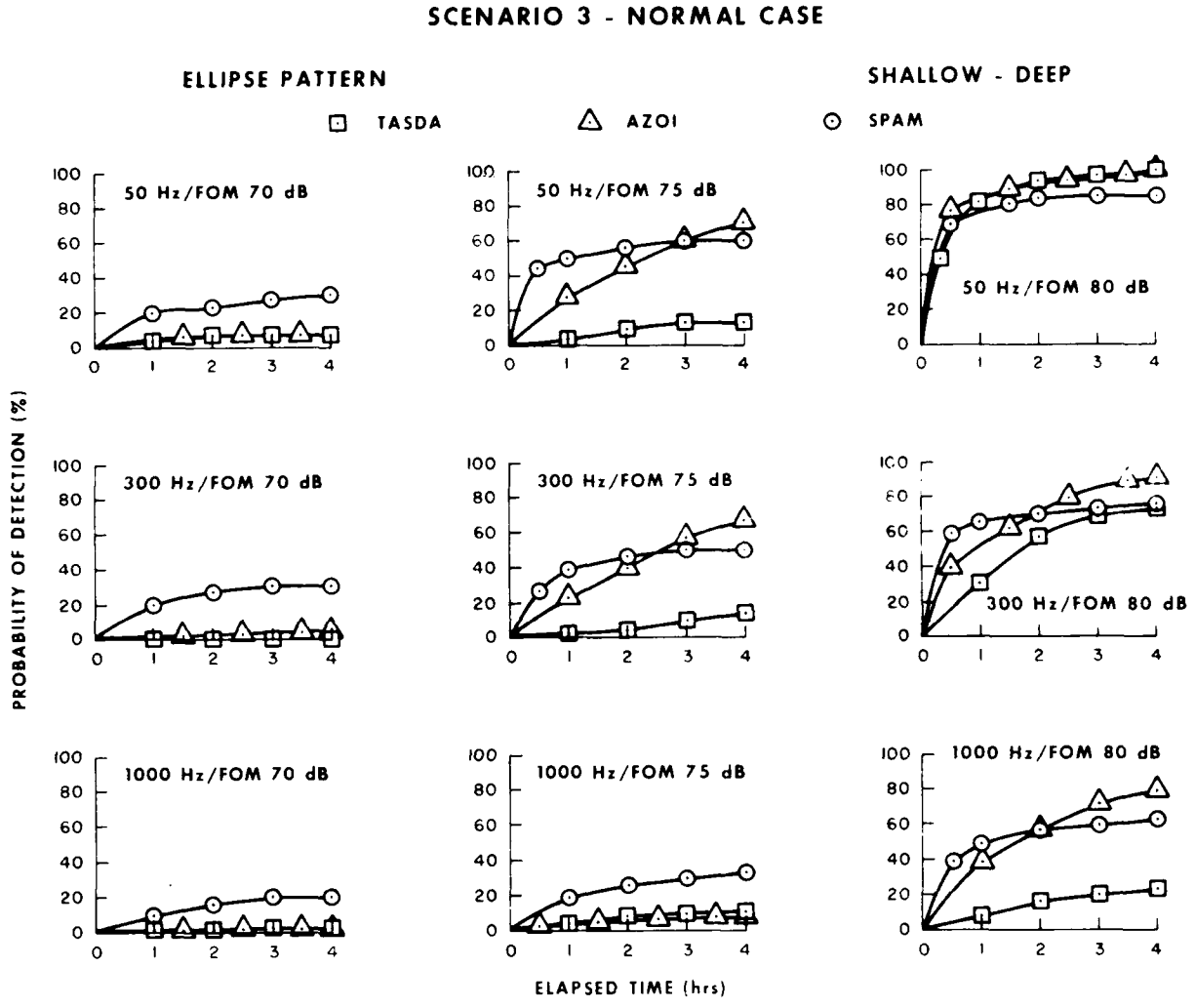

Figure C 51. Comparison of TASDA, AZOI and SPAM with a normal initial target location at one hour time late with a shallow deep target receiver combination in scenario 3 using the ellipse pattern.

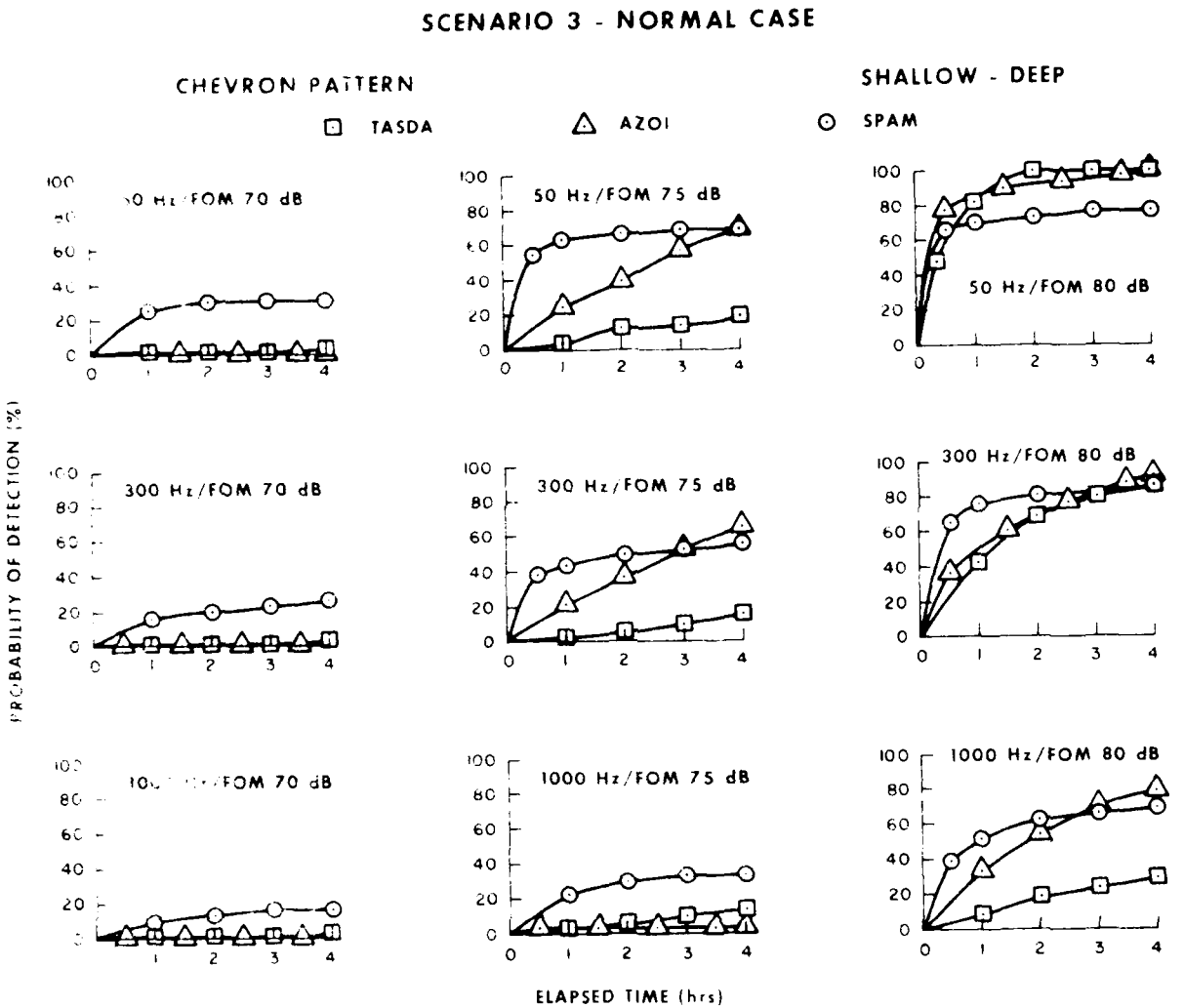

Figure C-52. Comparison of TASDA, AZOI and SPAM with a normal initial target location at one hour time late with a shallow-deep target for the chevron pattern in scenario 3 using the chevron pattern.

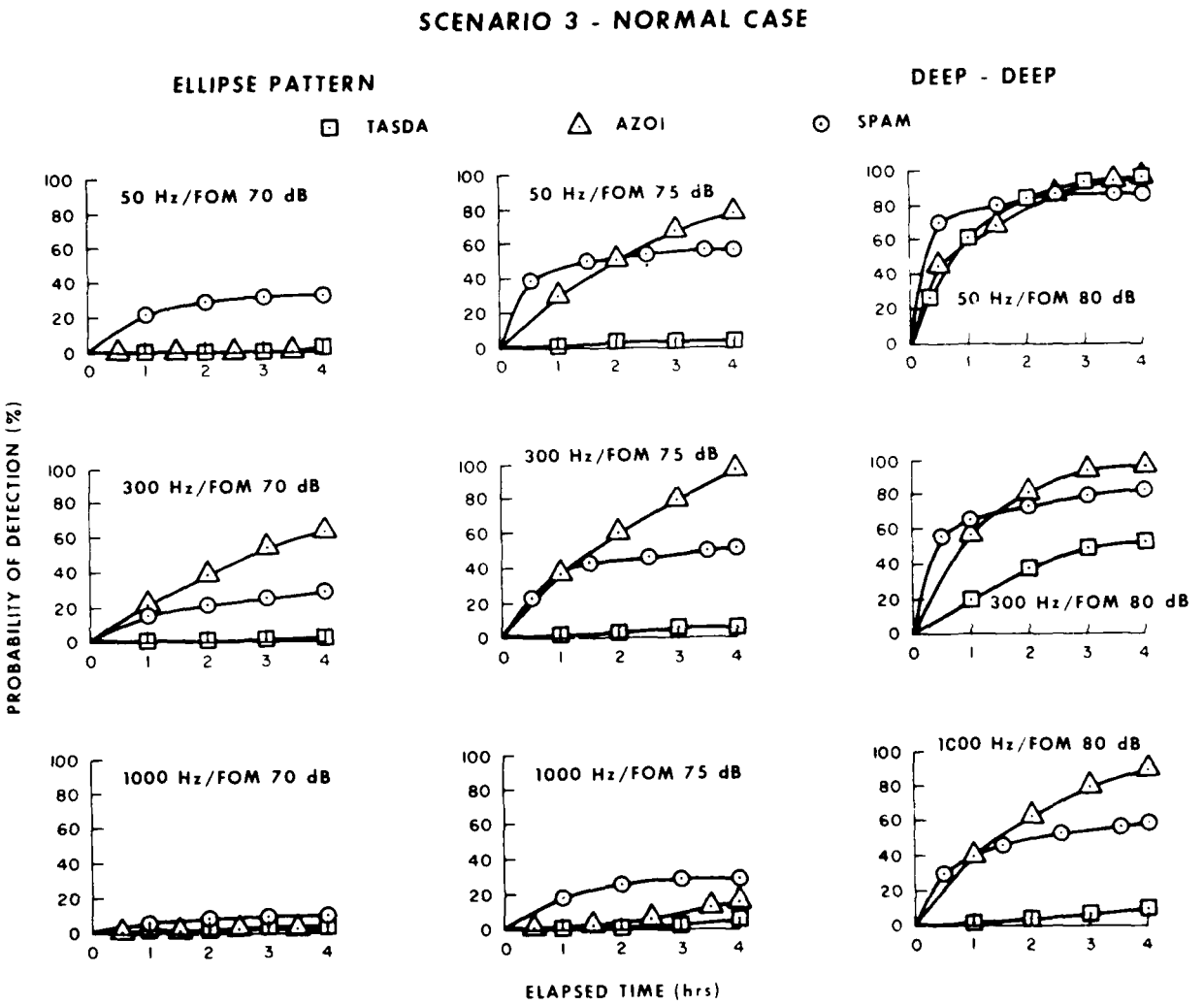

Figure C-53. Comparison of TASDA, AZOI and SPAM with a normal initial target location at one hour time late with a deep target and a deep receiver in scenario 3 using an ellipse pattern

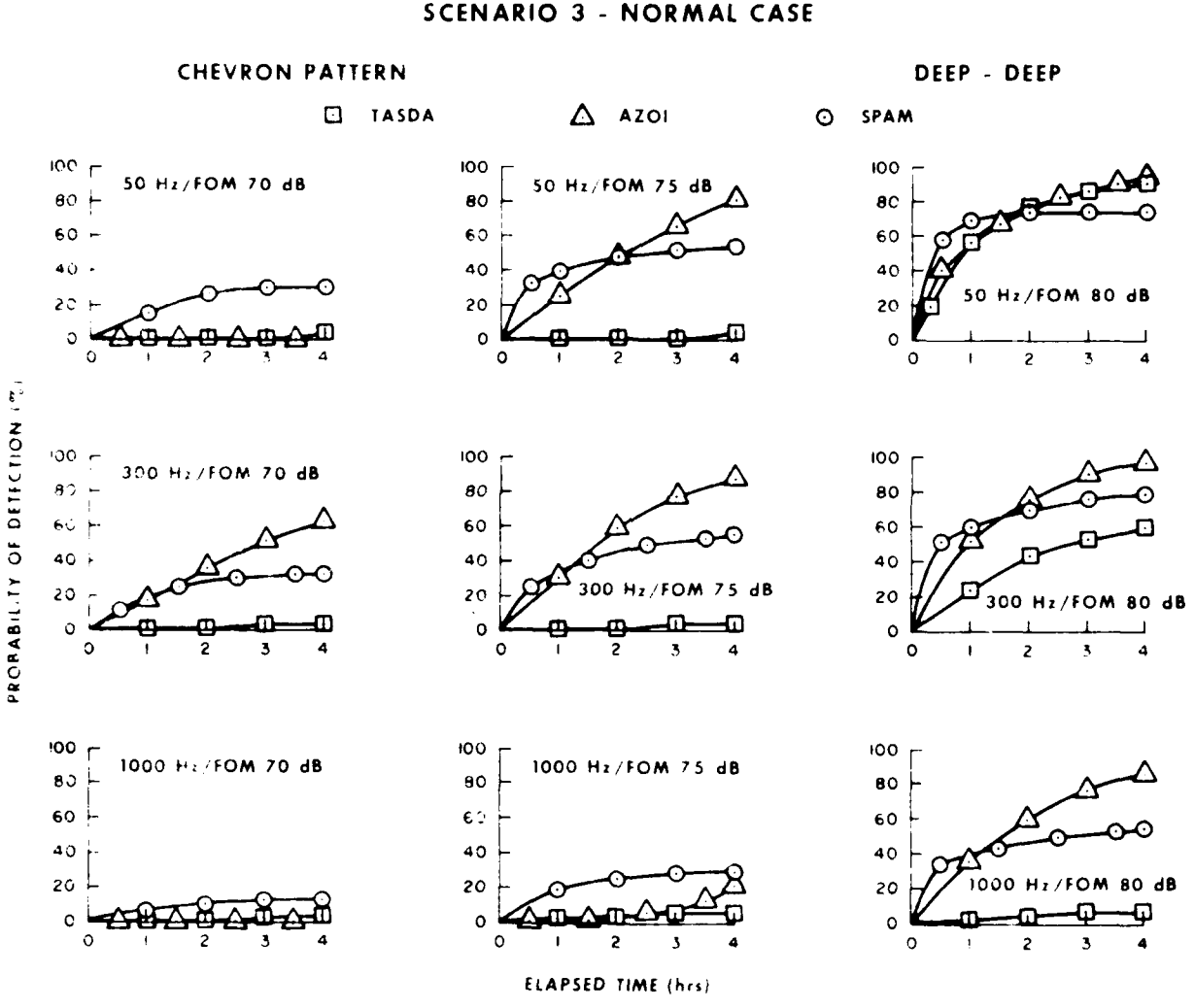

Figure C 54. Comparison of TASDA, AZOI and SPAM with a normal initial target location at one hour time late with a deep target set and a deep receiver in scenario 3 using the chevron pattern

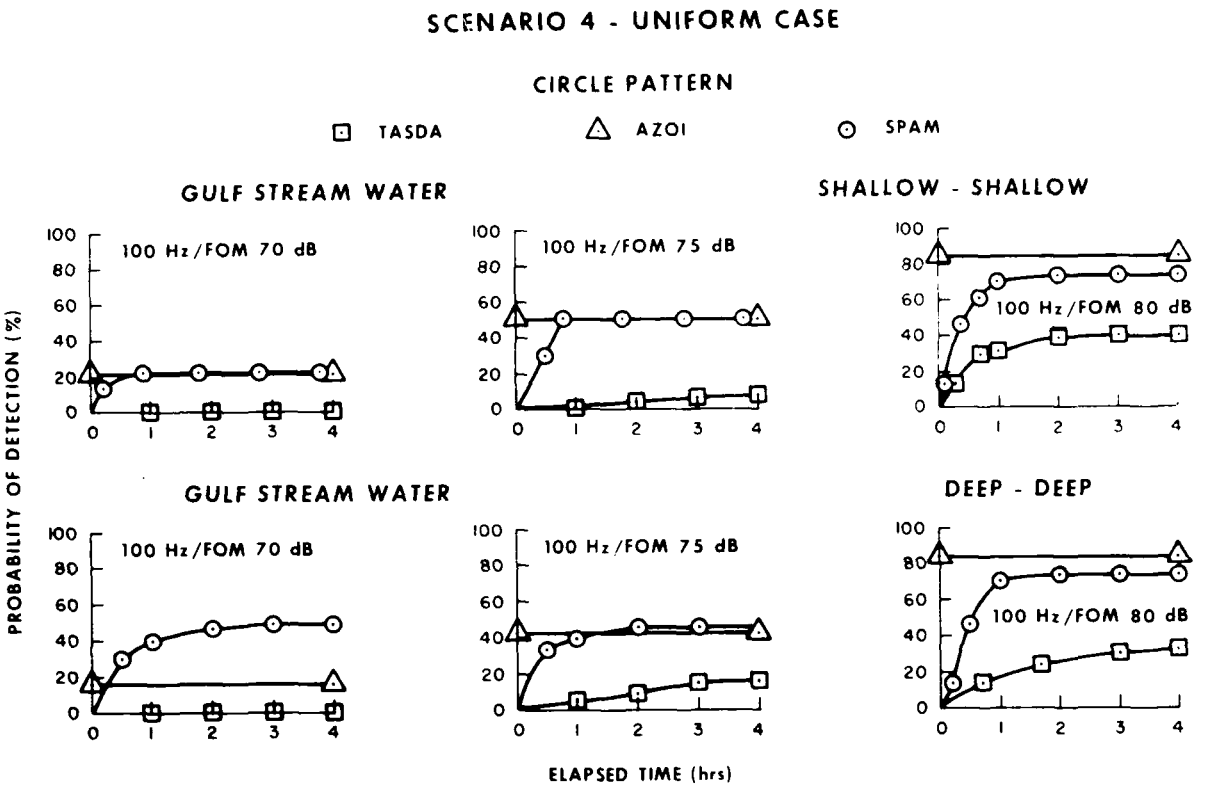

Figure C-55. Comparison of TASDA, AZOI, and SPAM with a uniform initial target location at one hour time late with a receiver frequency of 100 Hz in the Gulf Stream environment in scenario 4 using the circle pattern.

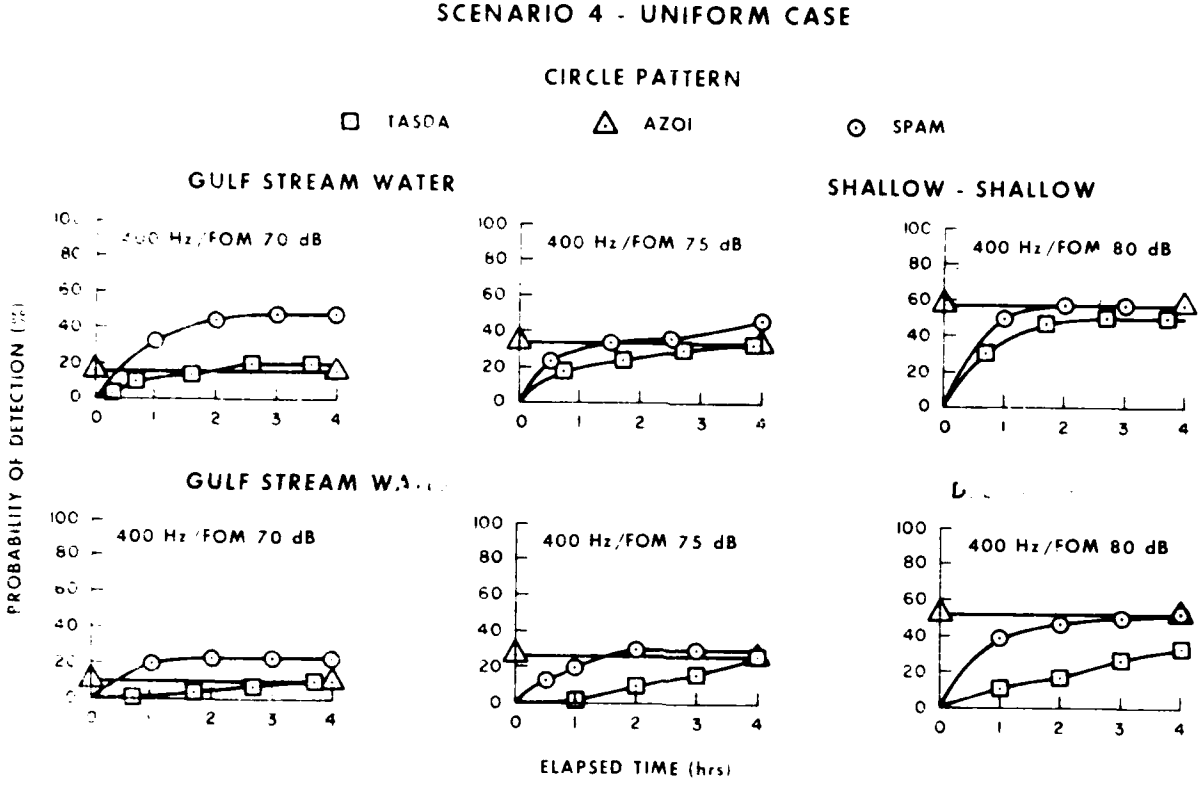

Figure [illegible]. Comparison of TASDA, AZOI, and SPAM with a uniform initial target location at one hour time late with a receiver frequency of 400 Hz in the Gulf Stream environment in scenario 4 using the circle pattern.

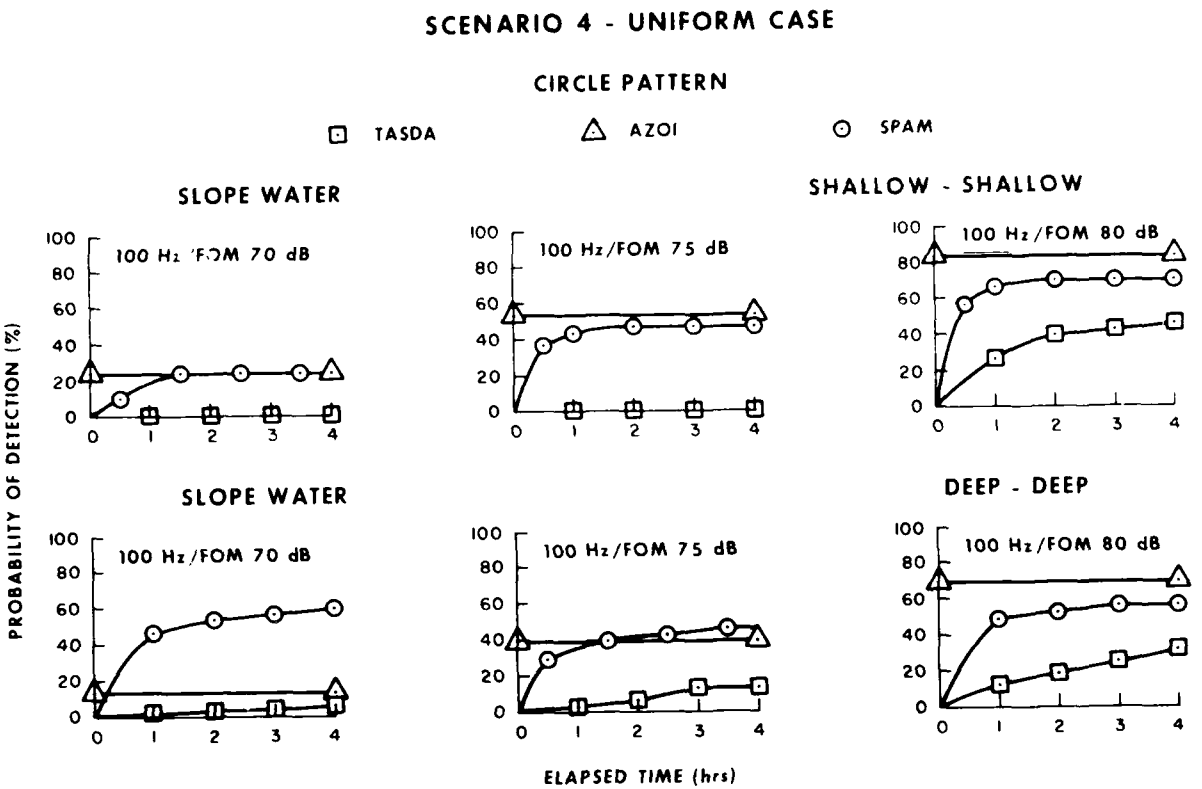

Figure C-57. Comparison of TASDA, AZOI and SPAM, with a uniform initial target location at one hour time late with a receiver frequency of 100 Hz in the slope water environment in scenario 4 using the circle pattern.

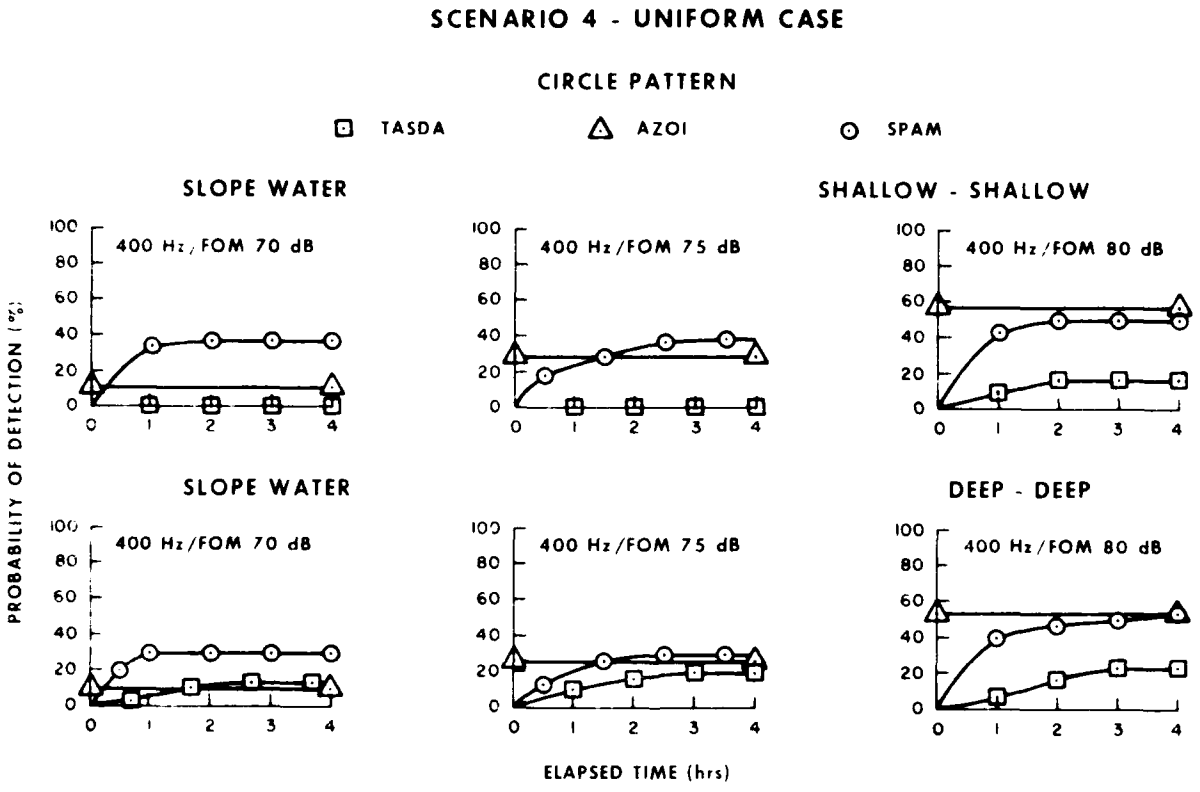

Figure C-58. Comparison of TASDA, AZOI and SPAM, with a uniform initial target location at one hour time late with a receiver frequency of 400 Hz in the slope water environment in scenario 4 using the circle pattern.

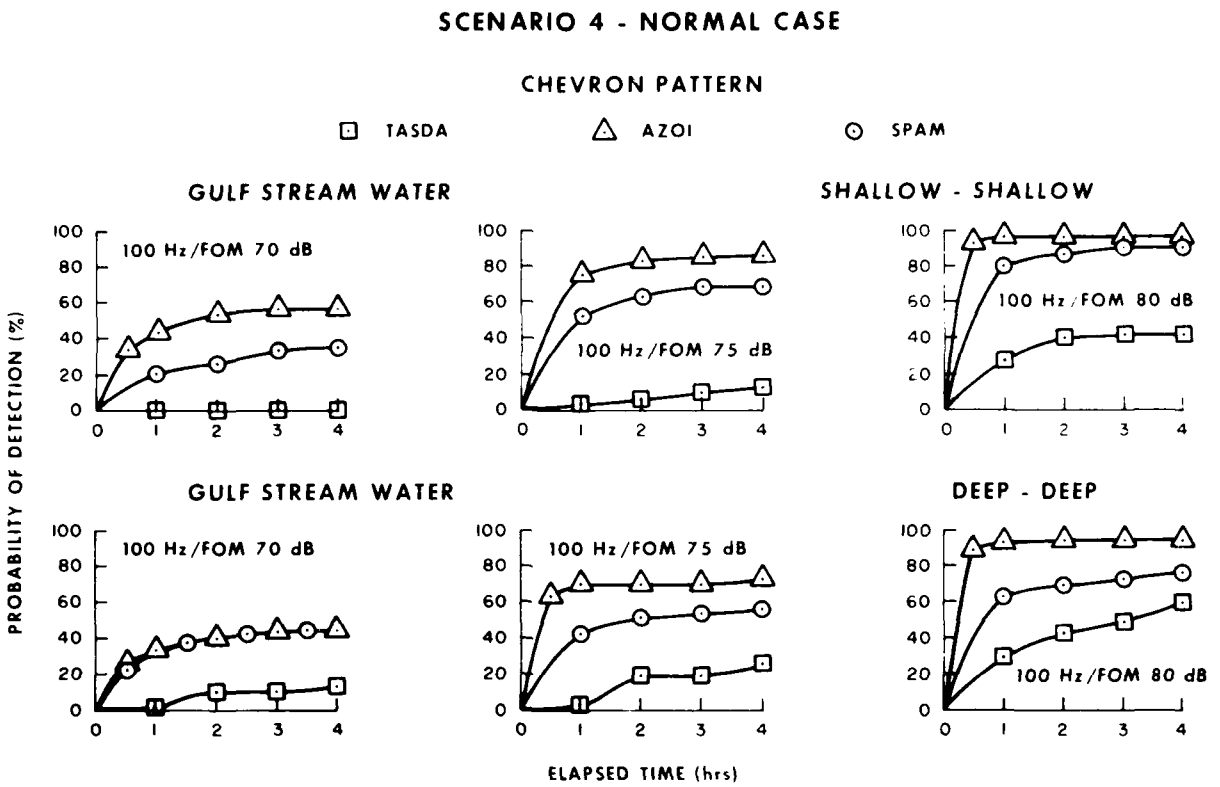

Figure C-59. Comparison of TASDA, AZOI, and SPAM with a normal initial target location at one hour time late with a receiver frequency of 100 Hz in the Gulf Stream environment in scenario 4 using the chevron pattern.

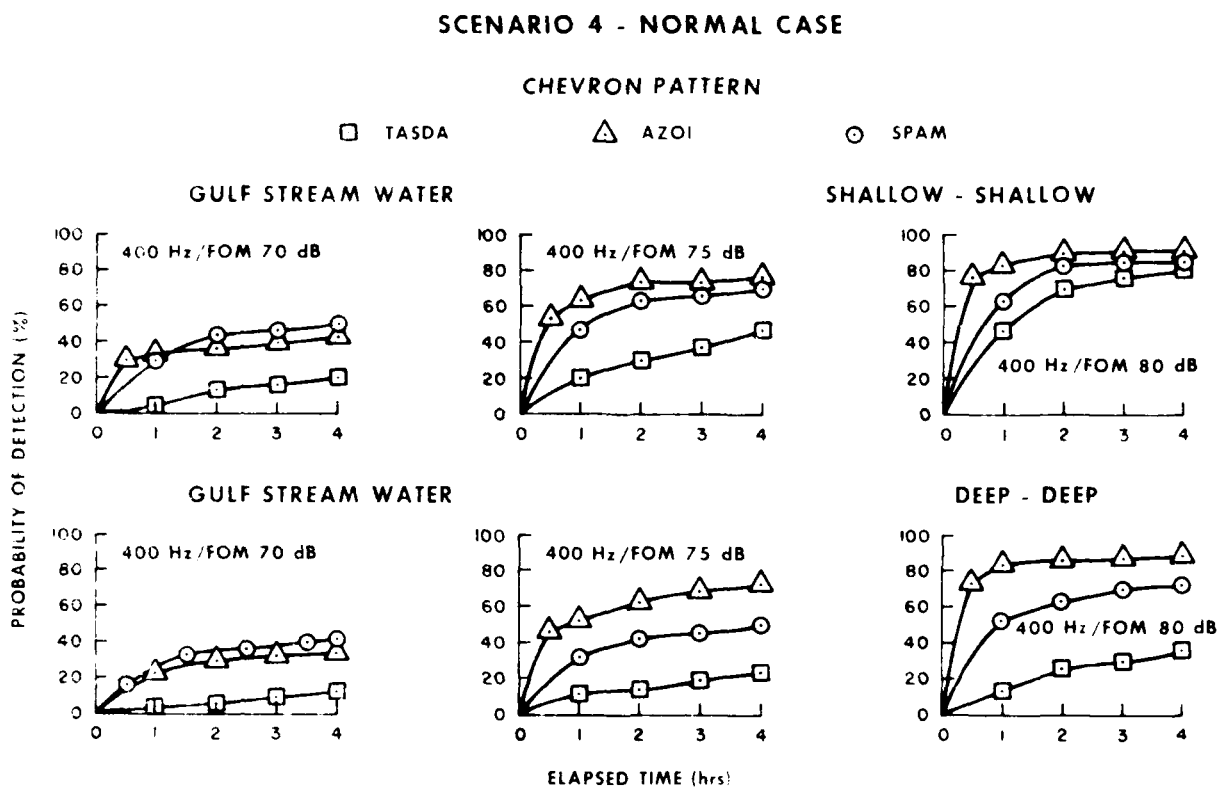

Figure C-60. Comparison of TASDA, AZOI, and SPAM with a normal initial target location at one hour time late with a receiver frequency of 400 Hz in the Gulf Stream environment in scenario 4 using the chevron pattern.

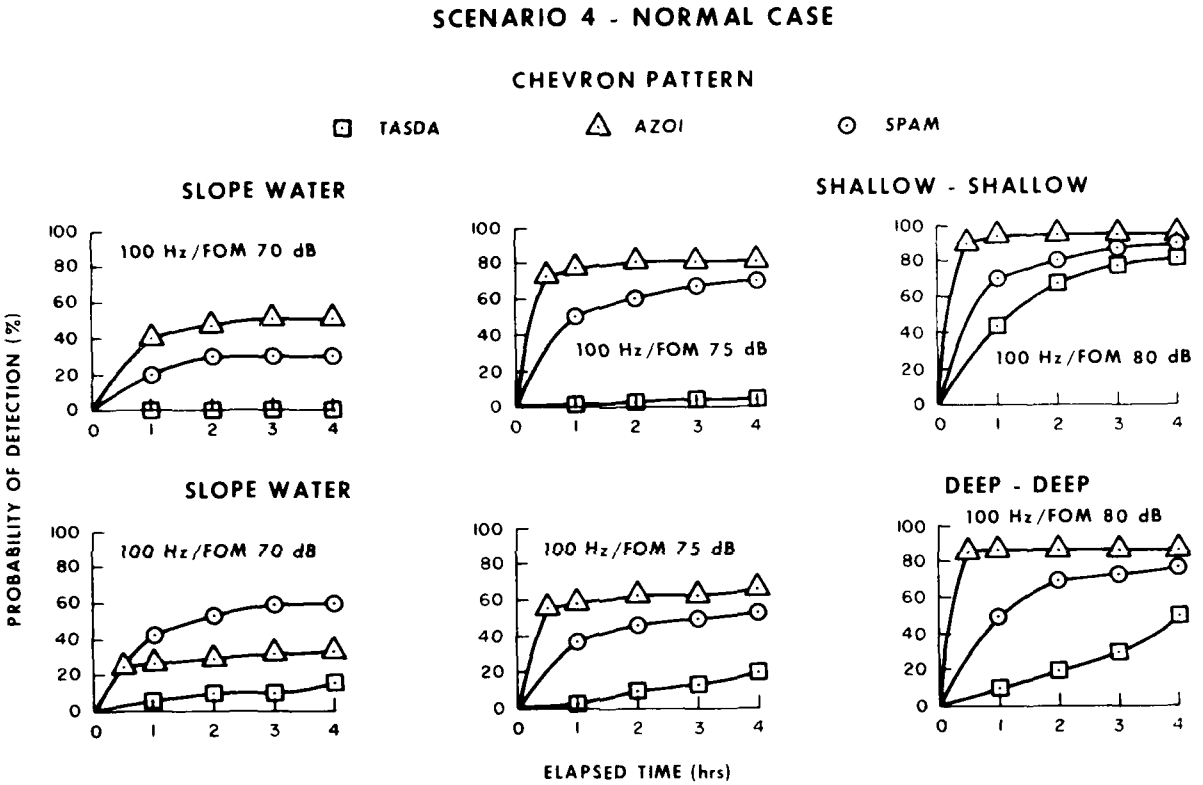

Figure C-61. Comparison of TASDA, AZOI and SPAM, with a normal initial target location at one hour time late with a receiver frequency of 100 Hz in the slope water environment in scenario 4 using the chevron pattern.

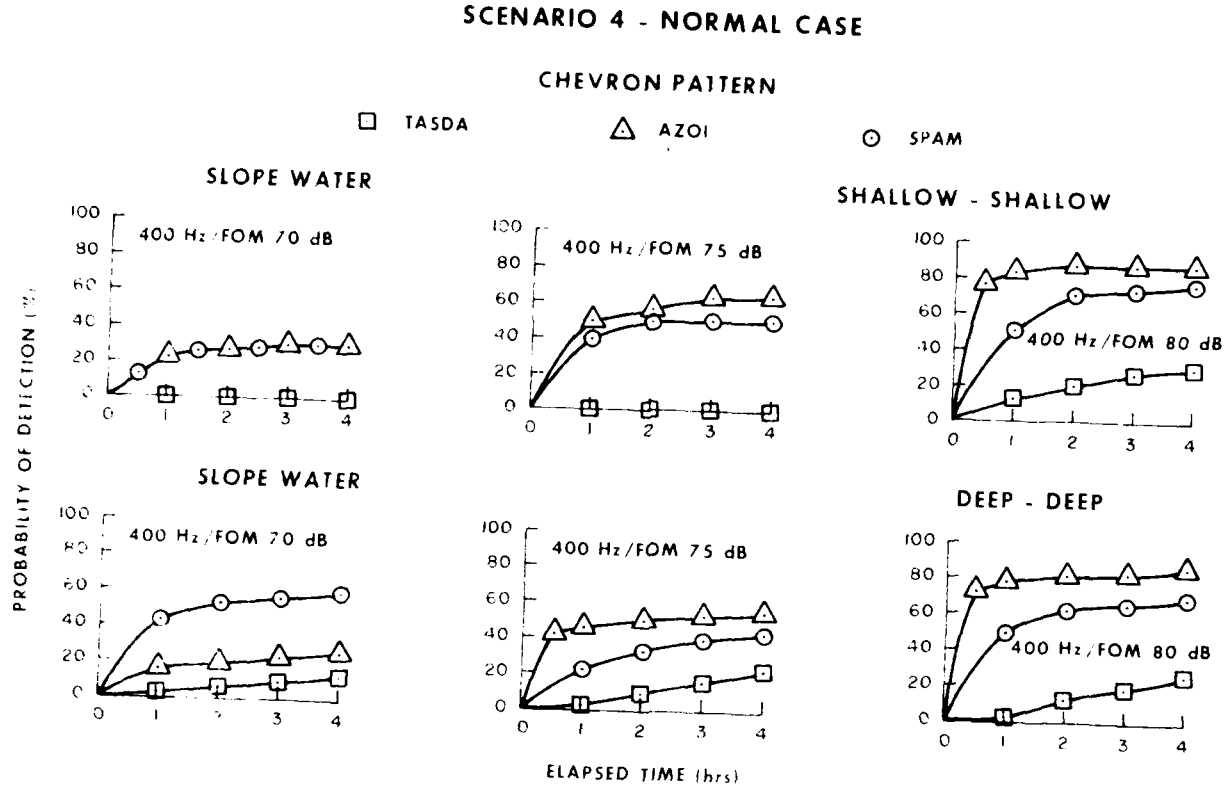

Figure C-62 Comparison of TASDA, AZOI and SPAM, with a normal initial target location at one hour time late with a receiver frequency of 400 Hz in the slope water environment in scenario 4 using the chevron pattern.

Scenario 1

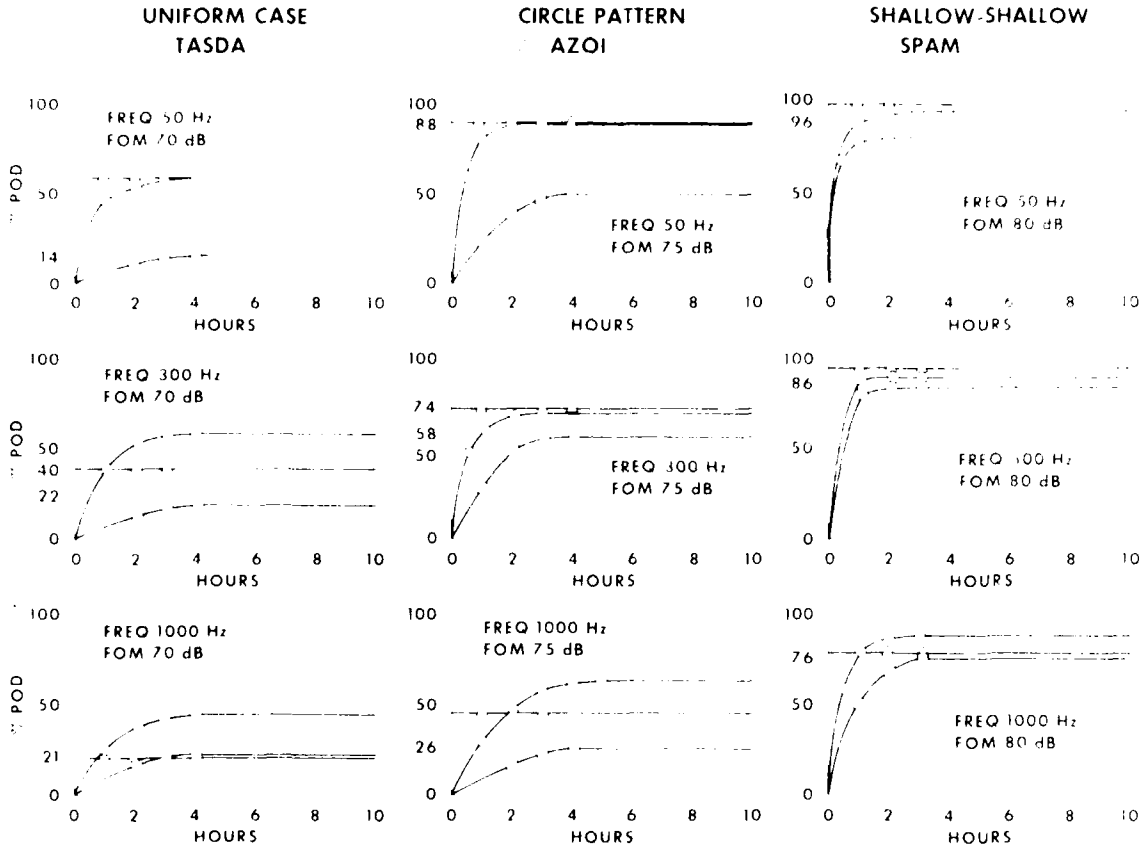

	FREQ 50 Hz			FREQ 300 Hz			FREQ 1000 Hz			
FOM	70	75	80	70	75	80	70	75	80	S-S%
CIRCLE (TASDA)	.14	.50	.96	.22	.58	.86	.21	.26	.76	49.9
CIRCLE (AZOI)	.54	.88	.99	.40	.74	.95	.20	.46	.78	66.0
CIRCLE (SPAM)	.55	.86	.81	.59	.72	.90	.41	.64	.85	70.3

Figure C-63. Scenario 1 - Eventual Probability of Detection for a shallow target and receiver. The eventual POD value is the maximum % POD attained by the curve. Eventual POD is obtained by observing the maximum POD for each CPOD curve. These maximum values are summed over frequency and FOM to give a percent POD for a uniformly distributed shallow target and a shallow receiver. Not for example: (.14 + .50 + .96 + .22 + .58 + .86 + .21 + .26 + .76)/9 = 49.9.

Table C-2: Scenario I
Eventual Probability of Detection
for a Uniform Target
at 30 min Time Late: Shallow - Shallow Case

UNIFORM TARGET

SHALLOW-SHALLOW (60ft-60ft)

	FREQ 50 Hz			FREQ 300 Hz			FREQ 1000 Hz		
COM	70	75	80	70	75	80	70	75	80
CIRCLE (TASEA)	.44	.50	.96	.22	.58	.86	.21	.26	.76
CIRCLE (AZOD)	.54	.88	.99	.40	.74	.95	.20	.46	.78
CIRCLE (SPAM)	.55	.86	.81	.59	.72	.90	.41	.64	.85
BRUSHTAC	.09	.41	.94	.17	.56	.80	.23	.29	.65
BRUSHTAC	.53	.85	.98	.40	.72	.93	.22	.47	.74
BRUSHTAC	.51	.83	.86	.45	.71	.91	.25	.45	.71
4-4-4-4	.11	.56	.97	.20	.58	.98	.20	.27	.80
4-4-4-4	.54	.88	.99	.40	.74	.95	.20	.47	.77
4-4-4-4	.67	.83	.86	.46	.85	.92	.40	.67	.81
5-5-5	.08	.56	.99	.08	.57	.99	.13	.21	.82
5-5-5	.47	.83	.99	.35	.68	.93	.16	.39	.70
5-5-5	.55	.82	.96	.53	.79	.93	.38	.71	.84
CHEVRON	.11	.52	.99	.16	.53	.99	.18	.32	.81
CHEVRON	.53	.87	.99	.40	.71	.95	.20	.45	.76
CHEVRON	.65	.78	.90	.56	.81	.90	.53	.63	.84

Table C-3: Scenario 1
Eventual Probability of Detection
for a Uniform Target
at 30 min Time Late: Shallow - Deep Case

UNIFORM TARGET — SHALLOW-DEEP (60ft-300ft)

FOM	FREQ 50 Hz			FREQ 300 Hz			FREQ 1000 Hz		
	70	75	80	70	75	80	70	75	80
CIRCLE (TASDA)	.00	.09	.88	.00	.06	.54	.00	.05	.21
CIRCLE (AZOI)	.33	.71	.96	.17	.47	.81	.06	.21	.49
CIRCLE (SPAM)	.42	.62	.78	.37	.61	.82	.34	.42	.70
BRUSHTAC	.00	.06	.66	.00	.07	.52	.00	.02	.15
BRUSHTAC	.32	.69	.94	.19	.46	.78	.08	.23	.49
BRUSHTAC	.39	.58	.79	.30	.45	.72	.33	.19	.53
4-4-4-4	.00	.07	.92	.00	.08	.63	.00	.03	.16
4-4-4-4	.32	.71	.96	.18	.47	.82	.07	.22	.50
4-4-4-4	.43	.57	.79	.42	.58	.82	.33	.34	.55
5-6-5	.00	.07	.93	.00	.03	.61	.00	.04	.14
5-6-5	26	.64	.94	.14	.40	.75	.05	.16	.40
5-6-5	.47	.69	.85	.37	.42	.88	.30	.26	.69
CHEVRON	.00	.11	.95	.00	.03	.65	.00	.04	.18
CHEVRON	.32	.70	.96	.18	.47	.81	.06	.21	.48
CHEVRON	.47	.65	.84	.42	.51	.79	.32	.45	.53

Table C-1: Scenario I
Eventual Probability of Detection
for a Uniform Target
at 30 min Time Late: Deep - Deep Case

UNIFORM TARGET

DEEP-DEEP (200ft-300ft)

	FREQ 50 Hz			FREQ 300 Hz			FREQ 1000 Hz		
LOS	70	75	80	70	75	80	70	75	80
CIRCLE (FASDA)	.00	.00	.59	.00	.01	.28	.00	.00	.02
CIRCLE (AZCOD)	.30	.67	.94	.23	.52	.84	.08	.23	.51
CIRCLE (SPAM)	.42	.64	.80	.49	.57	.83	.16	.31	.59
BRUSHTAC	.00	.00	.46	.00	.03	.40	.00	.00	.01
BRUSHTAC	.28	.64	.92	.21	.49	.80	.07	.22	.48
BRUSHTAC	.11	.60	.79	.41	.62	.81	.11	.35	.69
4-4-4-4	.00	.00	.54	.00	.01	.38	.00	.00	.01
4-4-4-4	.28	.65	.94	.21	.50	.82	.07	.22	.49
4-4-4-4	.36	.62	.83	.36	.66	.89	.13	.39	.67
5-6-5	.00	.00	.52	.00	.00	.40	.00	.00.	.00
5-6-5	.24	.58	.90	.18	.43	.76	.05	.16	.39
5-6-5	.43	.62	.81	.38	.69	.82	.14	.39	.58
CHEVRON	.00	.00	.60	.00	.00	.34	.00	.00	.01
CHEVRON	.28	.65	.93	.22	.50	.82	.07	.21	.47
CHEVRON	.36	.67	.85	.35	.57	.83	.09	.37	.62

Table C-5: Scenario 1
Eventual Probability of Detection
for a Normal Target
at 30 min Time Late: Shallow - Shallow Case

NORMAL TARGET — SHALLOW-SHALLOW (60ft-60ft)

	FREQ 50 Hz			FREQ 300 Hz			FREQ 1000 Hz		
FOM	70	75	80	70	75	80	70	75	80
ELLIPSE (TASDA)	.20	.97	.99	.26	.98	.99	.23	.37	.97
ELLIPSE (AZOI)	.97	.99	.99	.95	.99	.99	.86	.98	.99
ELLIPSE (SPAM)	.78	.86	.89	.70	.87	.94	.50	.79	.86
BRUSHTAC	.22	.89	.99	.25	.89	.99	.34	.39	.92
BRUSHTAC	.97	.99	.99	.96	.99	.99	.88	.98	.99
BRUSHTAC	.65	.82	.91	.66	.83	.95	.44	.71	.89
4-4-4-4	.16	.95	.99	.21	.96	.99	.16	.33	.99
4-4-4-4	.97	.99	.99	.96	.99	.99	.87	.99	.99
4-4-4-4	.71	.76	.87	.57	.89	.93	.49	.76	.88
5-6-5	.09	.92	.99	.15	.84	.99	.16	.24	.98
5-6-5	.94	.99	.99	.93	.99	.99	.78	.98	.99
5-6-5	.65	.83	.89	.55	.77	.94	.36	.64	.84
CHEVRON	.24	.94	.99	.28	.91	.99	.27	.36	.97
CHEVRON	.97	.99	.99	.96	.99	.99	.87	.98	.99
CHEVRON	.74	.84	.90	.62	.91	.92	.54	.79	.92

Table C-6: Scenario 1
Eventual Probability of Detection
for a Normal Target
at 30 min Time Late: Shallow + Deep Case

NORMAL TARGET — SHALLOW-DEEP (60ft-300ft)

FOM	FREQ 50 Hz			FREQ 300 Hz			FREQ 1000 Hz		
	70	75	80	70	75	80	70	75	80
ELLIPSE (CLASDA)	.02	.11	.99	.02	.14	.85	.03	.13	.29
ELLIPSE (AZOD)	.76	.98	.99	.71	.96	.99	.11	.80	.98
ELLIPSE (SPAM)	.52	.71	.87	.17	.71	.90	.31	.51	.71
BRUSHTAC	.00	.07	.96	.02	.16	.86	.06	.17	.29
BRUSHTAC	.80	.98	.99	.75	.97	.99	.50	.84	.98
BRUSHTAC	.13	.61	.83	.33	.66	.84	.24	.11	.72
4-4-4-4	.04	.17	.99	.02	.08	.85	.02	.15	.30
4-4-4-4	.77	.98	.99	.72	.96	.99	.16	.82	.98
4-4-4-4	.14	.71	.83	.10	.63	.80	.26	.17	.73
5-6-5	.01	.01	.97	.01	.05	.70	.01	.06	.18
5-6-5	.69	.96	.99	.64	.94	.99	.35	.72	.95
5-6-5	.15	.70	.84	.33	.56	.82	.30	.31	.71
CHEVRON	.03	.09	.98	.03	.18	.84	.00	.07	.25
CHEVRON	.79	.98	.99	.73	.96	.99	.16	.82	.98
CHEVRON	.10	.71	.85	.18	.58	.78	.12	.18	.73

Table C-7: Scenario 1
Eventual Probability of Detection
for a Normal Target
at 30 min Time Late: Deep - Deep Case

NORMAL TARGET — DEEP-DEEP (200ft-300ft)

	FREQ 50 Hz			FREQ 300 Hz			FREQ 1000 Hz		
FOM	70	75	80	70	75	80	70	75	80
ELLIPSE (TASDA)	.02	.05	.98	.02	.10	.63	.03	.05	.06
ELLIPSE (AZOD)	.86	.99	.99	.95	.99	.99	.74	.96	.99
ELLIPSE (SPAM)	.37	.76	.82	.42	.68	.88	.21	.35	.68
BRUSHTAC	.05	.08	.93	.06	.06	.49	.01	.02	.07
BRUSHTAC	.88	.99	.99	.96	.99	.99	.75	.96	.99
BRUSHTAC	.43	.71	.85	.36	.69	.89	.14	.37	.57
4-4-4-4	.03	.04	.96	.02	.05	.58	.01	.04	.07
4-4-4-4	.87	.99	.99	.96	.99	.99	.75	.97	.99
4-4-4-4	.46	.66	.88	.38	.72	.86	.14	.44	.70
5-6-5	.03	.03	.92	.03	.05	.77	.02	.03	.09
5-6-5	.82	.99	.99	.94	.99	.99	.67	.94	.99
5-6-5	.34	.65	.89	.46	.56	.82	.15	.41	.76
CHEVRON	.06	.08	.98	.05	.08	.57	.03	.04	.11
CHEVRON	.87	.99	.99	.96	.99	.99	.75	.96	.99
CHEVRON	.44	.76	.76	.49	.69	.84	.17	.53	.76

Table C-8: Scenario 1
Eventual Probability of Detection
for a Normal Target
at 1 Hr Time Late: Shallow - Shallow Case

NORMAL TARGET

SHALLOW-SHALLOW (60ft-60ft)

	FREQ 50 Hz			FREQ 300 Hz			FREQ 1000 Hz		
FOM	70	75	80	70	75	80	70	75	80
ELLIPSE (TASDA)	.23	.96	.99	.23	.92	.99	.21	.37	.99
ELLIPSE (AZCH)	.97	.99	.99	.95	.99	.99	.86	.99	.99
ELLIPSE (SPAM)	.75	.86	.84	.69	.86	.96	.48	.79	.85
BRUSHTAC	.17	.85	.99	.20	.88	.98	.18	.24	.92
BRUSHTAC	.97	.99	.99	.96	.99	.99	.88	.99	.99
BRUSHTAC	.64	.84	.91	.66	.85	.94	.43	.72	.88
4-4-4-4	.18	.92	.99	.20	.93	.99	.19	.32	.99
4-4-4-4	.97	.99	.99	.96	.99	.99	.87	.99	.99
4-4-4-4	.70	.77	.89	.56	.87	.91	.48	.75	.89
5-6-5	.08	.82.	.99	.14	.91	.99	.12	.17	.97
5-6-5	.94	.99	.99	.93	.99	.99	.78	.97	.99
5-6-5	.64	.83	.89	.55	.78	.94	.35	.65	.85
CHEVRON	.23	.92	.99	.22	.95	.99	.37	.46	.97
CHEVRON	.97	.99	.99	.96	.99	.99	.87	.99	.99
CHEVRON	.73	.80	.92	.63	.90	.94	.53	.79	.92

Table C-9: Scenario 1
Eventual Probability of Detection
for a Normal Target
at 1 Hr Time Late: Shallow - Deep Case

NORMAL TARGET — SHALLOW-DEEP (60ft-300ft)

	FREQ 50 Hz			FREQ 300 Hz			FREQ 1000 Hz		
FOM	70	75	80	70	75	80	70	75	80
ELLIPSE (TASDA)	.01	.09	.99	.01	.06	.89	.02	.10	.30
ELLIPSE (AZOI)	.76	.98	.99	.70	.97	.99	.44	.80	.97
ELLIPSE (SPAM)	.52	.74	.85	.47	.72	.87	.31	.53	.72
BRUSHTAC	.04	.19	.91	.07	.19	.81	.04	.17	.33
BRUSHTAC	.79	.98	.99	.74	.96	.99	.49	.83	.97
BRUSHTAC	.45	.62	.83	.32	.67	.84	.26	.39	.72
4-4-4-4	.00	.10	.99	.01	.12	.79	.02	.13	.28
4-4-4-4	.77	.98	.99	.72	.96	.99	.45	.81	.78
4-4-4-4	.41	.69	.80	.40	.60	.81	.26	.48	.73
5-6-5	.01	.04	.99	.00	.04	.69	.01	.08	.16
5-6-5	.78	.96	.99	.63	.93	.99	.34	.71	.95
5-6-5	.46	.69	.85	.34	.56	.84	.31	.29	.70
CHEVRON	.03	.14	.99	.04	.20	.89	.02	.13	.25
CHEVRON	.78	.98	.99	.73	.96	.99	.46	.82	.98
CHEVRON	.41	.73	.86	.47	.57	.79	.41	.47	.74

Table C-10: Scenario 1
Eventual Probability of Detection
for a Normal Target
at 1 Hr Time Late: Deep - Deep Case

NORMAL TARGET

DEEP-DEEP (200ft-300ft)

	FOM	FREQ 50 Hz			FREQ 300 Hz			FREQ 1000 Hz		
		70	75	80	70	75	80	70	75	80
ELLIPSE (TASDA)		.02	.04	.95	.04	.07	.59	.02	.03	.07
ELLIPSE (AZOD)		.86	.99	.99	.95	.99	.99	.74	.96	.99
ELLIPSE (SPAM)		.39	.78	.82	.39	.67	.87	.21	.33	.68
BRUSHTAC		.05	.06	.92	.02	.09	.55	.00	.01	.05
BRUSHTAC		.88	.99	.99	.96	.99	.99	.76	.96	.99
BRUSHTAC		.43	.71	.85	.38	.69	.89	.13	.37	.55
4-4-4-4		.02	.02	.96	.01	.04	.50	.00	.00	.03
4-4-4-4		.86	.99	.99	.96	.99	.99	.75	.97	.99
4-4-4-4		.44	.67	.90	.34	.71	.86	.15	.44	.68
5-6-5		.02	.03	.88	.02	.03	.69	.01	.01	.04
5-6-5		.81	.99	.99	.93	.99	.99	.66	.93	.99
5-6-5		.34	.65	.90	.47	.54	.81	.17	.41	.76
CHEVRON		.03	.03	.94	.02	.04	.52	.02	.04	.06
CHEVRON		.87	.99	.99	.96	.99	.99	.75	.96	.99
CHEVRON		.44	.76	.77	.46	.69	.84	.16	.54	.77

Table C-11: Scenario 1
Eventual Probability of Detection
for a Normal Target
at 4 Hrs Time Late: Shallow - Shallow Case

NORMAL TARGET

SHALLOW-SHALLOW (60ft-60ft)

	FREQ 50 Hz			FREQ 300 Hz			FREQ 1000 Hz		
FOM	70	75	80	70	75	80	70	75	80
ELLIPSE (TASDA)	.10	.84	.99	.12	.81	.94	.19	.23	.92
ELLIPSE (AZOI)	.95	.99	.99	.94	.99	.99	.80	.98	.99
ELLIPSE (SPAM)	.68	.86	.87	.60	.85	.94	.42	.70	.85
BRUSHTAC	.13	.70	.98	.10	.73	.92	.10	.14	.80
BRUSHTAC	.95	.99	.99	.94	.99	.99	.78	.95	.99
BRUSHTAC	.66	.83	.92	.65	.83	.95	.40	.67	.85
4-4-4-4	.10	.83	.99	.21	.84	.96	.15	.23	.92
4-4-4-4	.95	.99	.99	.94	.99	.99	.79	.96	.99
4-4-4-4	.66	.74	.87	.51	.79	.91	.45	.70	.85
5-6-5	.07	.81	.99	.12	.87	.99	.10	.17	.98
5-6-5	.91	.99	.99	.90	.99	.99	.70	.93	.99
5-6-5	.60	.81	.92	.52	.74	.93	.34	.57	.83
CHEVRON	.11	.78	.99	.10	.88	.99	.10	.18	.88
CHEVRON	.95	.99	.99	.95	.99	.99	.79	.96	.99
CHEVRON	.65	.75	.89	.59	.84	.91	.43	.75	.92

Table C-12: Scenario 1
Eventual Probability of Detection
for a Normal Target
at 4 hrs Time Late: Shallow - Deep Case

NORMAL TARGET — SHALLOW-DEEP (60ft-300ft)

	FOM	FREQ 50 Hz			FREQ 300 Hz			FREQ 1000 Hz		
		70	75	80	70	75	80	70	75	80
ELLIPSE (TASDA)		.01	.10	.96	.01	.10	.71	.00	.06	.12
ELLIPSE (AZOI)		.73	.97	.99	.67	.95	.99	.37	.73	.95
ELLIPSE (SPAM)		.48	.69	.86	.45	.70	.89	.32	.46	.68
BRUSHTAC		.01	.03	.70	.01	.03	.59	.01	.08	.12
BRUSHTAC		.73	.97	.99	.68	.95	.99	.38	.72	.93
BRUSHTAC		.43	.60	.82	.36	.66	.80	.26	.40	.67
4-4-4-4		.00	.04	.89	.03	.13	.61	.01	.06	.16
4-4-4-4		.72	.97	.99	.67	.95	.99	.37	.73	.95
4-4-4-4		.38	.68	.86	.38	.57	.75	.24	.36	.61
5-6-5		.00	.04	.97	.01	.05	.65	.00	.09	.15
5-6-5		.66	.94	.99	.58	.91	.99	.29	.64	.91
5-6-5		.43	.65	.82	.37	.51	.83	.29	.26	.63
CHEVRON		.00	.06	.95	.01	.02	.66	.01	.06	.11
CHEVRON		.75	.97	.99	.69	.95	.99	.38	.74	.95
CHEVRON		.38	.73	.83	.50	.49	.79	.39	.44	.68

Table C-12: Scenario 1
Eventual Probability of Detection
for a Normal Target
at 4 Hrs Time Late: Deep - Deep Case

NORMAL TARGET

DEEP-DEEP (200ft-300ft)

CASE	TIME LATE								
	FREQ 50 Hz			FREQ 300 Hz			FREQ 1000 Hz		
FOM	70	75	80	70	75	80	70	75	80
ELLIPSE (TASDA)	.01	.01	.90	.01	.03	.55	.00	.00	.01
ELLIPSE (AZOI)	.86	.99	.99	.96	.99	.99	.73	.96	.99
ELLIPSE (SPAM)	.35	.69	.80	.38	.63	.88	.23	.29	.63
BRUSHTAC	.01	.01	.64	.00	.01	.36	.01	.01	.03
BRUSHTAC	.85	.99	.99	.95	.99	.99	.74	.96	.99
BRUSHTAC	.41	.72	.85	.37	.67	.89	.12	.36	.54
4-4-4-4	.02	.02	.83	.00	.05	.43	.03	.05	.06
4-4-4-4	.85	.99	.99	.96	.99	.99	.73	.96	.99
4-4-4-4	.46	.63	.89	.40	.70	.84	.14	.41	.65
5-6-5	.00	.00	.73	.00	.02	.54	.00	.00	.01
5-6-5	.78	.98	.99	.92	.99	.99	.61	.91	.99
5-6-5	.34	.61	.92	.43	.54	.79	.14	.39	.73
CHEVRON	.02	.02	.77	.00	.02	.55	.01	.04	.07
CHEVRON	.87	.99	.99	.97	.99	.99	.76	.97	.99
CHEVRON	.45	.72	.74	.47	.66	.80	.16	.45	.72

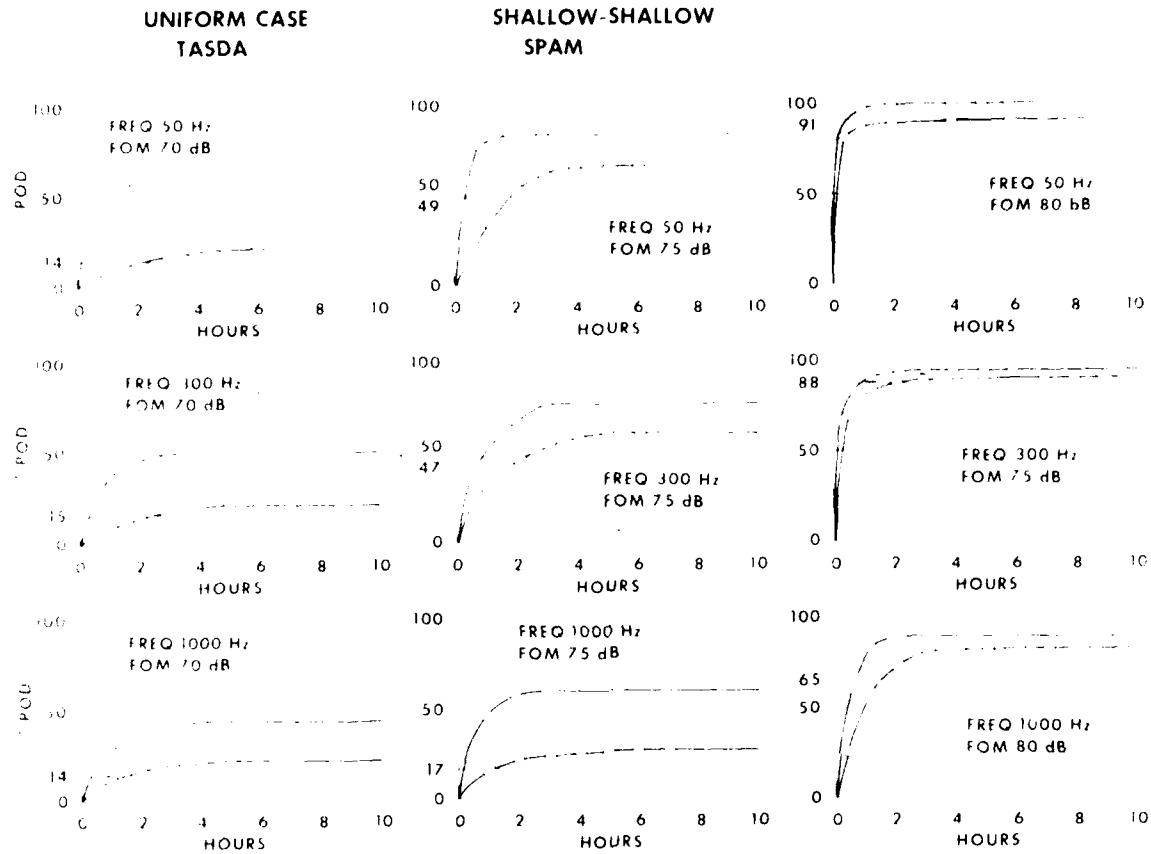

	FREQ 50 Hz			FREQ 300 Hz			FREQ 1000 Hz			
	70	75	80	70	75	80	70	75	80	S-S
CIRCLE (TASDA)	.13	.49	.91	.15	.47	.88	.14	.17	.65	47.2
CIRCLE (AZOI)	.01	.47	.92	.10	.42	.80	.03	.18	.54	38.5
CIRCLE (SPAM)	.51	.72	.83	.45	.62	.81	.44	.55	.78	63.4

Figure C-64. Scenario 2: Average Probability of Detection a shallow target and receiver. The average POD value is obtained by visually estimating the area under the CPOD curve. These average values are summed over frequency and FOM to give a percent POD for a uniformly distributed shallow target and a shallow receiver. Note for example: (.14 + .49 + .91 + .15 + .47 + .88 + .14 + .17 + .65)/9 = 47.2%.

Table C-13: Scenario 2
Average Probability of Detection
for a Uniform Target
at 1 Hr Time Late

UNIFORM TARGET

FOM	FREQ 50 Hz			FREQ 300 Hz			FREQ 1000 Hz		
	70	75	80	70	75	80	70	75	80
SHALLOW-SHALLOW (60ft-60ft)									
CIRCLE (TASDA)	.13	.49	.91	.15	.47	.88	.11	.17	.65
CIRCLE (AZOI)	.01	.47	.92	.10	.42	.80	.03	.18	.51
CIRCLE (SPAM)	.51	.72	.83	.45	.62	.81	.14	.55	.78
4-4-4-4	.21	.57	.98	.17	.52	.97	.17	.23	.70
4-4-4-4	.01	.48	.93	.12	.41	.82	.03	.24	.55
4-4-4-4	.45	.72	.73	.42	.71	.74	.32	.53	.60
SHALLOW-DEEP (60ft-300ft)									
CIRCLE	.00	.01	.71	.00	.07	.51	.00	.05	.16
CIRCLE	.00	.12	.76	.00	.04	.47	.00	.86	.13
CIRCLE	.38	.58	.70	.35	.50	.72	.29	.27	.46
4-4-4-4	.00	.05	.87	.01	.03	.49	.00	.05	.19
4-4-4-4	.00	.16	.75	.00	.06	.50	.00	.76	.19
4-4-4-4	.29	.48	.68	.27	.40	.66	.25	.24	.41
DEEP-DEEP (200ft-300ft)									
CIRCLE	.00	.00	.44	.00	.00	.21	.00	.00	.01
CIRCLE	.00	.19	.57	.04	.16	.48	.00	.06	.20
CIRCLE	.33	.61	.71	.31	.50	.75	.12	.35	.45
4-4-4-4	.00	.00	.52	.00	.01	.36	.00	.00	.01
4-4-4-4	.00	.14	.56	.00	.14	.49	.00	.03	.17
4-4-4-4	.35	.53	.74	.36	.60	.72	.16	.18	.51

Tabel C-14: Scenario 2
Average Probability of Detection
for a Normal Target
at 1 Hr Time Late

NORMAL TARGET — SHALLOW-SHALLOW (60ft-60ft)

	FOM	FREQ 50 Hz			FREQ 300 Hz			FREQ 1000 Hz		
		70	75	80	70	75	80	70	75	80
ELLIPSE (TASDA)		.21	.91	.99	.25	.90	.98	.24	.33	.98
ELLIPSE (AZOD)		.73	.95	.99	.72	.95	.98	.24	.85	.97
ELLIPSE (SPAM)		.57	.83	.81	.46	.81	.97	.35	.67	.85
CHEVRON		.31	.91	.99	.26	.89	.98	.31	.39	.96
CHEVRON		.73	.90	.99	.71	.96	.98	.18	.83	.96
CHEVRON		.61	.75	.76	.62	.74	.88	.46	.70	.76
							SHALLOW-DEEP (60ft-300ft)			
ELLIPSE		.03	.20	.96	.01	.11	.74	.04	.14	.29
ELLIPSE		.04	.78	.98	.03	.76	.97	.03	.10	.83
ELLIPSE		.36	.64	.82	.33	.60	.74	.29	.33	.65
CHEVRON		.01	.11	.97	.03	.14	.86	.03	.16	.35
CHEVRON		.02	.77	.99	.01	.76	.95	.01	.05	.85
CHEVRON		.45	.72	.70	.36	.57	.76	.22	.36	.73
							DEEP-DEEP (200ft-300ft)			
ELLIPSE		.03	.06	.87	.01	.05	.58	.01	.02	.05
ELLIPSE		.01	.85	.95	.63	.87	.94	.01	.65	.92
ELLIPSE		.38	.62	.86	.40	.63	.87	.17	.35	.67
CHEVRON		.03	.05	.92	.01	.05	.58	.03	.05	.07
CHEVRON		.01	.65	.98	.72	.95	.98	.00	.70	.96
CHEVRON		.34	.57	.76	.40	.59	.74	.16	.35	.57

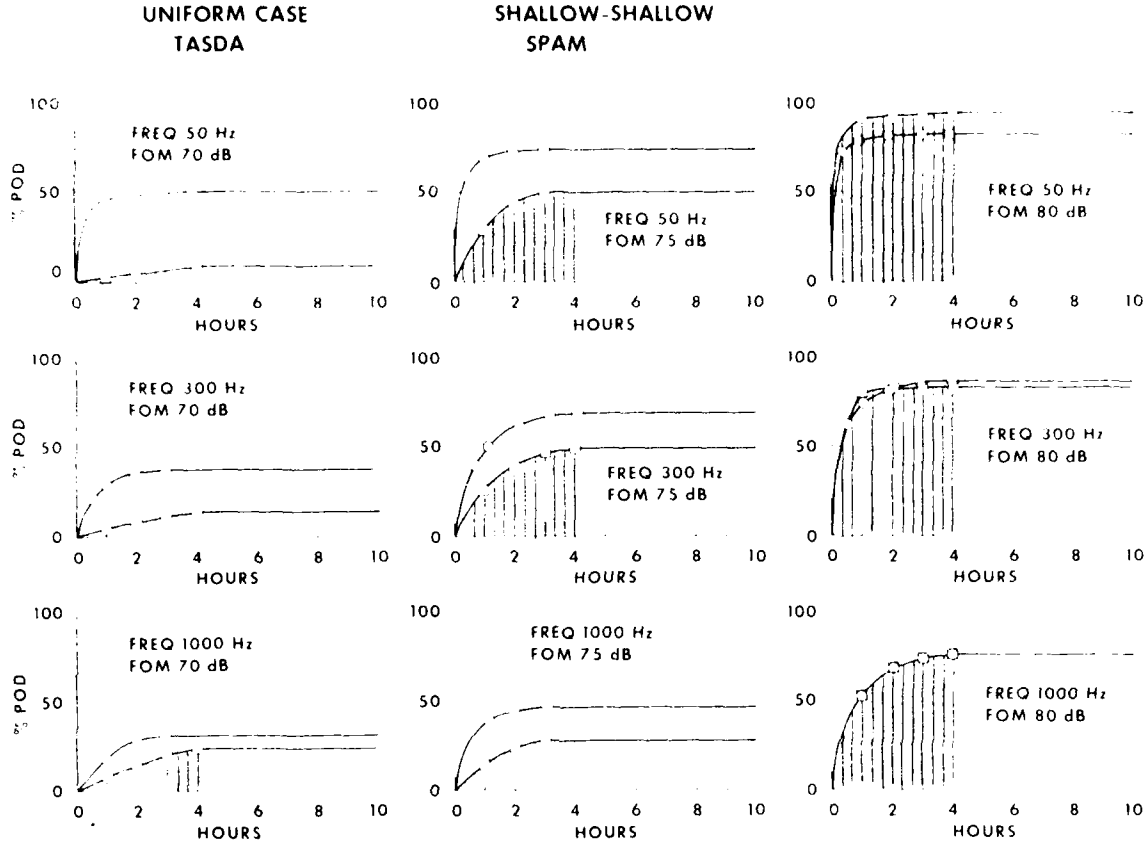

	FREQ 50 Hz			FREQ 300 Hz			FREQ 1000 Hz			
	70	75	80	70	75	80	70	75	80	S-S
CIRCLE (TASDA)	.13	.50	.95	.09	.43	.82	.22	.32	.73	46.0
CIRCLE (AZOI)	.05	.27	.76	.07	.24	.43	.02	.13	.35	25.8
CIRCLE (SPAM)	.48	.69	.81	.32	.57	.77	.25	.40	.63	55.2

Figure C-65. Scenario 3 and 4: Average Probability of Detection for a shallow target and receiver. The average POD value is obtained by summing the POD values at each time increment and dividing by the total number of time increments to estimate the area under the CPOD curve. The average values are summed over frequency and FOM to give a percent POD for a uniformly distributed shallow target and a shallow receiver.

Table C-15: Scenario 3
Average Probability of Detection
for a Uniform Target
at 1 Hr Time Late

UNIFORM TARGET

SHALLOW-SHALLOW (60ft-60ft)

	FOM	FREQ 50 Hz			FREQ 300 Hz		FREQ 1000 Hz			
		70	75	80	70	75	80	70	75	80
CIRCLE (TASDA)		.13	.50	.95	.09	.13	.82	.22	.32	.73
CIRCLE (AZOI)		.05	.27	.76	.07	.21	.13	.02	.13	.35
CIRCLE (SPAM)		.18	.69	.81	.32	.57	.77	.25	.40	.63
1-1-1-1		.18	.58	.98	.13	.54	.93	.17	.29	.76
1-1-1-1		.03	.26	.71	.06	.21	.41	.01	.11	.33
1-1-1-1		.37	.67	.71	.30	.61	.72	.21	.42	.57

SHALLOW-DEEP (60ft-300ft)

CIRCLE		.01	.06	.76	.00	.06	.47	.00	.11	.20
CIRCLE		.00	.10	.60	.00	.03	.26	.00	.97	.11
CIRCLE		.32	.17	.65	.17	.39	.62	.14	.18	.38
1-1-1-1		.00	.01	.86	.01	.07	.57	.01	.05	.16
1-1-1-1		.00	.08	.54	.00	.02	.22	.00	.00	.09
1-1-1-1		.19	.11	.69	.10	.31	.62	.11	.19	.36

DEEP-DEEP (200ft-300ft)

CIRCLE		.00	.01	.50	.00	.02	.33	.00	.00	.00
CIRCLE		.00	.06	.26	.05	.05	.19	.00	.00	.08
CIRCLE		.21	.48	.63	.16	.39	.64	.09	.20	.38
1-1-1-1		.00	.00	.52	.00	.00	.36	.00	.00	.02
1-1-1-1		.00	.06	.25	.03	.05	.18	.00	.00	.07
1-1-1-1		.19	.48	.70	.18	.40	.59	.10	.18	.38

Table C-16: Scenario 3
Average Probability of Detection
for a Normal Target
at 1 Hr Time Late

NORMAL TARGET

SHALLOW-SHALLOW (60ft-60ft)

	FREQ 50 Hz			FREQ 300 Hz			FREQ 1000 Hz		
FOM	70	75	80	70	75	80	70	75	80
ELLIPSE (TASDA)	.17	.73	.98	.11	.72	.94	.13	.19	.84
ELLIPSE (AZOI)	.44	.76	.97	.44	.68	.83	.09	.60	.79
ELLIPSE (SPAM)	.56	.76	.81	.35	.70	.83	.33	.54	.74
CHEVRON	.09	.70	.96	.18	.74	.94	.15	.19	.86
CHEVRON	.43	.76	.97	.43	.68	.84	.09	.60	.80
CHEVRON	.51	.79	.78	.46	.64	.79	.30	.58	.77
						SHALLOW-DEEP (60ft-300ft)			
ELLIPSE	.03	.09	.90	.01	.06	.51	.02	.08	.15
ELLIPSE	.02	.47	.90	.03	.43	.72	.03	.05	.59
ELLIPSE	.24	.55	.78	.24	.42	.69	.16	.26	.54
CHEVRON	.01	.11	.91	.01	.08	.63	.01	.07	.20
CHEVRON	.01	.41	.90	.01	.40	.70	.01	.03	.56
CHEVRON	.30	.64	.70	.24	.47	.76	.11	.29	.60
						DEEP-DEEP (200ft-300ft)			
ELLIPSE	.01	.02	.76	.02	.05	.34	.02	.02	.05
ELLIPSE	.02	.53	.77	.42	.62	.78	.02	.08	.64
ELLIPSE	.28	.50	.79	.26	.43	.71	.09	.24	.47
CHEVRON	.01	.01	.72	.02	.02	.11	.02	.04	.05
CHEVRON	.01	.50	.75	.39	.60	.76	.01	.07	.61
CHEVRON	.24	.18	.67	.25	.41	.68	.09	.25	.45

Table C-17: Scenario 4
Average Probability of Detection
for a Uniform Target
at 1 Hr Time Late

UNIFORM TARGET		GULF STREAM			SHALLOW-SHALLOW (100ft-150ft)		
		FREQ 100 Hz			FREQ 100 Hz		
	FOM	70	75	80	70	75	80
CIRCLE (PASDA)		.15	.30	.49	.01	.03	.38
CIRCLE (AZOD)		.21	.51	.82	.15	.32	.56
CIRCLE (SLAM)		.22	.42	.67	.11	.36	.50
		SLOPE WATER					
CIRCLE		.00	.01	.41	.00	.00	.12
CIRCLE		.16	.42	.71	.09	.26	.52
CIRCLE		.26	.61	.80	.39	.36	.50
		GULF STREAM			DEEP-DEEP (500ft-1000ft)		
CIRCLE		.02	.11	.24	.08	.13	.21
CIRCLE		.23	.54	.84	.10	.28	.57
CIRCLE		.43	.41	.56	.19	.27	.45
		SLOPE WATER					
CIRCLE		.09	.13	.17	.05	.09	.23
CIRCLE		.11	.40	.72	.08	.25	.54
CIRCLE		.10	.45	.65	.32	.37	.57

Table C-18: Scenario 4
Average Probability of Detection
for a Normal Target
at 1 Hr Time Late

NORMAL TARGET

GULF STREAM — SHALLOW-SHALLOW (100ft-150ft)

	FOM	FREQ 100 Hz 70	75	80	FREQ 400 Hz 70	75	80
CHEVRON SKEW	(TASDA)	.01	.06	.67	.11	.26	.62
CHEVRON SKEW	(AZOI)	.46	.78	.96	.40	.60	.81
CHEVRON SKEW	(SPAM)	.22	.42	.66	.36	.31	.42
SLOPE WATER							
CHEVRON SKEW		.02	.04	.61	.01	.04	.19
CHEVRON SKEW		.43	.77	.93	.24	.55	.84
CHEVRON SKEW		.25	.57	.75	.25	.43	.63
GULF STREAM — **DEEP-DEEP (500ft-1000ft)**							
CHEVRON SKEW		.07	.14	.42	.08	.15	.25
CHEVRON SKEW		.35	.69	.90	.26	.57	.82
CHEVRON SKEW		.51	.39	.51	.28	.27	.44
SLOPE WATER							
CHEVRON SKEW		.09	.12	.31	.06	.11	.13
CHEVRON SKEW		.30	.61	.87	.21	.48	.78
CHEVRON SKEW		.50	.42	.63	.50	.32	.56

DISTRIBUTION LIST

CNO (OP 952, 952D1) 1 EA	2
COMPATWINGSLANT (TAC D&E)	1
COMPATWINGSPAC (TAC D&E)	1
COMNAVSEASYSCOM (63D5, Library) 1 EA	2
COMNAVAIRSYSCOM (370P, Library) 1 EA	2
COMNAVAIRDEVCEN (203, Library) 1 EA	2
COMNAVOCEANCOM	1
MASWSPO	1
NORDA (321)	1
FLENVMOCEANCEN	1
NAVPGSCOL	1
NAVWARCOL	1
DTIC	[illegible]


END
DATE
FILMED
10-81
DTIC

AD-A104 415 NAVAL OCEANOGRAPHIC OFFICE NSTL STATION MS F/G 11/1
ASSESSMENT OF TACTICAL SONOBUOY COMPUTER PROGRAMS FOR ENVIRONME--ETC(U)
FEB 81 L J FUSILLO
UNCLASSIFIED NOO-TR-260 NL

3 of 3

SUPPLEMENTARY

INFORMATION

DEPARTMENT OF THE NAVY
U.S. NAVAL OCEANOGRAPHIC OFFICE
NSTL STATION
BAY ST. LOUIS, MISSISSIPPI 39522

IN REPLY REFER TO
Code 9200
8 February 1982

ERRATA

Naval Oceanographic Office

Technical Report TR260, "Assessment of Tactical Sonobuoy Computer Programs for Environmental Software Systems (U)," February 1981, should be corrected as indicated below:

1. Replace graph Lat 3935N Lon 7130W on page 10 with "peel and press" graph Lat 3936N Lon 7029W.

2. Replace graph Lat 3936N Lon 7029W on page 11 with "peel and press" graph Lat 3935N Lon 7130W.

Enclosures (12)

DEPTH	VELOCITY
0.0	1525.1
67.0	1526.9
90.0	1523.2
100.0	1523.4
111.0	1520.5
132.0	1519.2
147.0	1518.5
165.0	1516.7
181.0	1515.8
200.0	1514.5
312.0	1501.7
460.0	1491.2
600.0	1485.5
800.0	1481.7
1000.0	1481.4
1200.0	1483.8
1500.0	1488.9
2000.0	1497.4
2400.0	1503.5

SOUND VELOCITY PROFILE

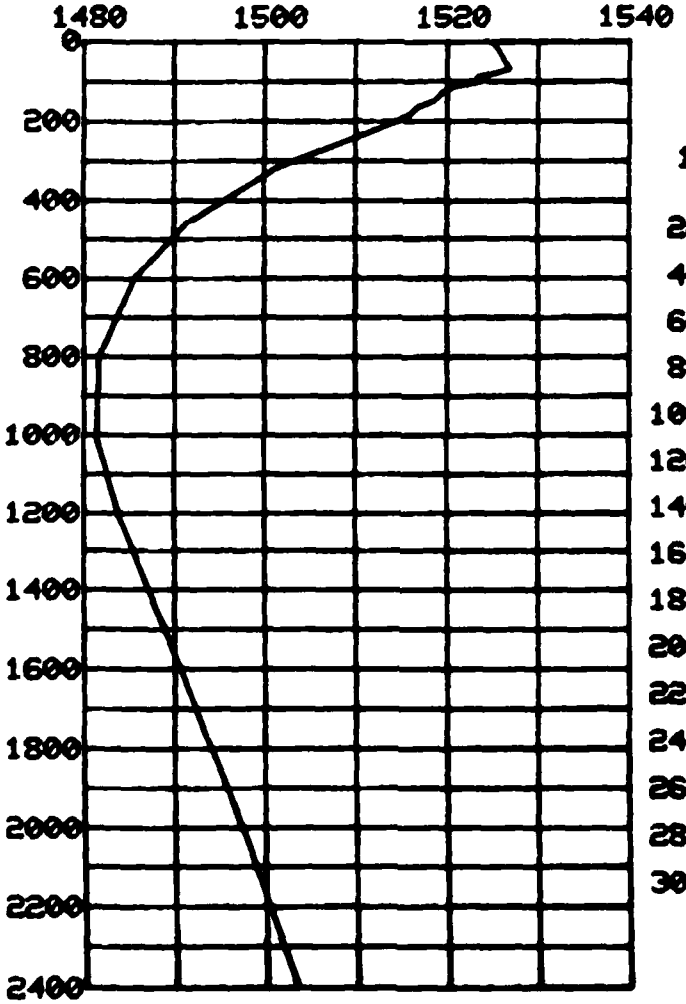

LAT 3936N LON 7029W
DATE 171169

(NEAR SURFACE)

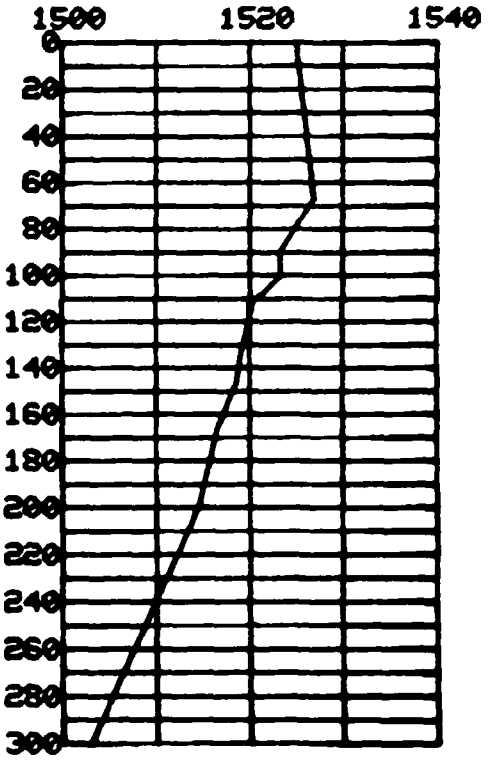

DEPTH	VELOCITY
0.0	1523.5
34.0	1524.1
41.0	1522.6
70.0	1522.3
82.0	1519.8
88.0	1515.6
99.0	1513.8
105.0	1513.3
121.0	1509.5
149.0	1507.9
178.0	1504.4
200.0	1502.6
312.0	1492.7
460.0	1483.0
600.0	1480.8
800.0	1481.7
1000.0	1483.9
1200.0	1486.3
1500.0	1490.6
2000.0	1497.6
2400.0	1503.2

SOUND VELOCITY PROFILE

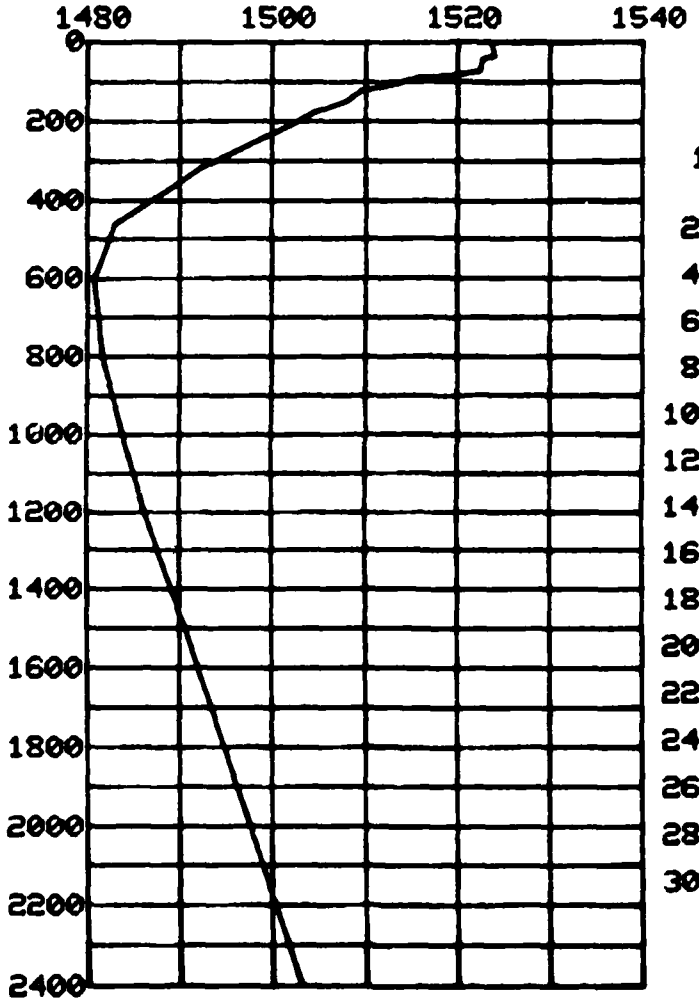

LAT 3935N LON 7130W
DATE 181169

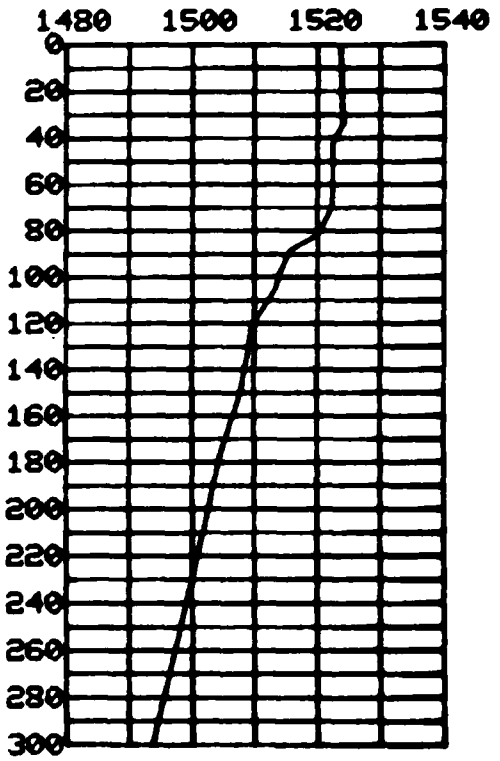


D
FI
3